MULTI-PROXY EVIDENCE OF LONG-TERM ENVIRONMENTAL CHANGE IN NORTHERN AUSTRALIA'S TROPICAL SAVANNAS

Maria Jose Rivera Araya

Master of Science, Geography
Bachelor of Science, Chemistry
Bachelor of Arts, Anthropology

A thesis submitted for the degree of
Doctor of Philosophy

College of Science and Engineering
James Cook University

December 2020

Acknowledgements

I sincerely thank:

My supervisors Michael Bird, Sean Ulm, Cassandra Rowe, Vladimir Levchenko and Jonathan Tyler for supporting my ideas throughout my PhD candidature. Thanks to Michael Bird for financial support during my fieldwork and labwork throughout my PhD.

Vladimir Levchenko and Patricia Gadd for supporting my AINSE PGRA application, for hosting me at ANSTO several times through the course of my PhD.

John Tibby, Ulrike Proske and Kathryn Taffs for their help interpreting diatom assemblages. Anne Alexandre for her help identifying phytoliths.

The Traditional Owners of the lands and waters we carried out fieldwork, including Anggamudi (also known as Angkamuthi), Wuthahti (alternatively Wuthathi) and Yadhaigana (alternatively Yadhaykenu). In particular Charles Woosop and the Apudthama Land Trust.

The AINSE team (Michael Rose, Sandy O' Connor, Michelle Durant, Nerissa Phillips) for their help during my AINSE PGRA visits.

My partner Maru, my family in Costa Rica.

My laboratory colleagues and friends.

I am also very grateful for the financial support provided for this PhD research project by the following organisations:

Australian Research Council (Laureate Fellowship to Michael Bird) Grant # FL140100044

Australian Institute of Nuclear Science and Engineering (AINSE) PGRA- Post Graduate Research Award # 12357

Centre of Excellence for Australian Biodiversity and Heritage Grant # CE170100015

Universidad de Costa Rica through the Academic Mobility Program

Australian Government Research Training Program Scholarship

Statement of Contribution of Others

Standard contributions were made by the supervisory team of Professor Michael Bird, Professor Sean Ulm, Dr. Cassandra Rowe, Dr. Jonathan Tyler and Dr. Vladimir Levchenko. This assistance included project design, technical support, and revisions and editing of this thesis.

Contributions of others to the thesis

Nature of assistance	Contribution	Names of contributors
Intellectual support	Proposal writing	Prof. Michael Bird
	Data Analysis	Prof. Michael Bird, Dr. Cassandra Rowe, Vladimir Levchenko
	Editorial assistance	Prof. Michael Bird, Prof. Sean Ulm, Dr. Cassandra Rowe, Dr. Jonathan Tyler
Financial support	Research costs	Prof. Michael Bird
	Stipend	JCU Postgraduate Research Scholarship
	Travel and research training	Centre of Excellence for Australian Biodiversity and Heritage
Data collection	Research assistance	Prof. Michael Bird, Dr. Cassandra Rowe, Vladimir Levchenko
	Sample collection	Prof. Michael Bird, Dr. Cassandra Rowe, Rainy Comley, Costjin Zwart

Abstract

There are few long-term records of climatic and environmental change from Cape York Peninsula in the tropical savannas of northeast Australia. This scarcity has constrained the development and understanding of climate and environmental change in the Australian's tropics, and thereby the ability to provide context for the long period of human occupation of the region. Lake sediment archives are widely used to recognize changes in climate, precipitation, and anthropogenic activities with the potential to significantly extend the length of the available observational record by many millennia. Despite the common use of lake sediment proxy indicators to reconstruct climate and environmental histories, existing research demonstrates the complications associated with building robust and accurate chronologies and interpreting the meaning of observed changes from multiple physical, biological and chemical sources of information.

This study was based upon a 1.72 m sediment core from Sanamere Lagoon (11.123°S 142.359°E) with the aim to develop a new record of climate and environmental change for northern Cape York Peninsula. The record spans the last ca. 33 thousand (ka) calibrated years before the present (cal BP), based on a robust chronology established by comparing age-models derived from multiple carbon fractions (pyrogenic carbon derived from hydrogen pyrolysis – hypy fraction -, macrocharcoal, microcharcoal, pollen concentrates, bulk sediment and cellulose). The age-depth model derived from the hypy fraction was the most reliable and consistent with the stratigraphic changes identified along the core, removing allochthonous carbon and post-depositional contamination. This chronology provided the basis for the climatic and environmental reconstructions from the Sanamere sediment core presented in this thesis.

Time series based on diatoms, phytoliths, hypy fractions, stable isotopes and elemental geochemistry (ITRAX micro X-ray fluorescence scanning) were used to understand the evolution of environmental conditions in the area surrounding Sanamere Lagoon. Four main periods of environmental change were identified (33 - 29.1 ka, 29.1 - 18.2 ka, 18.2 - 9.7 ka and 9.7 ka - present). During the first period, the lagoon formed by collapse of underlying laterite karst terrain, to a level below the local water table, ensuring a continuous record. The lagoon was filled following a wet event, likely related to a southward shift of the Intertropical Convergence Zone (ITCZ) during low sea levels. The results suggest a dominance of dry conditions during the first two identified periods (33 - 18.2 ka). However, no evidence of extreme dry conditions during the Last Glacial Maximum are recorded in the lake sediments. During this time Sanamere Lagoon was a small and shallow water body, with limited organic input. The lagoon expanded and deepened during 18.2 - 9.7 ka, in particular starting at 12.4 ka, following wetter conditions derived from increased monsoon activity and approach of the ocean following sea level rise. The last time period (after 9.7 ka) records increased organic input, related to wet conditions. Between 4.9 - 4.2 ka, high sedimentation rates changes in the diatom assemblage and geochemical indicators indicate further deepening of the lagoon. Finally, after a slight decrease in rainfall from ca. 4.2 ka, the lagoon stabilised to reach modern conditions.

Changes in vegetation and fire were recorded using phytoliths and the hypy fractions. The sequence was characterized by the presence of sedges and woody taxa from the beginning to ca. 9.7 ka, with a minimal contribution from grasses. The redevelopment of the monsoon, between 18.2 and 9.7 ka sustained the dominance of members of Cyperaceae at the site. After 9.7 ka, and particularly after 7.2 ka, wetter conditions sustained a higher proportion of arboreal taxa during the early and middle Holocene, compared to earlier periods. While fire activity is recorded through the entire sequence, activity increased only during the Holocene. Peaks in the accumulation rates of the hypy fraction at 9.3 and 7.4 - 7.1 ka indicate an increase in fire activity (sustained by a higher availability of biomass to burn) also during the early and middle Holocene.

The results suggest that sea level was a defining feature of the climate and development of Sanamere Lagoon since its formation. The position of the ITCZ and monsoon activity were also determinant factors in the development of the lagoon. This thesis also brings new insights into the changes in environmental conditions in northern Australia, a region with great potential for understanding the interactions between climate, vegetation, fire, and humans using the long-term perspective available from the Sanamere Lagoon sediment sequence.

This thesis makes a significant contribution to the understanding of environmental change (vegetation, fire and hydrology) in Australia's monsoonal tropics over the last 33,000 years. It also provides a method for building reliable radiocarbon chronologies in lake sediments, as reliable chronologies are critical for the interpretation of palaeoenvironmental archives in the tropics. Further records of environmental change from tropical Australia, a region that has been continuously inhabited by indigenous Australians for 65,000 years, will enable a more detailed understanding of regional monsoon (palaeo)dynamics and human environment interactions.

Table of Contents

List of Tables

List of Figures

Chapter 1. **Introduction**

1.1. **Introduction**

The tropics are home to approximately half of the world's population and occupy one third of its landmass. Alarmingly, a growing body of evidence shows that these areas will feel the heaviest effects of global warming and climate change (Wheeler and Braun 2013; Frank et al. 2015; Diffenbaugh et al. 2017). Increasing the number of local climatic and vegetation change records from the tropics is required to inform climatic projections and modelling relevant to managing these future changes. These models can contribute to tackling the environmental and economic impact of climate extremes (such as floods, droughts, and related changes in fire activity) in our societies. By lengthening the environmental and climatic data record to thousands of years beyond the historical instrumental record, the uncertainty in projections of future environmental change can be reduced (Kohfeld and Harrison 2000).

In particular, knowledge generated by studying long-term palaeoenvironmental records from northern Australia provides important contextual information about climate variability in the Australian sub-tropics, humid and monsoonal tropics. This information can be used, for instance, to improve environmental management strategies for Australian tropical savannas in the future, given their socio-economic importance for agriculture and pastoralism (Stoeckl and Stanley 2007).

Northern Australia is one of the world's best places to pursue long-term studies regarding human-environment relationships, given that there is evidence of at least 65,000 years of human occupation (Clarkson et al. 2017). Investigating this area of the world contributes to the understanding of the connections between environmental conditions and human societies.

To understand climate variability and sensitivity, knowledge of long-term changes on at least millennial timescales is required. Records derived from lake sediments have proven to be useful across a range of geographical areas to recognize changes in climate, precipitation, and anthropogenic activities (Leng and Marshall 2004; Meyers and Lallier-Vergès 1999). Lake sediments contain geochemical proxies from a range of

sources including the lake body and lake catchment and thus can record environmental and hydrological changes controlled by climate variations and anthropogenic activities (Leng and Marshall 2004). Records derived from lake sediments have proven to be useful across a range of geographical areas to recognize changes in land use, palaeoclimate, palaeoecology and palaeohydrology. Indeed, palaeolimnology, the use of lakes to derive information about the past environmental conditions, is a well-established field of study that makes essential contributions to our understanding of past environmental conditions (Cohen 2003; Catalan et al. 2013).

This project focuses on understanding the environmental history and geochronology of the Sanamere Lagoon in northern Cape York, tropical northern Australia (Figure 1.1). Two main considerations guided the development of the project: 1) Geochronology: to provide the information upon which to base optimized dating protocols for tropical lake sediments and 2) Environmental change and palaeohydrology: to create a high-resolution record of environmental change (sedimentological, vegetation and fire) for a region located in the tropical savannas of northern Australia.

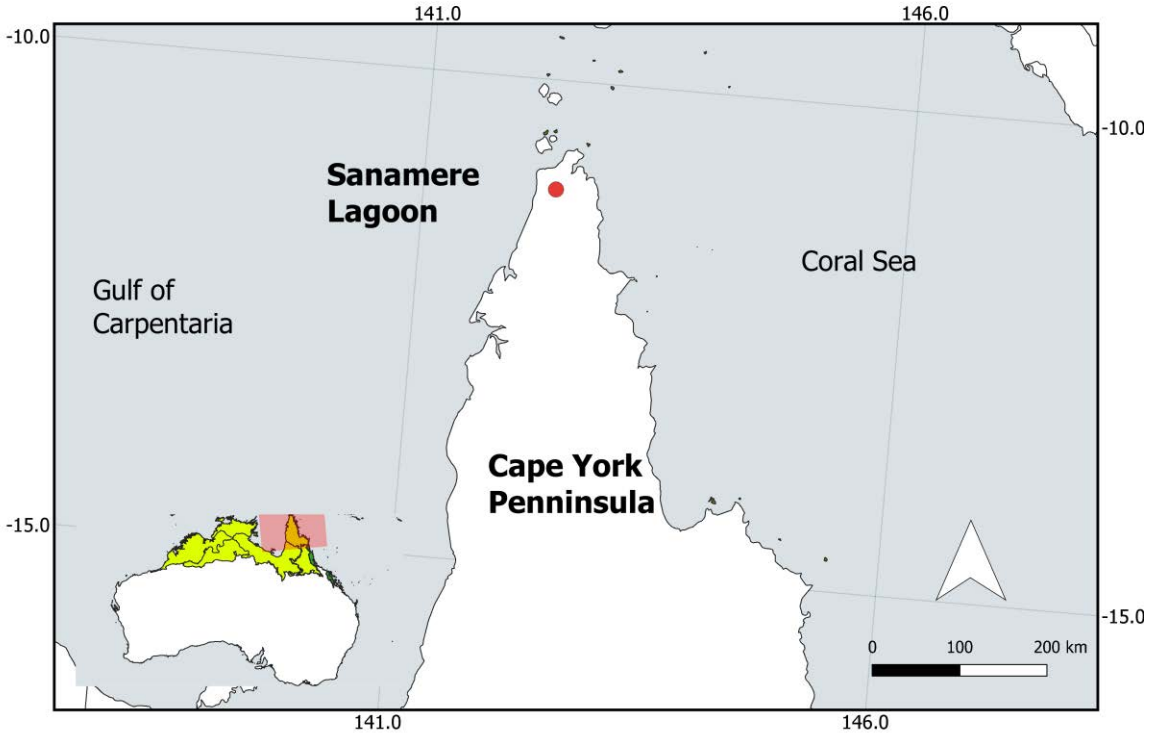

Figure 1.1 Sanamere Lagoon in Cape York Peninsula. Location of moden tropical savannas in Australia (yellow) and wet tropics (green) (based on Dinerstein et al. (2017)).

1.2. **Thesis aims**

1.2.1. **Geochronology**

Aim 1. Develop a protocol for building robust chronologies in tropical lake sediments using radiocarbon dating

Precise and accurate radiocarbon ages up to the radiocarbon dating limit of ~ 50,000 years (and the chronologies derived from dating) are critical for testing hypotheses of synchronous (or asynchronous) archaeological, environmental and climatic change and the interpretation of proxy records derived from lake sediment sequences. Although there have been many studies investigating methods for improving chronologies from lake sediment archives, most research attempting to identify the material most appropriate for dating has focused on temperate and Arctic regions. A single exception deals with peat cores in the tropics Indonesia, where pollen was found

to be the most reliable dating fraction (Wüst et al. 2008). The application of hydrogen pyrolysis (hypy) pretreatment to isolate stable polycyclic aromatic carbon ("Hypy fraction") for dating also appears to offer a viable approach to constructing chronologies from tropical organic spring deposits in north Western Australia, where other materials have been demonstrated to be unreliable (Field, Marx, et al. 2018). Importantly, no previous studies carried out in tropical lakes have tested a diversity of carbon fractions in the same sediment core, as the present study is proposing, to optimize a dating protocol to produce robust lacustrine chronologies.

Previous palaeoenvironmental studies have reported significant discrepancies between ages for different carbon fractions in lake sediments from the same depth. For example, in boreal and Arctic regions, lake sediment, wood and charcoal were found to be older than other macrofossil types, usually by several hundred years (Oswald et al. 2005). Discrepancies have also been found within different types of macrofossils, with some more prone to an apparent 'reservoir effect'. This effect can result in anomalously old radiocarbon ages of the dated samples by introducing pre-aged carbon (Alves et al 2018). For example, wood and charcoal were found to be older than other plant remains in some temperate ecosystems. A possible explanation is the slower decomposition and longer terrestrial residence time of these materials (Oswald et al. 2005).

Additionally, several studies have demonstrated that there are significant uncertainties associated with dating bulk sediment (Björck et al. 1998; Wüst et al. 2008). Although organic-rich sediments from lake deposits provide diverse materials to analyze for radiocarbon dating, there is considerable uncertainty regarding which organic fraction yields the most reliable radiocarbon ages and how these 'ages' relate to the actual time of deposition of the material. In addition, the relatively hot and moist conditions that characterize much of the tropics influence the preservation of materials that could be analyzed in these settings. For instance, aberrant radiocarbon results could be linked with poorly preserved or degraded charcoal, for example when the combustion yields are lower than usually expected (50-60 carbon % by weight) (Higham et al. 2009). Also, the materials used for radiocarbon dating are prone to contamination and reservoir effects, which are known to cause serious deviations in the obtained ages, relative to age of deposition. Therefore, as well as providing a robust chronology against which to interpret the record of environmental change at Sanamere Lagoon, the creation of more

effective and efficient pretreatment procedures for radiocarbon analyses is relevant to improving laboratory efficiencies, in turn lowering costs and increasing throughput.

The Sanamere Lagoon sequence offers a best case, tropical opportunity to a) investigate the consistency of the age models derived from the different carbon fractions that were radiocarbon dated, and b) study the causes of potential inconsistences in the radiocarbon dates and correlate the dates with potential disturbances/events along the length of the core.

Research questions:

How do the radiocarbon dates derived from diverse carbon fractions relate to each other within individual samples, and over time in multiple samples along the core?

How and why do reservoir and contamination effects manifest themselves in the radiocarbon measurements of different organic fractions?

How consistent are differences observed between the dated carbon fractions?

How might differences between the 'true' and 'observed ages' be minimized by selection and dating of a particular 'ideal' fraction?

1.2.2. **Environmental change and palaeohydrology**

Aim 2. Reconstruct past climatic variability in northern Cape York Peninsula using the Sanamere Lagoon sediment sequence

Aim 3. Reconstruct past vegetation and fire activity in northern Cape York Peninsula using the Sanamere Lagoon sediment sequence

Although Australia has been the target of large projects (OZ-INTIMATE, Australian INTIMATE) aiming to develop a climate event stratigraphy for the region (Reeves et al. 2013), there are very few records of past terrestrial environmental change of any time depth for the Australian tropics outside the Atherton Tablelands in the wet tropics (refer to chapter 2 for more details about past environmental records). Most (inland) pollen and charcoal records have focused on wetter parts of the region that

contain extensive, permanent lakes and swamps or are from the marine realm, in association with marine environmental proxies.

For each record, the calibrated chronology is used (thousand calibrated years before the present) and referred to as “ka” throughout. Continuous records of environmental change are scarce in the tropical savannas beyond the Holocene, given the poor preservation of proxy material due to the ephemeral nature of most lakes, due to seasonality of rainfall. A few studies in the Pilbara region of northwestern Australia and the Northern Territory have yielded some insights into the hydroclimate of the region (Denniston, Wyrwoll, Polyak, et al. 2013; Rowe et al., 2020, respectively). Most research has focused on building Holocene pollen records, such as in Groote Eylandt in the Gulf of Carpentaria (Shulmeister 1992; Shulmeister and Lees 1992; Shulmeister 1999), Vanderlin Island (Prebble et al. 2005), Mornington Island (Moss et al. 2015), Bentinck Island (Mackenzie et al. 2017), and northern Cape York (Rowe 2007, 2015). However, the only studies focusing in palaeohydrology in tropical Australia have been pursued in Lake Carpentaria (Jones and Torgersen 1988; McCulloch, De Deckker, and Chivas 1989; Reeves et al. 2007, 2008; Torgersen et al. 1985; Devriendt 2011). Other studies have reconstructed the terrestrial palaeoclimate records, which have been interpreted as providing indirect evidence of palaeohydrological conditions. More recently, palaeoecological records have also emerged from the Kimberley region in Western Australia (Field et al. 2017; Denniston, Wyrwoll, Polyak, et al. 2013) (see section 2.3.2).

During the last 33 ka, important environmental changes have influenced northern Australia (e.g. end of the last glacial period, reactivation of the monsoon, sea level changes, and the onset/intensification of El Niño-Southern Oscillation, ENSO). These changes impacted on and altered the vegetation composition and fire regime across the region. However, most terrestrial studies on this region have provided only Holocene records, covering ca. 12 ka or less (chapter 2). Marine records are longer compared to terrestrial records and have provided information about climate and vegetation in the tropics of Australia over the last 30 ka (Moss and Kershaw, 2007). However, these records are low in resolution, and they do not necessarily represent terrestrial conditions on the Australian continent. For instance, the significant changes in sea-level and coastline proximity over this time frame suggest that we have limited knowledge of the multiplicity of factors that may have influenced the climate conditions over thousands of years. Moreover, marine records are primarily based on pollen (which could be sourced

from different regions), and this variety of possible sources indicates these records may not represent local conditions. More terrestrial records, covering past glacial and interglacial periods contribute to track and better understand the dynamics between climate, vegetation, fire, and the local expressions of the environmental changes that occurred in the region.

While data for northern Australia is becoming more spatially and temporary refined, debates still remain on the climatic and vegetation responses that took place during the Last Glacial (31 ka - 22 ka) and Last Glacial Maximum (LGM) (22 ka - 18 ka) periods in the Australian tropical savannas (Reeves et al. 2013). For instance, regional syntheses indicate that drier, cooler conditions and low levels of carbon dioxide during the Glacial and LGM periods limited vegetation growth under these climatic conditions (mainly shrubs and herbs), but recent studies suggest that the local climatic responses were highly variable (Tierney, Russell, and Huang 2010). During the LGM, diverse proxy data reveal prolonged low temperatures and phases of extreme dryness (Rowe et al. 2019). For instance, several wet episodes were initially proposed to have taken place during the Glacial in northern Australia (Nott and Price 1994; Nott, Price, and Bryant 1996), but recently the ages were declared uncertain (May, Preusser, and Gliganic 2015). The available information for the Glacial and LGM periods in the northern Australian savannas is particularly limited, with interpretation further hindered by the low resolution and chronological uncertainties in the records (Marlon et al. 2013), along with the observation that there are as yet no studies of vegetation and fire patterns for these periods. However, most studies agree that after the LGM, biomass increased, and vegetation became more diverse in composition as precipitation, temperature and CO_2 increased (Clark et al. 2012). During the early Holocene, evidence from different sites suggests an increase in the frequency of fires starting at around 11 ka (Field, Tyler, et al. 2018) and the establishment of modern vegetation during the middle Holocene (Reeves et al. 2013; Haberle 2005; Field, Tyler, et al. 2018; Stevenson, Dodson, and Prosser 2001).

Fire has been recognised as a powerful ecological force, and the need to study fire across temporal scales has been highlighted recently (McLauchlan et al. 2020). The Australian tropical savannas are the most fire-prone regions in Australia (Bowman et al. 2010; Russell-Smith and Yates 2007; Russell-Smith and Edwards 2006). Previous studies in these ecosystems have determined rainfall seasonality, biomass growth and

human interventions to be the modern drivers of fire regime (Gill et al. 2000; Russell-Smith, Ryan, and Durieu 1997). Conversely, fire influences the climate system by releasing carbon (Bowman et al. 2009). Records of the long-term fire and vegetation dynamics of savanna ecosystems constitute an important resource from which to understand modern patterns of ecological change, and thereby improve vegetation and fire management practices in the region, along with providing information to aid the validation of vegetation change models (Power et al. 2008). However, little is known about the dynamics of vegetation and fire Australian tropical savannas in the past (Reeves et al. 2013).

Fire records older than ~12 ka are scarce in the seasonal tropics of Australia. As such, generalizations of the past biomass burning patterns in the region are based on records derived from the wet tropics (Atherton Tablelands, Papua New Guinea and Indonesia) (Haberle, Hope, and van der Kaars 2001; Mooney et al. 2011). These studies suggest that fire was infrequent over the Glacial and pre-glacial periods, with sites in the humid tropics (where information is available) showing peaks in biomass burning around 15 ka, probably a result of an increase in available woody fuel and increases in temperature and precipitation around this time (Haberle, Hope, and van der Kaars 2001; Mooney et al. 2011). In northern Australia, the records from Big Willium (7.2 ka) (Stevenson et al. 2015) and Girraween (9.7 ka and 7.7 ka) (Rowe et al. 2019) suggest increased burning during the middle Holocene. Variable fire patterns have been described for the Late Holocene, based on records from the Kimberley, northern Australia and the wet tropics (Rowe 2007, 2015; Field, Tyler, et al. 2018; Haberle 2005). Some studies have argued that this pattern in the later Holocene reflects an increase in climate variability associated with more active ENSO cyclicity (Mooney et al. 2011; Kershaw, Bretherton, and van der Kaars 2007).

There is a pressing need to extend our knowledge of the environmental dynamics of the seasonally dry parts of Australasia, particularly the Australian savannas that cover much of the Australian tropics (Figure 1.1). More research on the savannas is required to understand their response to climate change and variability in the magnitude of local to regional responses to climate forcing. These differences cause local signals to mask regional or continental scale responses to climate. For example, while in northern Cape York total annual rainfall has increased since 1950, regions along the southern Gulf of Carpentaria have become drier (BOM 2018).

Research questions:

Does the Sanamere sequence document periods of increased/decreased water availability in the past?

Is there palaeolimnological evidence to suggest past hydrological changes?

How do the results of this research relate to the palaeoclimate changes recorded elsewhere for northern Australia (e.g. wetter mid-Holocene (after 9 ka), aridity in early Holocene?

Does the Sanamere sequence document periods of changed fire and vegetation? And if so, how do these changes relate to hydrological change?

1.3. **Organization of the Thesis**

This thesis is organised according to the aims presented above. After the introductory first chapter, the second chapter presents the specific methodologies and workflow used in this PhD project, along with a general description of the study area and site. In addition, chapter 2 presents a literature review of the current knowledge of past climate, vegetation, and fire on Cape York Peninsula in Australia. In the third chapter, the sedimentology and stratigraphy of the Sanamere sediment core is described, and this forms the foundation for the subsequent chapters. The fourth chapter addresses aim I and contains the results of a comparison of several carbon fractions and pretreatments to determine the most reliable chronology for Sanamere Lagoon. Chapter 5 analyses the changes in climate and hydrologic conditions inferred from the lagoon sediment proxy records, while chapter 6 describes the vegetation and fire history of the area. Chapter 7 discusses the implications of the findings from chapters 3 to 6 and provides suggestions for future work (Figure 1.2). Each chapter includes a chapter summary at the end to facilitate the reading of the thesis.

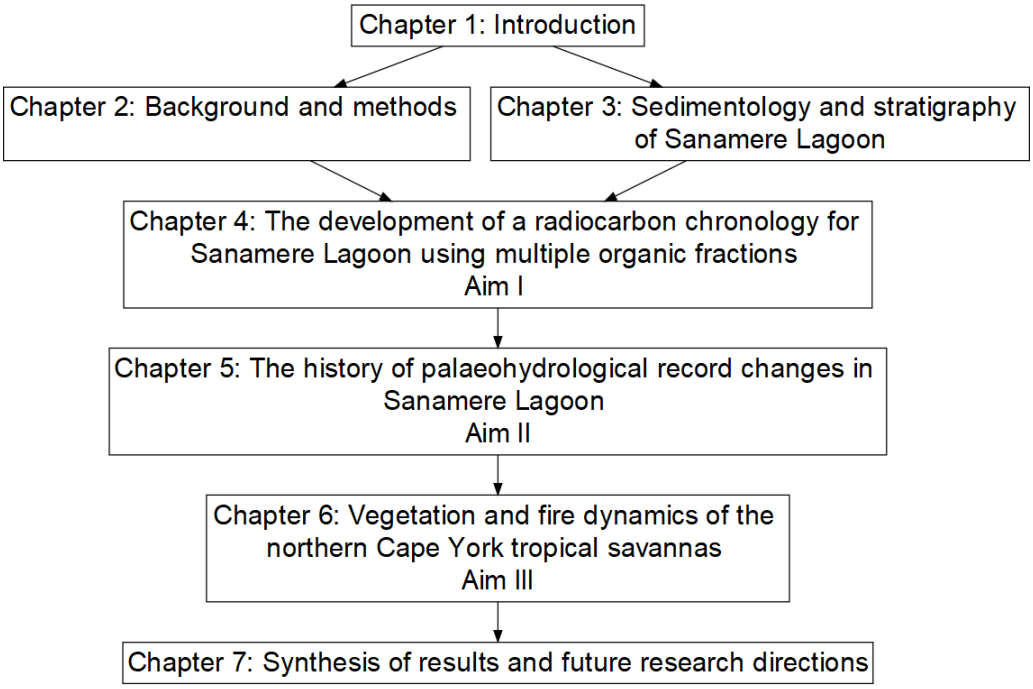

Figure 1.2. Flow chart of the thesis structure, linking thesis chapters to aims

1.4. Chapter 1 summary

Three basic aims are essential to understanding the environmental history of northern savannas of Cape York Peninsula: (1) Build a reliable chronology based on radiocarbon dating (2) Reconstruct the changes in palaeohydrology, and (3) Reconstruct the changes in vegetation and fire reflected at the site.

These aims elaborate upon two major themes: the standardisation of protocols to build radiocarbon dating chronologies and the understanding of past environmental changes. The research addresses these themes by analysing a lake sediment core from Sanamere Lagoon in Cape York Peninsula. Next, chapter 2 contextualizes the research question through a description of the study site and a review of the literature on past environmental change of Cape York, and the methodological perspectives that inform this research.

Chapter 2. **Background and methods**

This chapter includes a description of the study area and its modern and past climatic contexts. In turn, this chapter introduces methods used in the development of this thesis, with emphasis on the two main components (geochronology and environmental change).

2.1. **Study area**

Cape York Peninsula is located at the northernmost point of Queensland on the north-eastern coast of Australia. It lies between 10°S and 16°S and is one of the monsoonal regions of Northern Australia, along with the Kimberley and the Top End (Arnhem Land). The updated Koppen-Geiger climate system (based on long-term monthly precipitation and temperature station time series) classifies most of the Peninsula as a strongly seasonal tropical climate (tropical savanna), with just a small area of wetter Am (tropical monsoon) environment on the eastern coast (Peel, Finlayson, and McMahon 2007). Annual rainfall varies from 800 mm in the central-southern part to over 2000 mm near the Iron Range (Figure 2.1). Approximately 80% of the average annual rainfall falls during the four months from December to March (the so-called monsoonal 'wet season'). Temperatures are generally warm to hot, with means ranging between 21.5 °C and 30.9 °C across the region. Maximum temperatures can be over 40 °C in summer (Environment Science Services 1995).

The vegetation of Cape York Peninsula is dominated by *Eucalyptus* spp. woodlands, open woodlands, and open forests, which occupy 64 % of the area. The next most extensive vegetation group is the low open-woodlands, low woodlands, and tall shrublands, dominated by *Melaleuca* spp. (14.2 % of total area). Grasslands (6.1 %), rainforests (5.6 %) and heathlands (3.3 %) are the next most extensive vegetation types (Neldner et al. 1995; Fox et al. 2001) (Figure 2.2).

The region has an abundance of internationally and nationally important natural resources, including remnant rainforests, rich mineral reserves (bauxite, gold, kaolin, silica sand), and several rivers of high ecological significance, high biodiversity, and a strong Indigenous culture (Hitchcock et al. 2013).

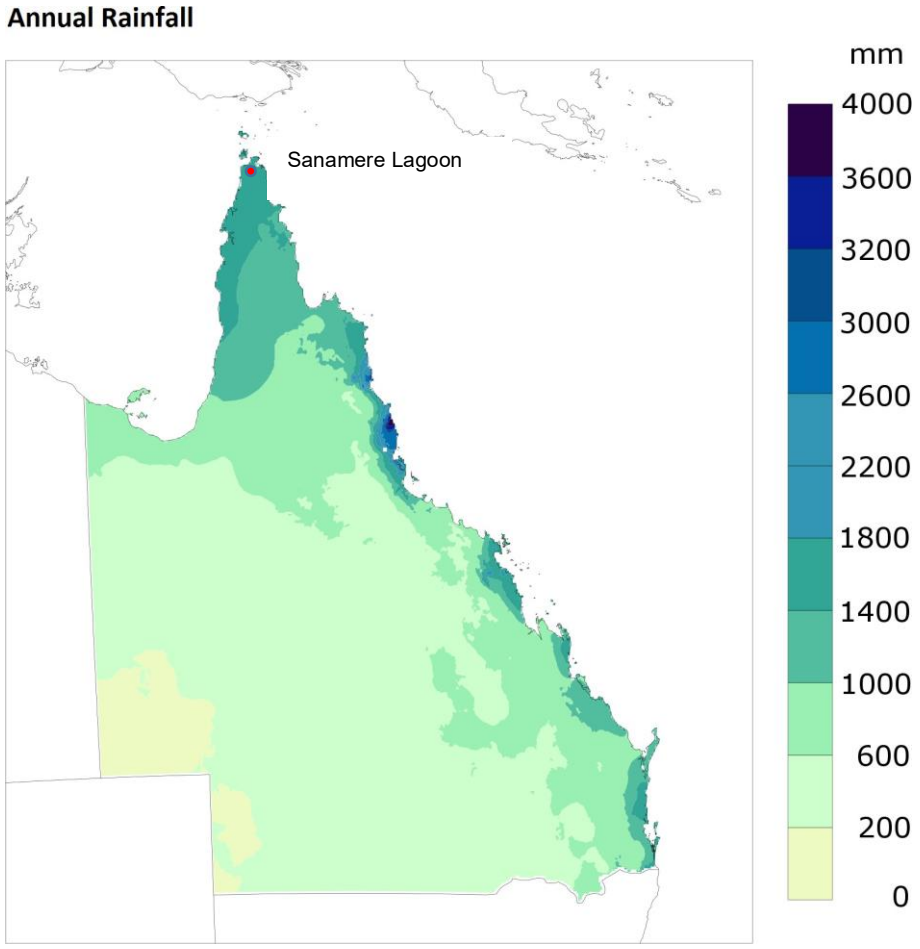

Figure 2.1. Average annual rainfall, 2012–2016. Source: Bureau of Meteorology Australian Water Availability Project gridded monthly data. Plotted by the Queensland Government Department of Environment and Science. Available at https://www.stateoftheenvironment.des.qld.gov.au/climate/climate-observations/annual-rainfall

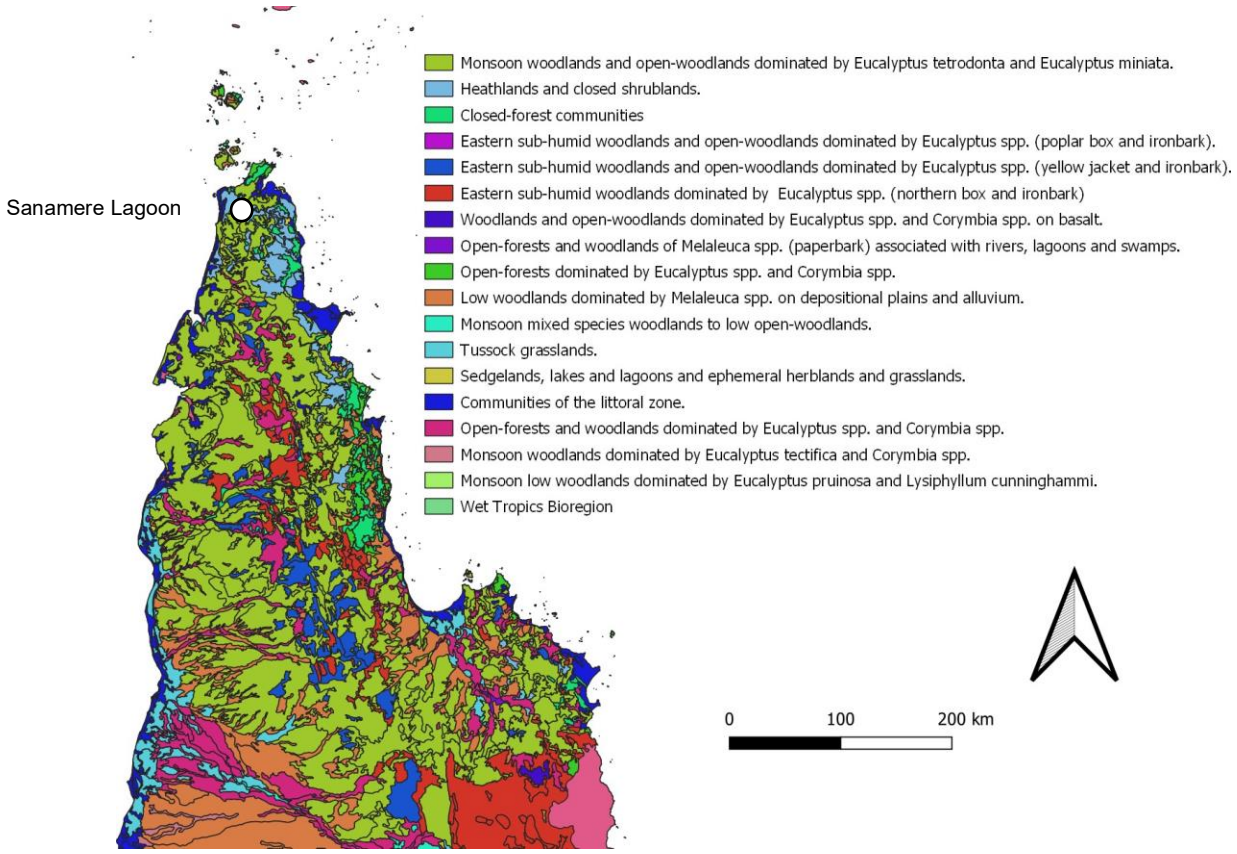

Figure 2.2. Cape York Peninsula vegetation (after Environmental Protection Agency, Brisbane and the Cooperative & Research Centre for Sustainable Development of Tropical Savannas, 2001).

2.2. **Study site**

Sanamere Lagoon (11.123°S 142.359°E; 15 m asl) is located close to the northern tip of Cape York Peninsula and is part of the Apudthama Land Trust Area, classified as Aboriginal Freehold land and managed under the Northern Peninsula Area Regional Council. The lagoon is 1 km north of the W-E flowing perennial Jardine River (Figure 2.3). The climate of the region is monsoonal with 88 % of the annual 1753 mm rainfall falling between December and April with a mean annual temperature of 27 °C (BOM 2018). Winds are predominantly from the north-northwest and southeast in January and July, respectively (BOM 2019) (Figure 2.4). Sanamere Lagoon is considered a sub-coastal wet heath swamp, and a palustrine system (a wetland with more than 30 % emergent vegetation) (Environment & Science 2018). Sanamere Lagoon is also referred as of value as a “wilderness wetland area” (Abrahams et al. 1995). The Anggamudi (also known as Angkamuthi), Wuthahti (alternatively Wuthathi) and Yadhaigana (alternatively

Yadhaykenu) people are the traditional owners of the Jardine River catchment (Australian Institute of Aboriginal & Torres Strait Islander Studies, 2020).

Although most lakes dry out in this region during the dry season (May - November), the dataset (Mueller et al. 2016; Commonwealth of Australia 2018) indicates that the deeper parts of Sanamere Lagoon have been permanently covered by standing water for the last 35 years, despite periods of significantly below average rainfall in this period (Figure 2.5). The water depth during the dry season is 1.2 m for most of the lake. At this level, several relict dune features are exposed, dating from the time of lagoon impoundment. The lake was probably formed as a result of the collapse of laterite karst to form a sinkhole-like depression below the local water table (Grimes and Spate 2008). During the wet season, the dune features are largely submerged and the lake outflows over the Jardine River.

Sanamere is in an enclosed basin surrounded by higher elevation land, with the highest point (57 m a.s.l.) to the north-northeast of the lagoon, close to the current Bamaga Road (Geoscience-Australia 2015). Based on topography, Sanamere Lagoon has an approximate catchment area of 9 km^2, with the lowest overflow point at ~17 m a.s.l. to the west of the lagoon (Figure 2.6).

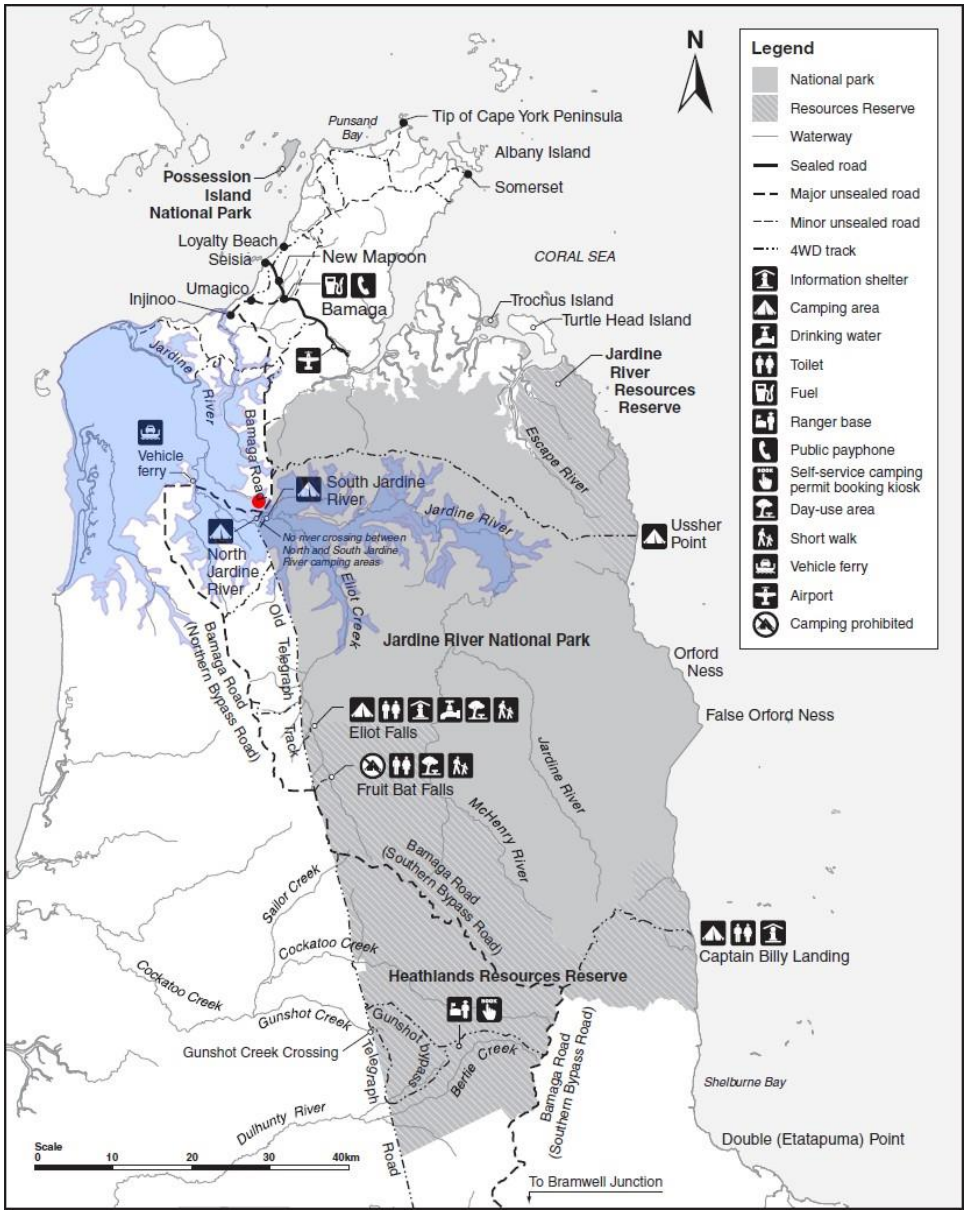

Figure 2.3. Map of the Jardine River National Park, Jardine River Resources Reserve and Heathland Resources Reserve, with Sanamere indicated in red and the Jardine River Wetlands Aggregation shaded blue (courtesy of Emma Rehn).

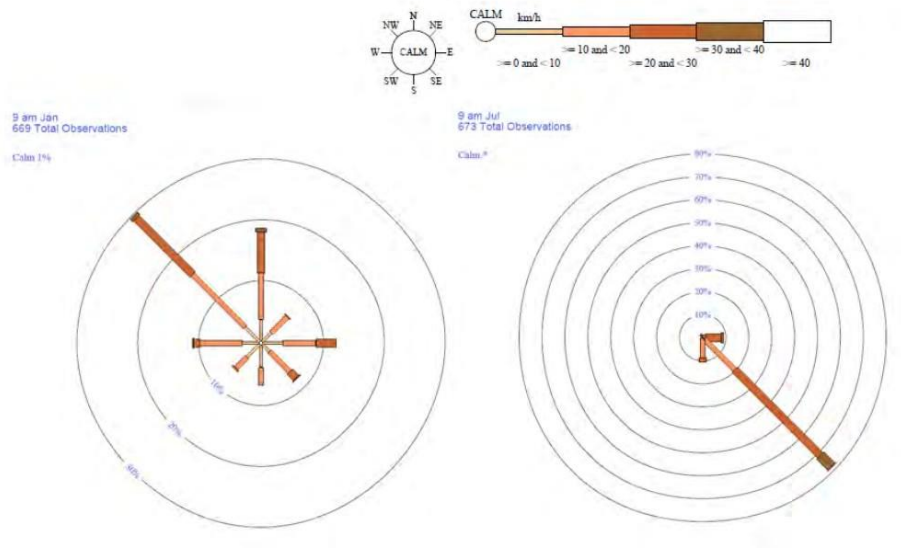

Figure 2.4. Average wind direction and speed 1995-2017, measured at 9 am in in January (left) and July (right), from Horn Island weather station (~ 50 km north of Sanamere Lagoon) ((BOM 2019)

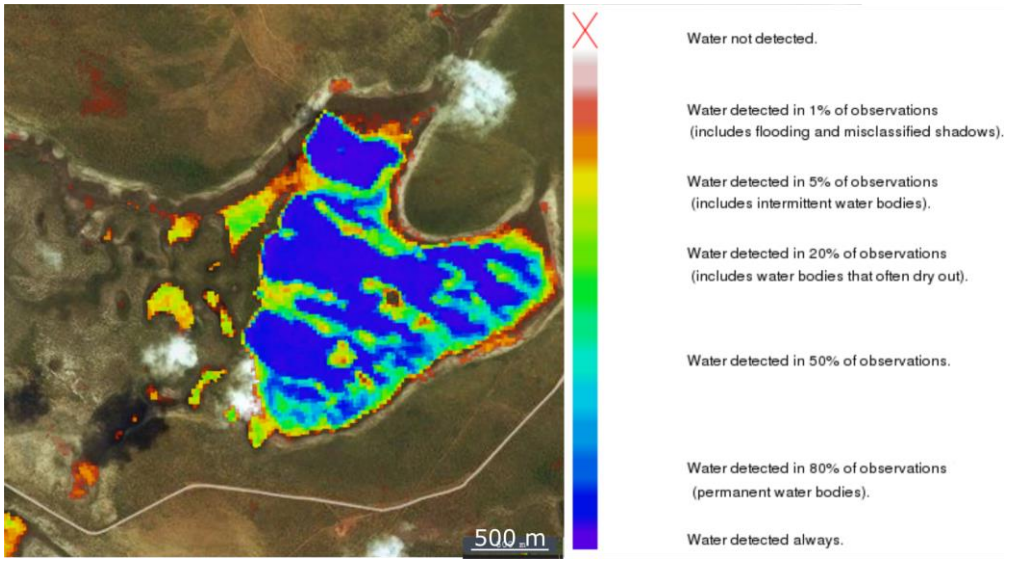

Figure 2.5. WOfS data showing permanency of water in the lagoon since 1986 with blue denoting areas permanently covered, possible relict dune features shown as low permanency areas, exposed in the dry season (Commonwealth of Australia 2018)

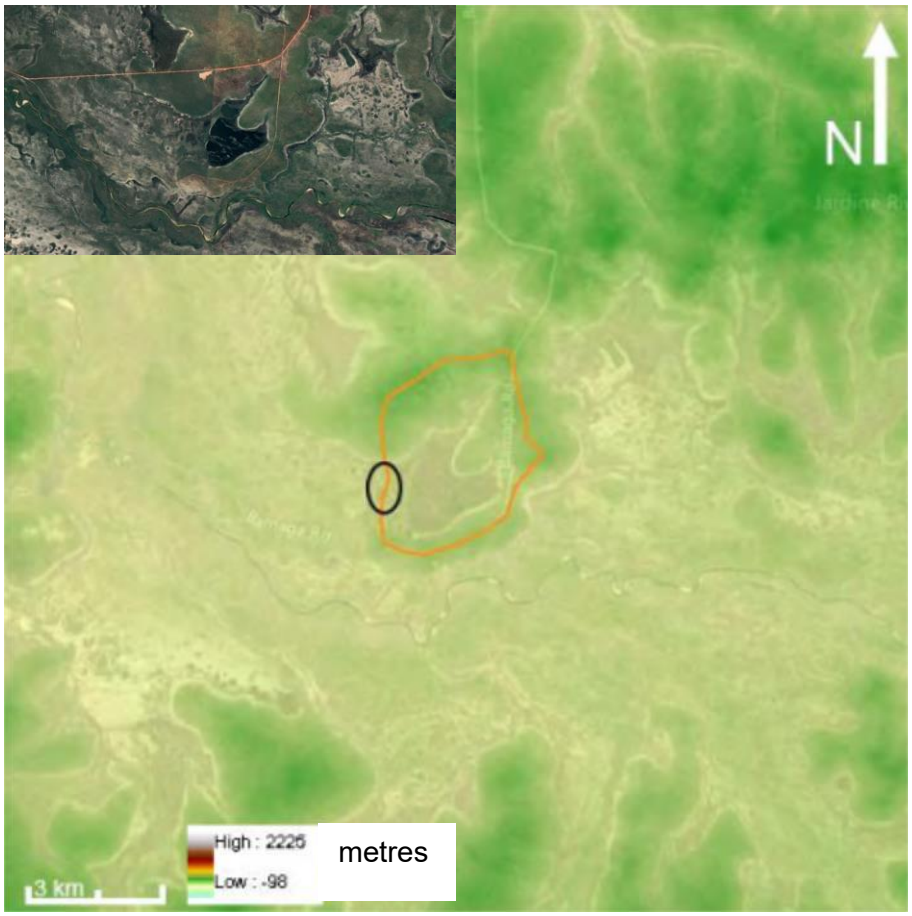

Figure 2.6. Digital elevation map of Sanamere Lagoon and surrounds, with the approximate catchment area of the lagoon marked in orange and western low point (outlet) circled in black. Darker green indicates higher elevation (diagram courtesy of Emma Rehn).

2.2.1. **Geology and lake formation**

The geology of the watershed is represented by middle Jurassic to Early Cretaceous Helby Beds (Geology 1:250,000 sheet SC54-15) (*Australian Geoscience Information Network* 2020), which are composed by clayey quartzose sandstone and pebble conglomerate, not underlain by carbonate-bearing lithologies. The lake is likely to have formed by a collapse into cavities formed by dissolution of underlying rock and it is an example of 'laterite karst' (Grimes and Spate 2008).

2.2.2. **Vegetation**

The vegetation around the lake edge is dominated by sedgeland, open-heaths, dwarf open-heaths and woodlands. Between the water's edge and 50 m distance sedges such as *Eleocharis sphacelate* dominate the landscape (Figure 2.7). Between 50 m and 300 m distance the vegetation transitions to an open, diverse heath and shrubland, incorporating species of, *Neofabricia*, *Asteromyrtus*, *Baeckea*, *Jacksonia*, *Hibbertia*, *Thryptomene*, *Allocasuarina* and *Grevillea* (Figure 2.8). At 300 m from the lake there is another transition to *Eucalytus* woodlands, especially *Eucalyptus tetrodonta* (Figure 2.9) (Neldner et al. 1995). Smaller woodland sub-canopy trees are common and include *Acacia*, *Grevillea glauca* and *Grevillea pteridifolia* as well as *Livisonia* palm, with *Asteromyrtus* present as shrub. *Banksia* and *Casuarina* are present in wetter low-lying areas. Grasses dominate the ground cover in this area (Poaceae) and leaf litter is greater than that found in the heathland.

The term 'open' is actually a quantified term (Specht, 1981). The thesis followed these vegetation structural guidelines and terminologies in the field observations. So, 'open' refers to between 30-70% foliage cover, whether in a forest or heathland or grassland. The openness itself at Sanamere is a legacy of both the seasonal climate, the poor soils (in organics/nutrients and moisture capacity) as well as historical into modern management schemes, and including managed fire (= a mix of natural and human).

Figure 2.7. Vegetation at the Sanamere Lagoon waterline, comprised of sedges and scattered *Pandanus*

Figure 2.8. Open heathland vegetation 50 metres from the waterline

Figure 2.9. *Eucalyptus* woodland at 400 m (right) from the waterline

2.2.3. **Soils**

Sanamere's catchment is characterized by deep bleached uniform yellow earthy sands with poor drainage, flooding and low fertility. Soils are primarily derived from sandstone (Kandosols and Tenosols) (Biggs and Philip 1995). Tenosols on undulating rises of sandstone comprise the largest unit within the Heathlands Landscape. Both the Kandosols and Tenosols are infertile.

2.2.4. **Fire**

Northern Australia is the most fire-prone area of Australia, with around 250,000–450,000 km^2 burnt each year (Russell-Smith 2016). Australian savannas are characterized by low nutrient soils and a seasonal wet/dry climate. They exist across highly connected landscapes, and with very few topographic barriers, intense 'wild' fire regimes are frequent and large in scale (Stevens et al. 2017). These fires are one of the main drivers of vegetation dynamics and climate in the area. For example, the role of fire in controlling the balance between grasses and woody vegetation in savannas have

been widely studied (Lehmann et al. 2011), and most literature suggests that frequent fire reduces woody growth rates and tree density, and creates an environment more suitable for C_4 grasses (Lehmann et al. 2011). However, recent studies debate the role of fire regimes to reduce canopy vegetative cover and argue that this role is much more limited in impact than often assumed (Veenendaal et al. 2018). In palaeoecological research, burning has also been related to the opening of woodland (canopy and subcanopy) and creating patches of different plant communities (Rowe 2015).

In the 18-year period spanning 2000-2019, the area immediately surrounding Sanamere Lagoon (catchment and beyond) burned on average every 3 to 7 years (Rangelands Fire Information 2020). Fire scars recorded in this period over the surface of the lagoon (Figure 2.10) are likely a result of error in the determination of fire scars (Rehn 2020). However, fire scars that extend substantially beyond the water surface may be assumed to represent real scars.

Most fires occur each year during the later dry season (July - November). During April to July, fires in northern Australia are associated with lower air temperatures, higher moisture content, burning of smaller areas and may leave unburnt patches. Fires occurring between August and November are typically high intensity and burn large areas (Evans and Russell-Smith 2020). Australian Aboriginal people have used fire to manage the landscape for millennia. However, in the early 20th century the removal of Indigenous people to missions might have reduced intensive management of fire regime (Cooke et al 2009).

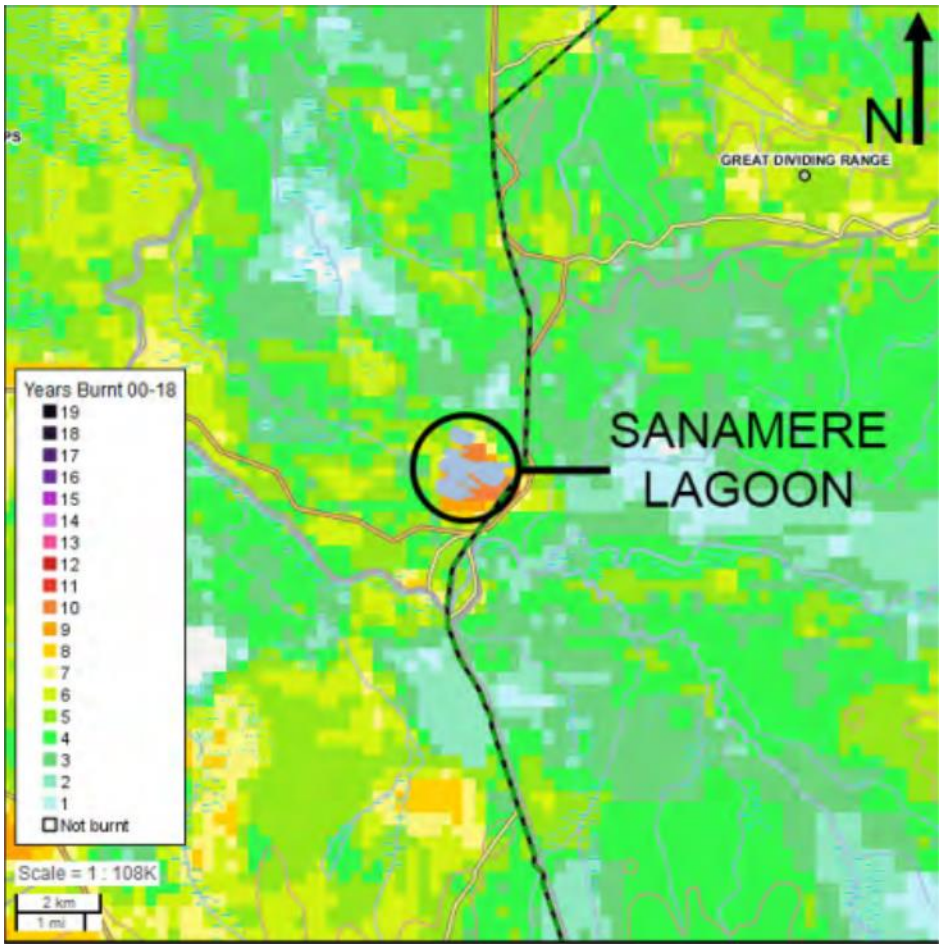

Figure 2.10. Number of years areas around Sanamere burned in the 10 years 2000 – 2018 (Rangelands Fire Information 2020)

2.3. Climatic context

2.3.1. Modern climate

The climate of the northeastern Australia's tropical savannas is largely determined by the annual movement of the monsoon system. Along with the monsoon, the southeasterly trade winds along the east coast during the dry season define most of the area (Shi et al. 2016). The monsoons are active from about November to March and are followed by a distinct seasonal drought for the remainder of the year. Tropical cyclones that form over the adjacent ocean also influence the climate of the Peninsula and cause extreme episodic rainfall events during the wet season. The main driver of Australian rainfall variability is ENSO in the Pacific Ocean (Risbey et al. 2009). However,

the Indian Ocean dipole (IOD) and Madden–Julian oscillation (MJO) also contribute to rainfall variability in northern Australia (BOM 2010).

The influence of the monsoon is controlled by the position of the Intertropical Convergence Zone (ITCZ) and the Indo-Pacific Warm Pool (IPWP). Their impact in the climate system is determined by the oceanic circulation system. For instance, the Indo-Pacific Warm Pool provides a large moisture source for the Northwest Monsoon and is an important component of the coupled ocean-atmosphere processes that gives rise to ENSO (Kershaw and van der Kaars 2012).

The monsoon system is divisible into three spatial components: the Northwest Monsoon that derives its moisture from the equatorial seas to the north and is considered to be 'pushed' by the Asian winter monsoon; the Pseudo-Monsoon of northwestern Australia that is driven by moist winds emanating from the Indian Ocean; and the Quasi-Monsoon that derives much of its moisture from easterly Pacific Ocean winds (Gentilli 1971). The Australian monsoon alternates between two seasonal phases linked to wind direction. In the winter phase, easterly trade winds bring dry conditions, and particularly the northern Australian region experiences an almost rainless dry season of about 7–8 months. In the summer, westerly winds bring sustained rainy conditions, torrential rains and, cyclones (Figure 2.11). As the two lesser influence climatic systems, information on IOD and MJO processes can be found via Risbey et al. 2009.

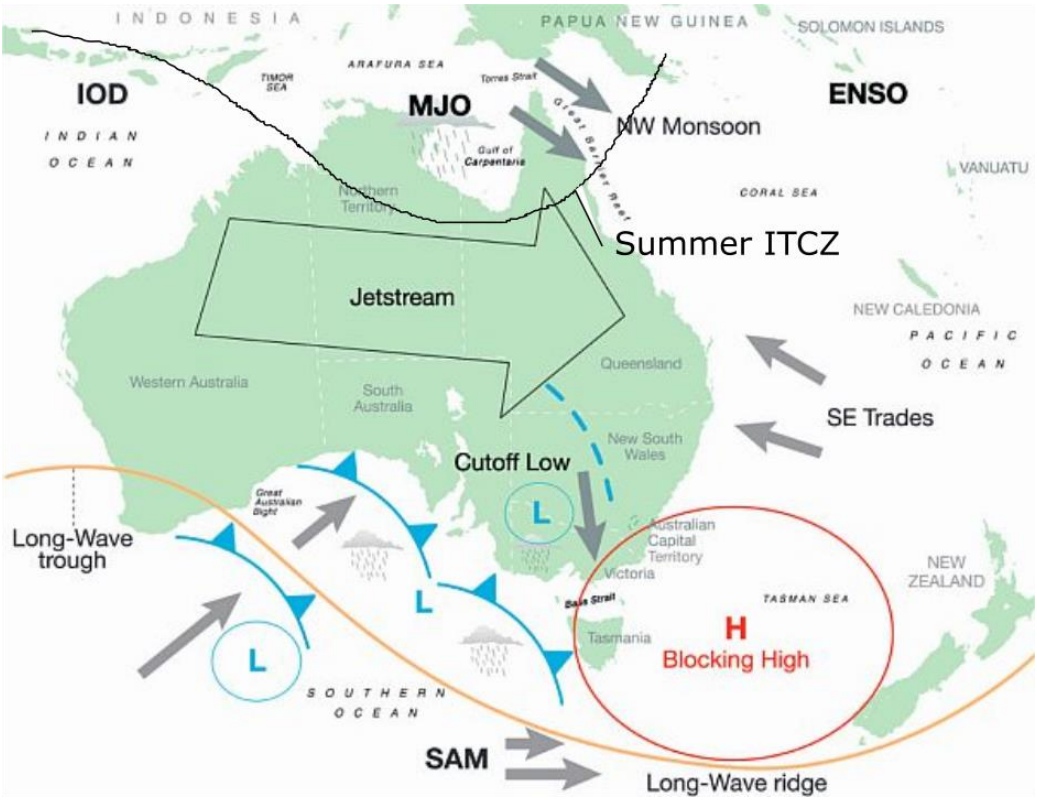

Figure 2.11. Influences on modern Australian climate. Modified from Risbey et al. (2009). © American Meteorological Society. Used with permission.IOD= Indian Ocean Dipole; MJO= Madden-Julian Oscillation

2.4. Past climate, vegetation, and fire

The following section summarises the current knowledge of past climate in the study area (covering ~ 800 km around the region), following the chronological divisions proposed by Reeves et al. (2013) and Burrows et al. (2016). The Glacial period is considered to span 30 ka – 18 ka, including the LGM (21 ka –18 ka); the Deglacial is considered to span 18 ka – 12 ka; and the Holocene is considered to begin at 12 ka. The Holocene is further split into three classifications: early (12 ka – 8 ka); mid (8 ka – 4 ka); and late (4 ka – present). Late Marine Isotope Stage 3 (MIS 3) extends from ~ 50 ka – 29 ka and Late Marine Isotope Stage 3 (MIS 2) from 30 ka - 14 ka. Where the text refers to climatic changes with no specific values, for example “warmer” or “drier”, these changes are in relation to the previous time period.

As mentioned in chapter 1, the past climate information available for northern Australia is limited (including monsoonal and ENSO dynamics). Besides the monsoon system, the climate of Cape York Peninsula was influenced by changes in sea level (section 2.3.3). Changes in the strength of the monsoon has been documented by studies in adjacent regions (Jiang et al. 2015; Denniston et al. 2017; Yan et al. 2018), along with past changes in sea level and shorelines. However, the data available for several sites in the region are not representative of the entire area. Near Cape York, the longest records (beyond the Holocene) are derived from upland areas to the south (Atherton Tablelands) or marine records which experience local environmental conditions that are not necessarily representative of lowland sites (Shulmeister and Lees 1995) (Figure 2.12, Table 2.1).

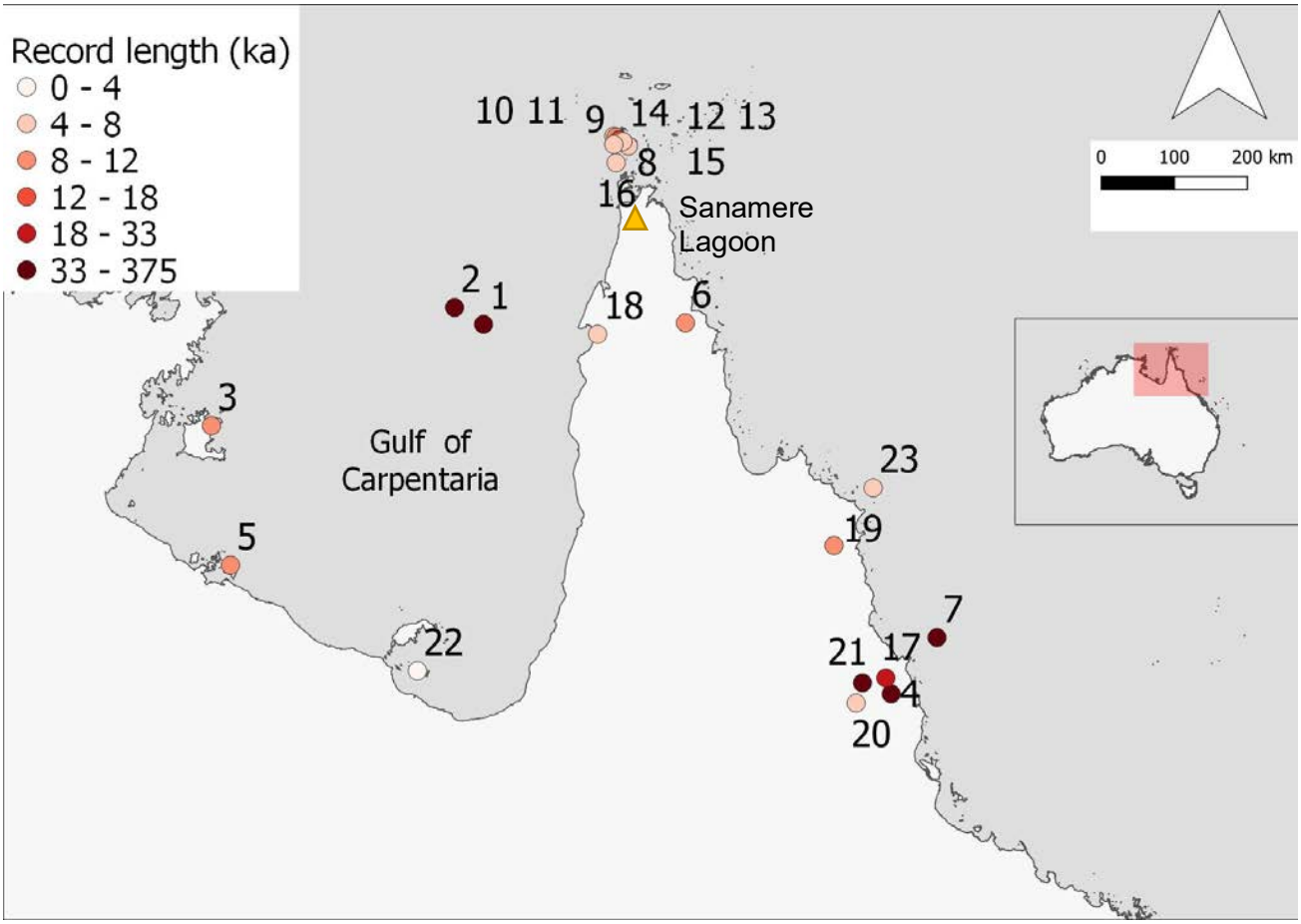

Figure 2.12. Location of sites mentioned in the text, with a focus on Cape York and surrounding areas (refer to Table 2.1 for details)

Table 2.1. Latitude, longitude and length of the past environmental records discussed in the text

Number	Site	Latitude (decimal degrees)	Longitude (decimal degrees)	Type	Length (ka)	References
1	Lake Carpentaria GC2	-12.52000	140.3500	lacustrine	36.00	Torgersen et al., 1985, 1988
2	Lake Carpentaria MD32	-12.30000	139.9700	lacustrine	130.00	Chivas et al., 2001; Reeves et al., 2008; Devriendt, 2011
3	Four Mile Billabong, NT	-13.85000	136.7800	swamp	10.00	Shulmeister and Lees, 1995
4	Lynch's Crater, QLD	-17.37000	145.7000	lacustrine	234.75	Kershaw, 1981; Turney et al., 2006; Kershaw et al., 2007
5	Lake Walala, NT	-15.68000	137.0300	swamp	10.00	Prebble et al., 2005
6	Three Quarter Mile Lake, QLD	-12.50000	143.0000	lacustrine	8.30	Luly et al., 2006
7	ODP820	-16.63000	146.3000	marine	250.00	Moss and Kershaw, 2000; 2007
8	Mua, Torres Strait	-10.18000	142.2500	swamp	6.00	Rowe, 2007
9	Argan Swamp	-10.05000	142.0600	coastal	5.52	Rowe, 2007
10	Badu 15	-10.06000	142.0900	terrestrial	9.00	Rowe, 2007

Number	Site	Latitude (decimal degrees)	Longitude (decimal degrees)	Type	Length (ka)	References
11	Bar20	-10.10000	142.1200	coastal	2.83	Rowe, 2007
12	Boigu Gawat Core 1	-10.10000	142.1400	coastal	4.57	Rowe, 2007; Rowe, 2015
13	Boigu Gawat Core 2	-10.10000	142.1400	coastal	13.82	Rowe, 2007; Rowe, 2015
14	Tiam Point	-10.12000	142.1800	coastal	7.70	Rowe, 2007
15	Zurath Islet	-10.16000	142.0600	coastal	6.50	Rowe, 2007
16	Waruid	-10.40000	142.0900	coastal	6.00	Rowe, 2007
17	Lake Euramoo	-17.15990	145.6286	lacustrine	23.48	Haberle, 2005
18	Big Willum	-12.64929	141.8470	lacustrine	8.00	Stevenson 2015
19	Isabella Swamp	-15.42127	144.9486	swamp	9.20	Stephens and Head 1995
20	Witherspoon Swamp	-17.49000	145.2400	swamp	7.90	Moss 2012
21	Bromfield Swamp	-17.22440	145.3227	swamp	37.00	Burrows 2014; Burrows 2016
22	Bentinck Island	-17.06660	139.4830	coastal	2.40	Mackenzie et. al, 2017; Mackenzie et al., 2020
23	Lizard Island	-14.66500	145.4630	coastal	8.00	Proske and Haberle, 2012

2.4.1. **Glacial (30 ka - 21 ka) and LGM (21 ka - 18 ka)**

The longest palaeoecological records from northern Australia come from Lake Carpentaria, and several studies have defined the extent and lake level fluctuations during the late Quaternary in this region (Jones and Torgersen 1988; McCulloch, De Deckker, and Chivas 1989; Reeves et al. 2007, 2008; Torgersen et al. 1985; Devriendt 2011). Torgersen et al. (1985) estimated the regional evaporation to precipitation ratio to have remained twice the modern ratio between 41 ka to 12 ka, suggesting drier conditions. Additionally, irregular patterns of precipitation during the LGM are suggested by the highly variable ratios of magnesium to calcium (Mg/Ca), sodium to calcium (Na/Ca), strontium to calcium (Sr/Ca), and δ^{18}O.

Additional evidence of aridity in northern Australia comes from analysis of aeolian dust activity (De Deckker, Corrège, and Head 1991; De Deckker 2001) in the Gulf of Carpentaria. The most pronounced arid period peaks around 21.5 ka, corresponding to the start of the period of lowest global sea level and glacial advance. Other peaks were found at ~ 25.5 ka, ~ 29.5 ka, 24 ka, and 19.3 ka (De Deckker 2001). Furthermore, evidence of fluvial activity in the north of Australia generally supports drier conditions through the LGM (Nanson et al. 1991; Nanson, East, and Roberts 1993).

There are no terrestrial records of climate, vegetation, and fire in Cape York between 30 ka - 18 ka. All the available records are from south of Cape York in the humid, not seasonal, tropics on the Atherton Tablelands. In this area, three sites have been extensively studied: Lynch's Crater (Kershaw, Bretherton, and van der Kaars 2007; Turney et al. 2006, 2004), Lake Euramoo (Haberle 2005), and Bromfield Swamp (Burrows et al. 2016). The available lines of evidence suggest the Glacial and LGM periods to be drier and cooler than today in this sector. Before the LGM, palynological analyses report dry, open woodlands on the Atherton Tablelands, Lynch's Crater and Lake Euramoo (Turney et al. 2004; Kershaw 1994). Vegetation records from Lynch's Crater, Lake Euramoo (Haberle 2005) and ODP820 (Moss and Kershaw 2007) suggest the dominance of sclerophyll woodland (i.e. Casuarinaceae and Myrtaceae). Except for Lynch's Crater, other records from the region indicate increased presence of grasses during the LGM (Petherick, Moss, and McGowan 2011). Further evidence of elevated values of Poaceae during the LGM is found in the pollen record from nearby marine core

ODP820 (Moss and Kershaw 2007). Burrows et al. (2016) suggested marked changes in effective precipitation (towards drier conditions) at 32.7 ka, 30.1 ka, 24.7 ka, and 21.9 ka in Bromfield Swamp.

In the broader tropical Australasian region, most studies agree on evidence of drier, cooler conditions between ca. 33 ka and 18 ka across the area (Denniston, Wyrwoll, Asmerom, et al. 2013; DiNezio and Tierney 2013; Reeves et al. 2013), with a lesser number reporting the existence of wetter events, some of them episodic (Nott, Price, and Bryant 1996; Muller et al. 2008; Burrows et al. 2016; Denniston et al. 2017). For instance, extreme flood events just before 23 ka were detected by Nott, Price, and Bryant (1996) and Nott and Price (1999), although the timing of these events should be taken with caution as ages could be overestimated (May, Preusser, and Gliganic 2015). Muller et al. (2008) found evidence of wet conditions during Heinrich events at 30 ka – 29 ka and 24 ka – 23 ka in Lynch's Crater. Changes in monsoon strength during the LGM have been proposed by several studies (Jiang et al. 2015; Denniston et al. 2017; Yan et al. 2018). For example, Yan et al. (2018) found that while the annual mean precipitation over the Australian monsoon region decreased, the annual precipitation range of summer to winter was enhanced.

Except for Lake Carpentaria, all studies from the region have fire records, most of them younger than ca. 12 ka. Both Lynch's Crater and ODP 820 have records for the LGM and the Glacial, with high charcoal values during the LGM (Kershaw 1994; Moss and Kershaw 2007; Kershaw, Bretherton, and van der Kaars 2007) or increased availability of biomass (e.g. sclerophyll woodland) for burning (Kershaw 1994).

2.4.2. **Deglacial (18 ka - 12 ka)**

The increase in lake level at Lake Carpentaria during the Deglacial suggests wetter conditions in the region, possibly associated with reactivation of the monsoon. While wetter conditions are reported in Lake Euramoo related to the growth of *Eucalyptus* woodland, Lynch's Crater and the ODP 820 records show evidence of dry conditions based on vegetation (Kershaw and Nix 1988; Moss and Kershaw 2007; Turney et al. 2004; Kershaw, Bretherton, and van der Kaars 2007). Likewise, in Broomfield Swamp decreases in effective precipitation at 13.9 ka – 13.4 ka and 11.9 ka have been identified (Burrows et al. 2016).

Fire records in the dry tropics report negligible or low burning activity during this period (Rowe et al. 2019; Field et al. 2017). Conversely, Lake Euramoo, demonstrates fire was much more prominent in the landscape starting at 16.8 ka.

2.4.3. Holocene (12 ka - Present)

Early Holocene (12 ka - 8 ka)

Warmer and wetter conditions have been proposed to be dominant during the early Holocene in the northern Australian tropics. Records from western Gulf of Carpentaria (Four Mile Billabong and Walala) point to effective precipitation rising from ca. 10 ka to 5 ka. The very few studies from the savannas of Cape York are limited to those derived from lake sediment cores with records beginning at the middle Holocene. These studies include Big and Little Willum (Proske et al. 2017; Stevenson et al. 2015) and Three-Quarter Mile Lake (Luly, Grindrod, and Penny 2006), and propose an increase in effective precipitation ca. 7.9 ka, consistent with studies from the Atherton Tablelands and the Kimberley (Shulmeister 1992; Haberle 2005; Denniston, Wyrwoll, Polyak, et al. 2013; Rowe et al. 2019). In Big Willum, as open water developed from ca. 7 ka – 5 ka, grass and sedge declined as the swampy basin bottom became fully submerged. Several coastal sites in the area (Western Torres Strait, Lizard Island) record widespread mangrove forest development led by the early Holocene sea level rise (Rowe 2007; Proske and Haberle 2012). Changes in vegetation suggest increased rainfall in Lake Euramoo. Haberle (2005) found the maximum rate of increase in rainforest between 9.6 ka and 8.7 ka. These changes are most likely to represent the local establishment of closed canopy rainforest under the influence of increasing precipitation at Lake Euramoo (and the Atherton Tablelands more generally).

Mid and Late Holocene (8 ka - Present)

The middle Holocene has also been identified as a period of increased precipitation in northeastern Australia's humid tropics and Western Torres Strait. In Broomfield Swamp, geochemical evidence derived from elemental counts (ITRAX) (rise in Ti and Ge) suggests a wetter period (8.5 ka - 5.9 ka) compared to the periods before and after (Burrows et al. 2016). Another phase of increased precipitation for Lake Euramoo is suggested around 7.3 ka to 6.3 ka, when rainforest achieved its maximum extent across the Atherton Tablelands. Shulmeister (1999) places the mid-Holocene

precipitation maximum between 5 ka - 3.7 ka for the Northern Territory and north Queensland. In the Torres Strait, the prominence of island rainforest elements during the early-mid Holocene likely reflects the timing and influence of higher rainfall and humid climate. Additional evidence of a wetter phase is present at 6 ka in Lizard Island, where a possible cyclone event was documented (Proske and Haberle 2012). Extensive stable mangrove communities dominated coastal Torres Strait, starting at 6 ka and 3 ka (Rowe 2007). Overall, pollen from northern Australia also reflects woodland expansion at this time, and modern vegetation established (Proske, Heslop, and Haberle 2014). Whiterspoon Swamp also shows a wetter phase during the mid-Holocene, with an increase in sedges and sclerophyll taxa (Moss et al. 2012).

Quantitative estimates derived from offshore pollen records also indicate peak precipitation between 7 ka and 6 ka (van der Kaars, De Deckker, and Gingele 2006). These changes are associated with the flooding of the continental shelf and the 'big swamp phase', as sea levels increase during the deglaciation and early Holocene (Woodroffe, Thom, and Chappell 1985).

Two increases in charcoal accumulation were identified at 8 ka in Lake Euramoo (Haberle 2005), while in Big Willum a peak was identified at 7.2 ka (Stevenson et al. 2015). Vanderlin Island in the Gulf of Carpentaria shows an increase around 6 ka. In summary, these peaks suggest increased burning during the middle Holocene in the area, potentially related to greater available woody biomass.

In northern Australia, the late Holocene (4 ka to present) is associated with climatic variability, peat/wetland establishment and localised episodic aridity. For example, the available records from Lake Euramoo and Lynch's Crater agree that this period was characterised by increased seasonality according to pollen evidence (Haberle 2005; Reeves et al. 2013). Similarly, Head and Fullager (1992) identify "increasing climatic variability" in the last 3000 years from dune instability in the East Kimberley. Evidence and derived discussions from several sites across northern Australia from Lees (1992), Shulmeister (1999), and Gagan et al. (2004), including the western Torres-Strait (Rowe 2007) point to conditions during the mid-to-late Holocene being as much drier than the previous early-to-mid Holocene phase. This evidence includes geomorphological evidence from dunefields, sea surface temperature (SST) reconstructions from foraminiferal Mg/Ca and vegetation reconstruction derived from

pollen Haberle (2005) identifies drier conditions and increased rainfall seasonality after ca. 4 ka. Stevenson et al. (2015) note the end of a “warm and wet period” at ca. 5 ka at Big Willum Swamp and identify the period between 1 ka - 0.4 ka as the period of “greatest variability” at the site. Similarly, in Witherspoon swamp, Moss et al. (2015) identified a period of dry conditions starting at 2 ka.

Burrows et al. (2016) identified a dry event in the Bromfield Swamp and Quincan Crater records at 4.1 ka as a possible indicator of “substantial climate change”. Mackenzie et al. (2017) describe variable conditions over the last 1.25 ka in the South Wellesley Islands, including storm events, wet conditions at one site around 0.750 ka and a drying trend beginning in the last 150-50 years across three swamps.

The Late Holocene was also a period of wetland and peat establishment at several sites (Rowe 2015; Stevenson et al. 2015; Luly, Grindrod, and Penny 2006). In the Torres Strait Islands, freshwater swamps developed by 2.6 ka with palynological records dominated by *Melaleuca* and the herbaceous swamp taxa *Leptocarpus* and Cyperaceae (Rowe 2015). Records at Boigu Gawat 1 and Boigu Gawat 2 in Torres Strait, suggest that wetlands became more productive, organic material increased and coastal influence was reduced (Rowe 2007, 2015). Records in the Gulf of Carpentaria show expansion and development in the late-Holocene. Walala swamp in Vanderlin Island was fully developed by 4.5 ka with organic sediments increasing in the last 2 ka (Prebble et al. 2005). Four Mile Billabong also expanded in the last 1 ka. At Big Willum swamp increased precipitation is maintained between 2.2 ka and 1.3 ka (Proske et al. 2017).

Locations such as the Torres-Strait (Rowe 2015) show an increase in charcoal accumulation (and therefore, fire) during the last millennium before the present. Big Willum in Western Cape York shows peaks after 2 ka. Variable patterns of burning have been identified during the Late Holocene (Rowe 2007, 2015; Field, Tyler, et al. 2018; Haberle 2005). Some studies have argued that this pattern in the later Holocene reflects an increase in climate variability associated with more active ENSO cyclicity (Mooney et al. 2011; Kershaw, Bretherton, and van der Kaars 2007). A summary of the available records is presented in Table 2.2.

Table 2.2. Summary of palaeonvironmental records for Cape York Peninsula

Time period	Summary of records
33 – 18 ka	Drier conditions and irregular patterns of precipitation. Pronounced arid periods around 21.5 ka. Drier and cooler conditions. Marked changes in effective precipitation Decreased fluvial activity
18 – 12 ka	Wetter conditions as Lake Carpentaria's level increased. Decreases in effective precipitation, especially at the end of the period
12- 8 ka	Effective precipitation rising
8 ka - Present	Peak in precipitation between 7 and 6 ka

2.4.4. **Palaeogeography of Cape York Peninsula (33 ka - Present)**

This section presents the available information on changes on palaeogeography, specifically sea level and dune formation in northern Australia and the broader region. Cape York Peninsula underwent major changes in geography during the last 33 ka, especially related to changes in sea level. By compiling a range of Late Quaternary sea-level indicator data, Brooke et al. (2017) and Lambeck et al. (2014) found an abrupt decrease in sea level ca. 30 ka (from - 83 m to - 126 m) in the Australian/South Pacific region (Figure 2.14, Figure 2.15 and Table 2.2). In Lake Carpentaria, during MIS 3 (57 ka- 29 ka), fully lacustrine conditions are confirmed by the ostracod Ba/Ca ratios, and the lake level corresponding to the - 60 m bathymetric contour, including increased intensity of fluvial sediment transport occurred during the MIS 3 and MIS 1 (Reeves et al. 2008).

Additional records from Lake Carpentaria indicate that lake levels dropped during the LGM (from the 59 m bathymetric contour during mid-MIS 3 to the 63 m bathymetric contour during the LGM). Episodes of sand deposition (aeolian or fluvial origin) at 26 ka, 24 ka and 21.5 ka at Lake Carpentaria are interpreted as arid events (De Deckker 2001) that closely match periods of elevated monsoon rainfall in the Ball Gown Cave record (northwestern Australia) (Denniston, Wyrwoll, Asmerom, et al. 2013). During the LGM,

large fluctuations of the lake level at the seasonal and interannual time scale are inferred from the $\delta^{18}O$ values and trace-element ratios of ostracod shells (Devriendt 2011). Fluvial activity continued through this period to maintain Lake Carpentaria permanently in the deeper regions of the basin. The sedimentary record indicates a temporary contraction of the lake to around the − 63 m contour (23–19 ka), during which the sea was at its lowest level (approximately − 125 m) (Brooke et al. 2017; Yokoyama et al. 2001).

Lowered glacial sea level exposed the Sahul shelf, the continental shelf extending over from the northern coast of Australia to the island of New Guinea, south of the Gulf of Carpentaria and the Timor Sea. Its exposure could have sizable impact on IPWP climate given their central location between areas of deep convection of the IPWP (Di Nezio et al. 2016) (Figure 2.13).

Low sea levels during the LGM also influenced dune formation and emplacement in tropical Australia (Figure 2.16). Dune emplacements in Cape Arnhem (Lees et al. 1995), Cape Flattery and Shelburne Bay between 24 and 18 ka appear to represent a period of widespread dune activity associated with the LGM. Dune formation occurred at glacial low sea levels when wide areas of continental shelf became exposed to wind action (Lees, Yanchou, and Head 1990; Lees 1992, 2006) (Figure 2.15).

Lagoons also record aeolian and dune activity. For example, in Native Companion Lagoon (NCL), in North Stradbroke Island (southeast Queensland), the significant local sand and dust content of the NCL record for this period indicate that the dunes surrounding NCL were active, most likely in response to a reduced cover of vegetation. The LGM is shown as the period of maximum aeolian sedimentation, because of decreased precipitation (Petherick, McGowan, and Kamber 2009). Loss of vegetation cover and subsequent destabilization of dunes would account for the increased deposition of local North Stradbroke Island sediments in Native Companion Lagoon at this time (Petherick, McGowan, and Kamber 2009; McGowan, Petherick, and Kamber 2008).

Figure 2.13. Sahul ca. 20 ka. Yellow line denotes modern coastline. Source: http://sahultime. monash.edu.au/

In a regional context, several studies have highlighted the impact of changing sea levels on the hydroclimate. For example, DiNezio and Tierney (2013) highlight the importance of continental shelf exposure during low sea levels on IPWP hydrology during the LGM, when comparing the results from several studies in the region. The study by Di Nezio and Tierney (2013) suggests that sea level is a first-order driver of tropical hydroclimate on glacial–interglacial timescales, and that the exposure of the Sunda Shelf best explain the pattern of hydroclimatic change inferred from the proxies. Dry conditions may have been maintained until flooding of the Sunda–Sahul shelf, at the end of the deglaciation, according to several studies (e.g. De Deckker, Tapper, and van der Kaars 2003; DiNezio and Tierney 2013).

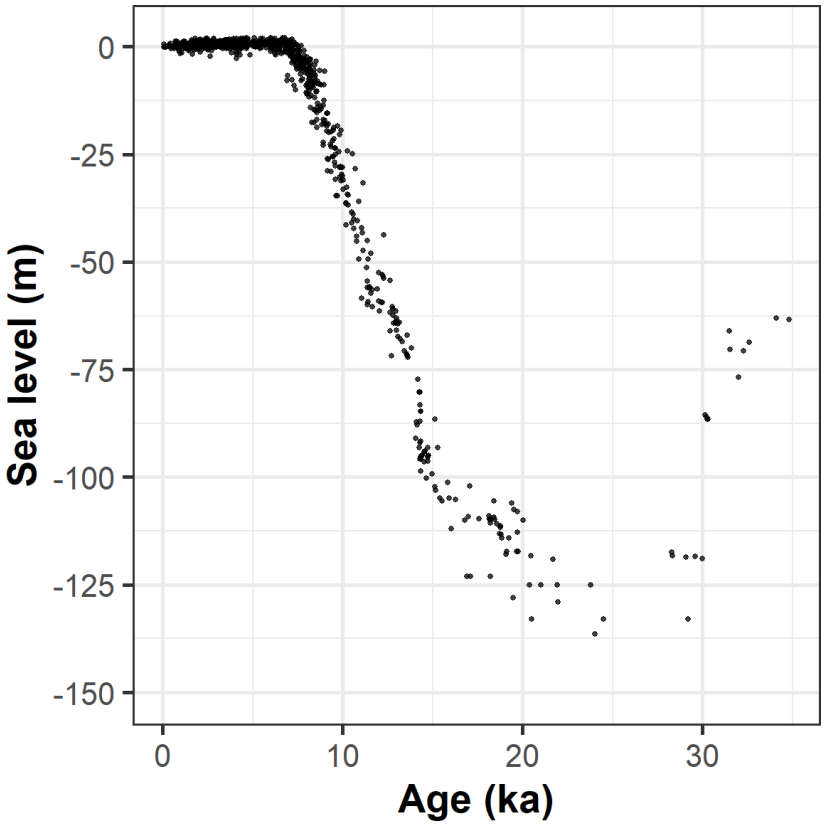

Figure 2.14. Changes in sea level according to Lambeck et al. (2014)

At Lake Carpentaria, beginning at 18 ka there is evidence of increased run-off and weathering. Increasing contributions from southern rivers and decreased salinity during 18 ka - 15 ka are interpreted as evidence of the reactivation of the monsoon (Devriendt 2011). Sedimentological evidence suggests a significant increase in lake level and extent after 18 ka (Reeves et al. 2008). This is confirmed by freshening of the lake and a considerable decrease in the lake water $\delta^{18}O$ variability after 18 ka (Reeves et al. 2008).

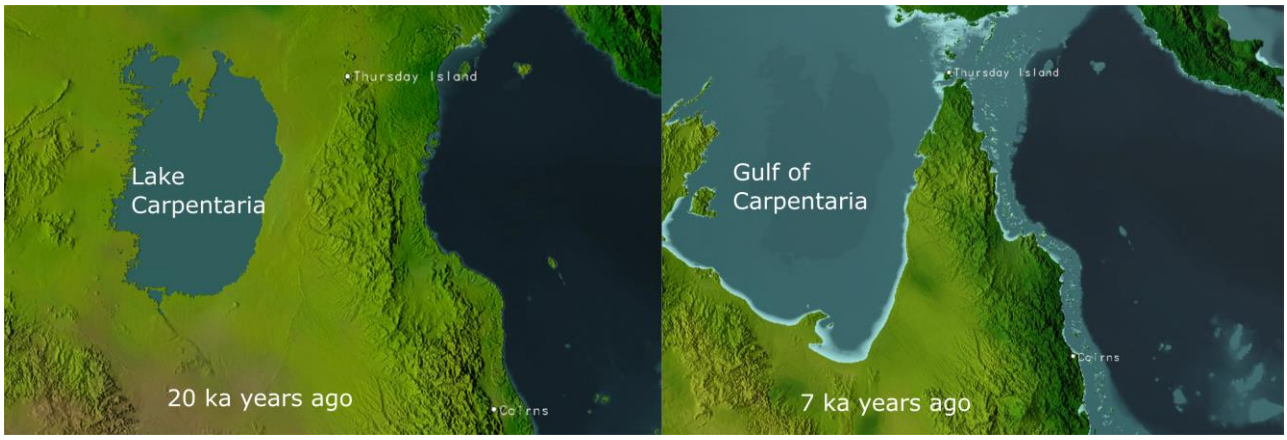

Figure 2.15. Changes in sea level in the Gulf of Carpentaria (after Brooke et al. 2017 and Lambeck et al. 2014)

Table 2.3. Main sea level changes in the Gulf of Carpentaria

Age (ka)	Event	Reference
57 – 23	Low sea levels	Reeves 2008
23 – 18	Lowest sea levels	Devriendt 2011
18 – 14	Increase in sea level	Devriendt 2011
14.1	Sea level rise rapidly	Brooke 2017
11.7	Breaching of the Arafura Sill	Sloss 2018
10.5	Full marine conditions	Sloss 2018
7.7- 4	High stand	Sloss 2018
4- Present	Present day sea level	Sloss 2018

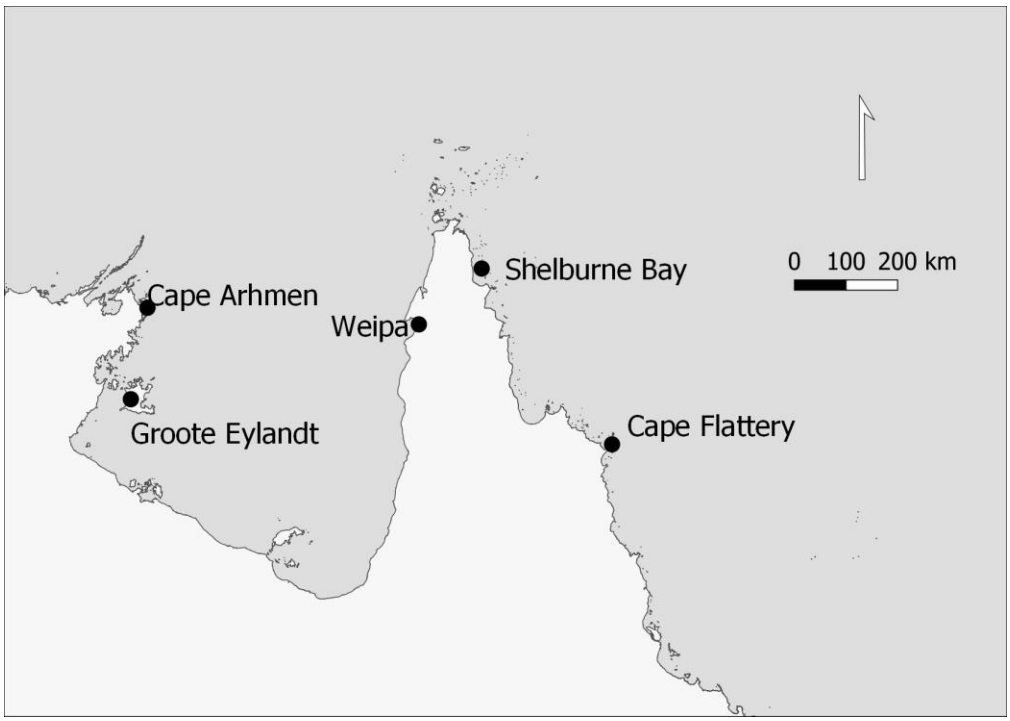

Figure 2.16. Sites with evidence of dune activity in Cape York Peninsula and surroundings

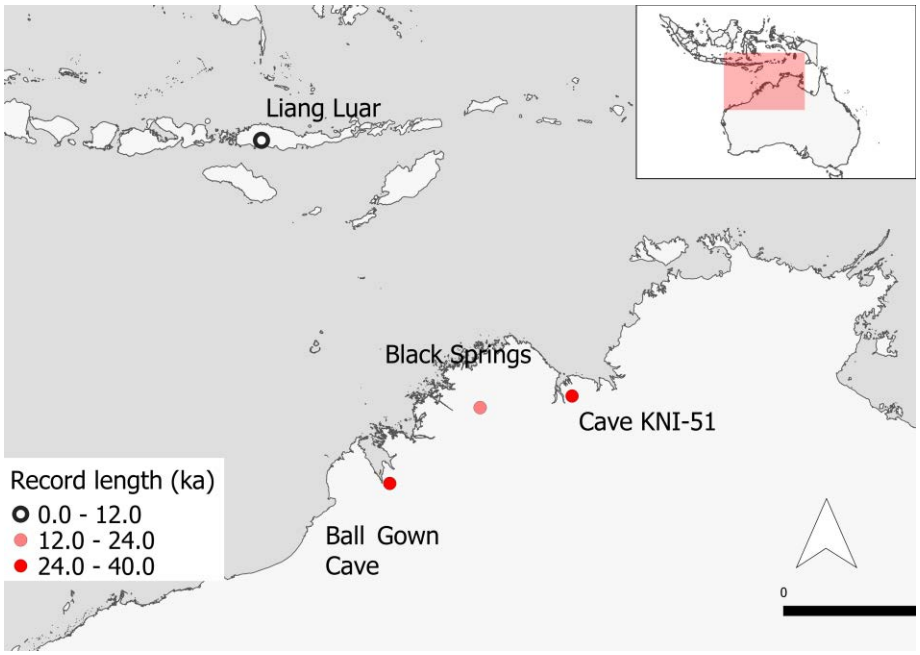

Figure 2.17. Location of sites mentioned in the text (Western Australia and Indonesia)

The maximum lake level (> 3 m average depth) and extent (> 100,000 km^2), as well as the lowest salinity, are recorded between 14 ka and 12 ka, suggesting the monsoon reached northeastern Australia around this time (Reeves et al. 2008). A shell-rich layer (19.0 ka – 17.1 ka) indicates a highly productive environment, associated with an influx of fresh water and increased precipitation. These changes are reflected in the sea level curve built by Brooke et al. (2017).

In the western equatorial Pacific (Sulawesi, Indonesia), dry conditions during the late glacial were terminated as a result of rising sea levels and the inundation of shallow continental shelves in the region, after the onset of deglaciation (DiNezio and Tierney 2013; Griffiths et al. 2013). Significant changes in speleothem $\delta^{18}O$ also coincide with the rapid flooding of the Sahul (ca. 12 ka – 11 ka) and Sunda (ca. 8.5 ka) shelves (Krause et al. 2019). The corresponding changes in speleothem $\delta^{18}O$ at Sulawesi (Krause et al. 2019) likely represent a combination of the reorganisation of local water masses, changes in source moisture pathways and intensification of the Walker circulation caused by enhanced convection over newly formed seas in the western equatorial Pacific region (Griffiths et al. 2009; DiNezio and Tierney 2013; Krause et al. 2019).

From ca. 12 ka important changes in sea level are recorded based on studies from Lake Carpentaria and the South Wellesley Archipelago (Sloss et al. 2018). From 12 ka, oceanic waters transgressed the Arafura Sill, and by 10.7 ka, the Lake Carpentaria region had become marine (McCulloch, De Deckker, and Chivas 1989; Chivas et al. 2001). Full marine conditions were attained in the Gulf of Carpentaria by 10.5 ka. Sloss et al. (2018) found that sea-level rose from −53 m (depth of the Arafura Sill) (Reeves et al. 2008; Sloss et al. 2018; Harris et al. 2008) at ca. 11.7 ka to ca. –25 m by 9.8 ka (Sloss et al. 2018) culminating in a mid-Holocene sea-level highstand (7.7 ka – 4 ka) and a corresponding period of increased precipitation and temperature during the Holocene. Coastal flooding facilitated increased moisture and heat transfer/transport fuelling monsoon activity. Data from Karumba, in the southern Gulf of Carpentaria (Chivas et al 2001), indicate that sea level was 2.5 m higher around 6.4 ka. Possibly, these conditions would expose Sanamere Lagoon to moisture and wind from the sea more than ever before. After 2 ka, sea level fell to present level (Lewis et al. 2013).

Additional studies from stalagmites in southeast Indonesia (Griffiths et al. 2009) also support the idea that lowered sea level had a large effect on IPWP hydroclimate from the LGM to 9.5 ka, when the Sunda Shelf was nearly flooded. Moreover, the early Holocene intensification of monsoon precipitation was driven by sea-level rise, which increased the supply of moisture to the Indonesian archipelago. Monsoon precipitation intensified even more rapidly from 11 ka to 7 ka, when the Indonesian continental shelf was flooded by global sea-level rise.

A drying trend is noted in several of the records during the mid-Holocene (Ball Gown Cave (oxygen and carbon stable isotope of stalagmites), Black Springs (pollen and elemental analyses of organic springs) and speleothems (oxygen isotope values) of Flores, coincident with increased precipitation in Borneo. A contraction of the IPWP is also recorded in the corals of this region (Reeves et al. 2013) (Figure 2.17).

The re-establishment of vegetation caused by rising sea levels during the mid-Holocene also contributed to dune stabilisation. The impact of sea level regression during the late Holocene is also documented in Bentinck Island, where the mangrove community transitioned to woodland and wetland dominated vegetation over the last 850 years (Mackenzie, Moss, and Ulm 2020). These changes also determined the timing of wetland development on the site, transitioning from coastal environments to wetlands between 0.8 and 0.4 ka (Mackenzie et al. 2017).

2.5. **Background to the methods used in the thesis**

The following sections develop the theoretical framework to interpret the results from chapters 3, 4, 5 and 6. Chapter 3 examines the sedimentology and stratigraphy of the Sanamere lake sediment core. Chapter 4 examines six carbon fractions in the sediment samples to determine which fraction and technique pre-treatment is most appropriate to obtain reliable radiocarbon dating results. Chapters 5 and 6 describe the palaeoenvironmental reconstruction for Sanamere Lagoon using multiple proxy records.

2.5.1. **Geochronology (Aim I)**

Radiocarbon dating

The ubiquitous presence of carbon in lacustrine environments makes radiocarbon dating one of the most commonly used and established techniques to date lake sediments. Carbon has three naturally occurring isotopes, two of which are stable (C-12 and C-13) and one (^{14}C) which is unstable, or radioactive. The production of ^{14}C takes place as a result of several nuclear reactions of ^{14}N with cosmic rays to form ^{14}C and a proton. Within hours, ^{14}C atoms undergo oxidation to form carbon dioxide ($^{14}CO_2$). Once a ^{14}C-tagged CO_2 molecule reaches the surface of the earth, it enters the carbon cycle (Aitken 1990; Wood 2015). About 85 % of ^{14}C remains in ocean water and the rest stays in terrestrial environments. Here, plants fix it in their cellular structures by photosynthesis, while other organisms obtain it secondarily by ingestion. Metabolic processes maintain the ^{14}C content of living organisms in equilibrium with atmospheric ^{14}C. These metabolic processes cease at the death of an animal or plant and the amount of ^{14}C will begin to decrease by decay at a rate determined by the ^{14}C half-life. The radiocarbon age of a given sample is based on measurement of residual ^{14}C content (Arnold and Libby, 1949; Aitken 1990; Wood 2015).

Some of the challenges associated with working with radiocarbon dating include changes in the natural production rate of radiocarbon in the atmosphere, as well as sample integrity. Regarding the first factor, atmospheric production of radiocarbon has varied through time, and these changes cause offsets between radiocarbon ages and calendrical ages. Calibration curves calculated by dating materials of precisely known age, such as tree rings have been used to overcome this discrepancy (Aitken 1990). IntCal20, the most updated calibration curve includes a wealth of new data and was extended to 55,000 cal BP. This curve comprises statistically integrated evidence from floating tree-ring chronologies, terrestrial macrofossils from lake sediments, foraminifera from marine sediments, speleothems, and corals, using improved evaluation of the time and location variable ^{14}C offsets from the atmosphere (reservoir ages, dead carbon fractions) for each dataset (Reimer et al 2020).

Regarding the second factor, the ability of ^{14}C determination to accurately date an event depends on the integrity of the sample and the degree of association between

the dated material and the event of interest. The integrity of the sample can be compromised by the incorporation of foreign carbonaceous materials into a sample matrix. For lake sediments, stratigraphic mixing, for example, by bioturbation is a common and serious problem, as it compromises the integrity of the sample. Bioturbation is one of the main causes of younger particles being reworked included in older deposits and vice versa. Erosion and floods can cause remobilized older carbon to be included in younger deposits. Samples that are in contact with groundwater could have absorbed inorganic carbonates that may alter the 'true' date. The effect of contaminants can be mitigated if information about the age of the contaminant, and the percentage contribution of the contaminant is available, though this is rarely possible (Aitken 1990; Olson, 1986; Wood 2015, Wohlfarth et al. 1998).

Selection of carbon fraction and pretreatment

Given the importance of the integrity of the sample to the reliability of radiocarbon dating, the selection of the carbon fraction to date and the pretreatment to apply is fundamentally important. There is general agreement about the suitability of some materials for dating, including very delicate materials, such as whole terrestrial leaves (which are unlikely to survive long periods of transport and reworking). There is more controversy around the general suitability of some macrofossils and charcoal, which have been reported to account for anomalous ages. Macrofossils (leaves, seeds, fruits) can take up contamination from fungi, when carbon from fungal spores and microorganisms is incorporated into the sample (Wohlfarth et al. 1998) and have been shown to yield systematic differences between series of paired analyses on two types of macrofossils (leaves and seeds) (Turney et al. 2000). Other materials, including bulk sediment and pollen, have been widely used, but previous studies have shown them to yield anomalous ages in at least some cases (Wang, Amundson, and Trumbore 1996). Stable polycyclic aromatic carbon (SPAC) or hypy fraction has been proposed as an alternative to the issues shown in other materials (Field et al 2018; Orr et al 2020).

Hypy fraction

Pyrogenic carbon (PyC) (hereafter Hypy fraction) with an aromatic ring size of > 7, is the solid carbonaceous residue remaining after hydrogen pyrolysis (hypy) and it is a demonstrably indigenous component of the original charcoal (Meredith et al. 2012). As such, the hypy fraction is likely to produce a reliable radiocarbon age, as the processes

remove labile carbon including contaminants (> 98 %) (Orr et al. 2020). Although a relatively new technique, hypy has been successfully applied in a number of different studies (Bird et al. 2014; Field, Tyler, et al. 2018). Incomplete removal of modern contamination has been shown for charcoal formed at < 350 °C as a small fraction of the labile carbon component may also be pyrolysed during HyPy treatment (Bird et al. 2014). During hypy, samples undergo pyrolysis aided by high hydrogen pressures in the presence of sulphided molybdenum catalyst (Ascough et al. 2009, 2010; Wurster et al. 2012).

One of the uncertainties related to the use of hypy includes the presence of a possible inbuilt 'reservoir' age associated with a period of storage in a lake catchment. This intrusion could cause the hypy results to older ages by an unknown amount (Ascough et al 2010; Bird et al. 2014; Orr et al. 2020). However, it is unlikely that this could cause such large offsets compared to what would be expected for the younger samples having between 2 and 5 % unremoved modern contamination (Wood 2015). Furthermore, total pyrogenic carbon content measured using the hypy technique is less likely to be biased by individual charcoal fragments, each of which may have some (unknown) residence time prior to deposition in the lake sediment and/or degree of unremoved contamination.

Bulk organics (bulk organic matter)

When no macro-organic remains are visible in lake sediment matrices, dating bulk sediments is the one of the most commonly used options. The organic components of bulk sediments are divided in three main categories, according to their solubility in acid and base (van der Plicht, Streurman, and van Mourik 2019; Bayliss 2009).

Humic acids: alkali soluble, acid insoluble and thought to derive from the decay of plant material that grew on the site as the sediment accumulated (Bayliss 2009).

Humin: acid and alkali insoluble, thought to consist of the physical remains of the plant/algal material. Humins are generally considered to be the most stable C fraction within the sedimentary profile (Pessenda, Gouveia, and Aravena 2001).

"Total organic" fraction: remains after the acid soluble fraction has been removed. "Humic acid" and "humin" fractions combined (Bayliss 2009).

Given the multiple sources from which carbon could have derived (Bronk Ramsey 2008), the contribution of contaminants increases considerably for any bulk organic matter fraction. Several studies have found this fraction to be consistently younger than other fractions given the possibility of contamination with younger carbon (Wang, Amundson, and Trumbore 1996; Pessenda, Gouveia, and Aravena 2001).

Pollen concentrate

Pollen concentrate is used as another alternative when macroscopic carbon fractions are not available. Several studies have found pollen concentrates to yield older ^{14}C dates compared to other fractions (Neulieb 2013; Fletcher et al. 2017), while others have found it to be younger (May et al. 2018), yielding significantly different chronologies compared to other fractions. In part this may be due to the greater mobility of pollen and pollen sized material in some environments (Clymo and Mackay 1987) and therefore, the possibility of being reworked. In addition, the porous structure and high surface to volume ratio of the pollen grain walls make them prone to store exogenous carbon materials (Kilian et al. 2002). These impurities can lead to unreliable ages (Fletcher et al. 2017).

Cellulose

Although cellulose is considered one of the fractions that yields reliable dates, the extraction of holocellulose is commonly complex and in some cases unreliable. For instance, during the early Holocene, differences of up to 1000 years are observed between lake sediment cellulose and terrestrial plant fossils (Kitagawa et al. 2007). This disagreement is probably caused by the contribution of ^{14}C-depleted cellulose synthesized by aquatic plants/algae in the lake (Kitagawa et al. 2007).

Furthermore, the most commonly used procedures to extract cellulose are time-consuming and require excessive organic solvents (Wolfe et al. 2007). Recently, Gillespie (2019) implemented a novel extraction protocol that includes the use of less toxic chemicals (such as HCl, NaOH and $NaClO_2$) in quicker steps to overcome the disadvantages inherent in the previous procedures.

Macro/microcharcoal

Macrocharcoal (> 250 μm) and microcharcoal (< 250 μm,> 63 μm) are very commonly dated when available and considered to be inert. However, standard pretreatment can lead to unremoved contamination and samples can be destroyed after this procedure, with no remaining material to be dated (Bird and Ascough 2012). Additionally, Bird (2007) showed that chemical modifications can occur on the surface of charcoal and that its porous nature makes it especially prone to absorb exogenous carbon and microbes. Iron carbonate (siderite) and oxides of different cations may also be formed during diagenesis. If this source of carbon is not removed, it can lead to anomalous dates (Bird 2007).

Although they are usually not separated, Carcaillet et al. 2001 suggest that microcharcoal and macrocharcoal represent different sources, with microcharcoal coming from further way from the site deposition (as fine particles are more likely to be transported by wind or water over long distances before deposition in the location from which they are ultimately collected) compared to macrocharcoal, which is unlikely to move long distances. This difference could yield different radiocarbon dates for macro and microcharcoal from the same sample.

2.5.2. **Environmental change and palaeohydrology (Aims II and III)**

Chapter 5 presents a multi-proxy record of geochemical (micro X-ray fluorescence [μXRF] scanning), carbon and nitrogen content and associated stable isotopes, physical (grain size) and biological (diatom) proxy data sets for Sanamere Lagoon. The chapter aims to develop a record of hydroclimatic changes in an under-studied region of northeast Australia. Chapter 6 contributes to refining the vegetation and fire record using a phytolith, carbon isotope and pyrogenic carbon-based reconstruction of Sanamere Lagoon in northern Cape York, Australia. The following sections present the methodological foundation for these chapters.

Diatoms

Carbonates are one of the most commonly used materials in palaeohydrological studies, and they are used to infer the isotope composition of the lake water at its time of formation, and by inference the isotope composition of precipitation. Precipitation isotope

ratios have been correlated with mean surface air temperature at mid-to high-latitudes, or with the amount of precipitation in tropical areas. However, in non-alkaline, dilute, open lakes, carbonates may be rare or absent. In lakes where carbonate is not preserved, silica bodies can be used as an alternative isotope proxy host to carbonates (Hu and Shemesh 2003; Lamb et al. 2005). For example, diatoms are photosynthetic algae that secrete a shell composed of opaline silica ($SiO_2 \cdot nH_2O$) and are present in many lake sedimentary records (Stoermer and Smol 2001). In very alkaline lakes (> pH 9) or lakes where silica is limited, diatoms are often preserved only in low concentration (Barker, Fontes, and Gasse 1994).

Diatom species inhabit specific environments based on their tolerance ranges and morphology (Battarbee et al. 2002). For palaeoenvironmental purposes, classification systems use pH, habitat and salinity as determinant variables to understand changes in diatom abundance in the past. Habitat can be placed into two categories: benthic and planktic species. Planktonic species live as free-floating cells in the plankton of ponds, lakes and oceans. Benthic species form attachments to surfaces and are further classified according to their attachment to the substratum. Epilithic species attach to rocks and geological surfaces, epipsammic species to sand grains, epizoic species to animals and epiphytic species are those that attach themselves to plants and other algae species. Finally, epipelic species are those that live on the benthos or sediment on the bottom of the aquatic environment while endopelic species live within sediment (Battarbee et al. 2002) (Table 2.3 and Table 2.4).

Diatoms are a common proxy, used extensively in tropical areas to infer lake level, with the first studies pursued in Africa (Gasse and Street 1978; Gasse 1987). Diatom composition and relative abundances potentially offer a more precise measure of palaeohydrological change than palynological data (Prebble et al. 2005; Wolin and Stone 2010). Other lake characteristics that are derived from these organisms include pH, sedimentary processes, changes in evaporation, salinity, turbidity and trophic status of a water body (Proske et al. 2017). Diverse applications and research questions in Arctic and subartic regions include peat water content, flood frequency, river discharge, effective moisture and ice cover (Moser et al. 2000).

Diatoms have provided considerable information about the palaeohydrology and hydroclimate of many tropical regions, including Australia (Luly, Grindrod, and Penny

2006; Prebble et al. 2005; Proske et al. 2017; Tibby and Haberle 2007), with the majority of the studies pursued in the east portion of the continent. For example, autecological information from different species indicate changes in the water level of lakes (Proske et al. 2017; Tibby and Haberle 2007) or major shifts in local hydrology, e.g. from a perennial swamp to open lake. Perennial lake conditions are identified by the overlap between planktonic/benthic and littoral/benthic diatom taxa (Prebble et al. 2005).

The environmental inferences drawn from diatoms are based on the autecology of individual diatom species or the study of the interactions of each species with the living and nonliving factors of its environment. For example, inference models link diatom ecological tolerances with physico-chemical variables that can be used to and infer palaeoecological conditions (Battarbee et al. 2002). On Cape York Peninsula, diatom composition is correlated with total alkalinity, bicarbonate concentration, pH, electrical conductivity (EC) and latitude (Negus et al. 2019). This correlation confirms the potential of using these organisms as palaeoclimate proxies in this area.

Table 2.4. Diatom classification according to salinity (based on van Dam, Mertens, and Sinkeldam 1994)

Description	Salinity (%)
fresh	< 0.2
fresh brackish	< 0.9
brackish fresh	0.8 - 1.8
brackish	1.8 - 9.0

Table 2.5. Diatom classification according to pH (based on van Dam, Mertens, and Sinkeldam 1994)

Classification	pH
acidobiontic	optimal occurrence at pH < 5.5

Classification	pH
acidophilous	mainly occurring at pH < 7
circumneutral	mainly occurring at pH-values about 7
alkaliphilous	mainly occurring at pH > 7
alkalbiontic	exclusivey occurring at pH > 7
indifferent	no apparent optimum

Sediment and isotope geochemistry

Titanium concentration and grain size analysis are commonly used to infer runoff and transportation of clastic materials into a lake (Vázquez et al. 2017). As with other proxies based on sediment physical properties, this depends on a clear understanding of climatic effects on sedimentology for a specific catchment (Douglas, Brenner, and Curtis 2016). The presence of elements such as iron, titanium and aluminum in lake and marine sediments often indicate times of greater material transport under conditions of higher precipitation and consequent runoff. The drivers of bulk sediment elemental geochemistry vary widely, and often need to be determined for each catchment and sedimentary system (Brodie et al. 2011).

The $\delta^{13}C$ measurements of bulk sediments can be used to infer changes in the source of organic carbon in lake sediments. In some cases, such measures provide insights into vegetation change, and distinction between terrestrial and aquatic input, C_3 (trees and shrubs) and C_4 plants (tropical grasses), which can be related to climate (Mays et al. 2017). Refer to section 5.2.3 and 5.2.5 for more information about sediment, isotope geochemistry and interpretations of nitrogen isotopes.

Grain size

Variability in clastic grain size can indicate changing lake levels, and the amount and energy of runoff into a sedimentary basin. Likewise, grain size analysis can be an indicator of the amount and intensity of flood events (Conroy et al. 2008). Some studies suggest that increased precipitation in closed-basin lake catchments transport larger grains from the catchment. Therefore, grain size in the sediment is seen as a function of

the intensity and/or amount of rainfall (Chen et al. 2004). Grain size measurements inform on the sources of detrital material and may help determine possible depositional processes (fluvial or aeolian) prevailing through different periods (Burrows et al. 2016). In Lake Barrine, in northeast Australia, grain size analysis, along with other proxies, was taken to indicate fluctuations in water level (Walker 2007). One of the limitations of grain size analysis is the possibility of not detecting small to medium events in the record.

Fire

Optical charcoal analysis is commonly used as a proxy for fire activity in the past. Although the use of hypy fractions as a tracer of past fire activity is in its infancy, the study by Bird et al. (2019) found that hypy fractions are able to reproduce similar fire activity signals when compared to charcoal counting records in northern Australia, with the advantage of removing the time-consuming particle counting step. Furthermore, the measurement of the carbon isotope composition of the pyrogenic carbon provides information on the proportions of C_3 and C_4 (grass) vegetation being burnt.

In the study by Bird et al. (2019), the recurrence of fire regimes (linked to changes in vegetation and climate) were derived using pyrogenic carbon abundance measured by hydrogen pyrolysis (Wurster et al. 2012) (section 2.4.1.1). However, the results from optical charcoal analysis and the Hypy fraction are not directly comparable as the proportion of pyrogenic carbon (Hypy fraction) to charcoal increases with increasing fire intensity (therefore representing higher intensity fires compared to the macroscopic and microscopic charcoal particles) (Bird and Ascough 2012).

The study of fire regime in the past mostly relies on the measurement of charcoal abundance in sediments (Higuera et al. 2010), and particle counting, either manually (Ali et al. 2009) or using computer-assisted tools (Conedera et al. 2009). As an alternative, the abundance of pyrogenic carbon (measured by an incandescence-based method) has been found to work as a moderate tracer of historical fire activity (Chellman et al. 2018).

Vegetation

Carbon isotopes

The source of organic matter input into a lake can be determined using bulk sedimentary organic carbon isotope values. The stable carbon isotope composition of forests varies with the type of forest present and end-members of corresponding biomes have different $\delta^{13}C$ values (Farquhar et al 1982). For instance, for tropical rainforest the carbon isotopic value is -27 ‰; for tropical seasonal forest -24.8 ‰ and for tropical deciduous forest -22 ‰ (Diefendorf et al. 2010; Kohn 2010). Those $\delta^{13}C$ values above baseline $\delta^{13}C$ values for tropical deciduous seasonal forests, unambiguously indicate that by implication, tropical grasses were a substantial part of the environments and that the hydroclimate was significantly drier and/or more seasonal than when $\delta^{13}C$ values are lower (Wurster et al. 2019). As an example, the $\delta^{13}C$ values for forest end-members in tropical savannas are expected to be -25 ‰. Therefore $\delta^{13}C$ values above ~ -24 to -25 ‰ unambiguously indicate the presence of tropical grasses and that the hydroclimate was significantly drier and/or more seasonal than when values are lower than this threshold (Diefendorf et al. 2010).

In addition, understanding the variation in C_4 vs C_3 being burnt through analysis of pyrogenic carbon in a sedimentary record can provide insight into the balance of trees versus grass in the surrounding area and hence possible environmental conditions at the time of burning (Wurster et al. 2017). Thus, the $\delta^{13}C$ of pyrogenic carbon ($\delta^{13}PyC$) can be used to make inferences about the vegetation being burnt. It is however important to understand the relationship is unlikely to be direct due to fractionation processes during initial pyrolysis and subsequent transport (Saiz et al. 2015).

Phytoliths

Phytoliths are silica bodies that form in living plants. Since different plant species produce different phytolith morphotypes, phytoliths can be used to identify plant assemblages and thereby to study palaeovegetation. Phytoliths have been increasingly used in plant palaeoecology studies not only because of their potential to elucidate changes in vegetation patterns, and represent local vegetation growth, but because of their resistance to degradation under tropical environmental conditions that are often unfavorable for pollen preservation (Rashid et al. 2019; Testé et al. 2020). Phytolith analysis is therefore used to identify the past vegetation communities in a particular

landscape. The analysis relies on morphotype counts and the delineation of classes of morphotypes that are indicative of plant groups.

Multiplicity and redundancy are two of the main limitations of phytolith analyses. Multiplicity refers to the production of range of different morphotypes by each plant, as deposition of silica often occurs at several sites in the plant tissue. Furthermore, redundancy refers to the overlap in the shapes of the silica bodies formed inside plants, even between taxa that are not closely related. Additionally, phytoliths are biased against non-grasses in many ecosystems.

Although multiplicity and redundancy in phytoliths can limit the vegetation inferences in detail, some morphotypes can be still ascribed to certain plant groups (Neumann et al. 2019; Daniau et al. 2019): Poaceae (saddle, bilobate, trapezoid oblong, elongate), Poaceae/Cyperaceae (bulliform, cuneiform bulliform, elongate entire cylindrical, elongate psilate, elongate blocky, elongate rugose, elogate facetated, blocky), woody dicotyledons (globular psilate) and non-diagnostic. According to Strömberg et al. (2018), vegetation inferences are statistically robust for assemblages with a clearly skewed morphotype distribution. For example, 90% woody dicotyledons phytoliths vs. 10% Poaceae phytoliths.

While pioneer studies using phytoliths targeted the development of agriculture and dietary practices in archaeological contexts (e.g. Piperno, Bush, and Colinvaux 1991; Kealhofer and Piperno 1998), phytolith analysis has been increasingly used in plant paleoecology studies because of its potential to identify past changes in vegetation patterns. In the tropics at least, this is because they represent local vegetation and are more resistant to degradation under environmental conditions that are not favorable for the preservation of other plant proxies such as pollen (Rashid et al. 2019; Testé et al. 2020). Despite their long history of use internationally, the application of phytoliths in Australian palaeoecology remains limited to a handful of studies in the Australian tropics (Wallis 2003, 2001), and their potential utility remains largely unexploited.

2.6. **Chapter 2 summary**

Sanamere Lagoon is located in the dry tropics of northern Australia, where monsoon dynamics, modulated by phenomena such as ENSO is currently the main

determinant of climate. Previous studies report significant changes in geography (sea level, shoreline, dune activity) that influenced, or were influenced by, climate in the past. Although several studies have provided results on past environmental change in the tropics of Australia, no records older than 8 ka are available for Cape York Peninsula. This thesis uses a multiproxy approach to contribute to fill the gaps associated with the past hydrology, vegetation and fire at Sanamere Lagoon, including elemental, isotopic (δ^{13}C and δ^{15}N), diatom, phytolith and pyrogenic carbon (Hypy fraction) analyses. Additionally, this thesis builds a reliable chronology for the Sanamere Lagoon sediment core by analysing and comparing the radiocarbon results from six different carbon fractions.

Chapter 3. **Sedimentology and stratigraphy**

This chapter describes the coring techniques used during fieldwork, along with the sedimentology and stratigraphy of the sediment core collected. This information helps form the basis for the interpretation of the following three chapters.

3.1. **Fieldwork and coring techniques**

Sanamere Lagoon was cored using a floating platform with hydraulic coring-rig, positioned at the approximate centre of the water body (11.123°S, 142.359°E). Fieldwork was undertaken in July 2017 (Figure 3.1). The coring location was chosen based on previous reconnaissance work carried out in May and April 2016. Although the coring technique allowed the preservation of the sediment-water interface, visual inspection of the core suggested the disturbance of this section. At the time of sampling, water depth was 1.2 m. A stainless-steel tube of 100 mm diameter and 1.6 mm wall thickness was used when coring to ensure a large volume of sample material was obtained. A single sediment core of 1.72 m was collected, cut in four portions and frozen onsite immediately so it maintained stratigraphic integrity. This column represents the entire sediment sequence in the lagoon, as the corer bottomed on laterite bedrock. The four portions were stored frozen at James Cook University, Cairns until further analysis. A series of water depth measurements were taken across a transect to build a cross section of depths (Figure 3.2).

3.2. **Methods**

3.2.1. **Core processing**

We returned the core sections to the cold room (4–5 °C) in the Advanced Analytical Centre at James Cook University, Cairns. We opened the core tubes longitudinally, photographed the core sections, and described sediment colors (Munsell, 1970 version) and textures using standard methods (Schnurrenberger, Russell, and Kelts 2003). Subsequently, each core section was divided into three slices and each one was sub-sampled at 1 cm intervals. Two slices were stored frozen and intact for ITRAX analyses and archive purposes. The wet weight was recorded for each sample, samples

were freeze-dried, and the ‘dry’ weight was also recorded for use in calculation of bulk density. One section of each core was scanned using the ITRAX micro X-ray Fluorescence (μXRF) core scanner at the Australian Nuclear Science and Technology Organisation (ANSTO). The scans included optical and X-ray photographs of all sections.

Figure 3.1. Sanamere fieldwork

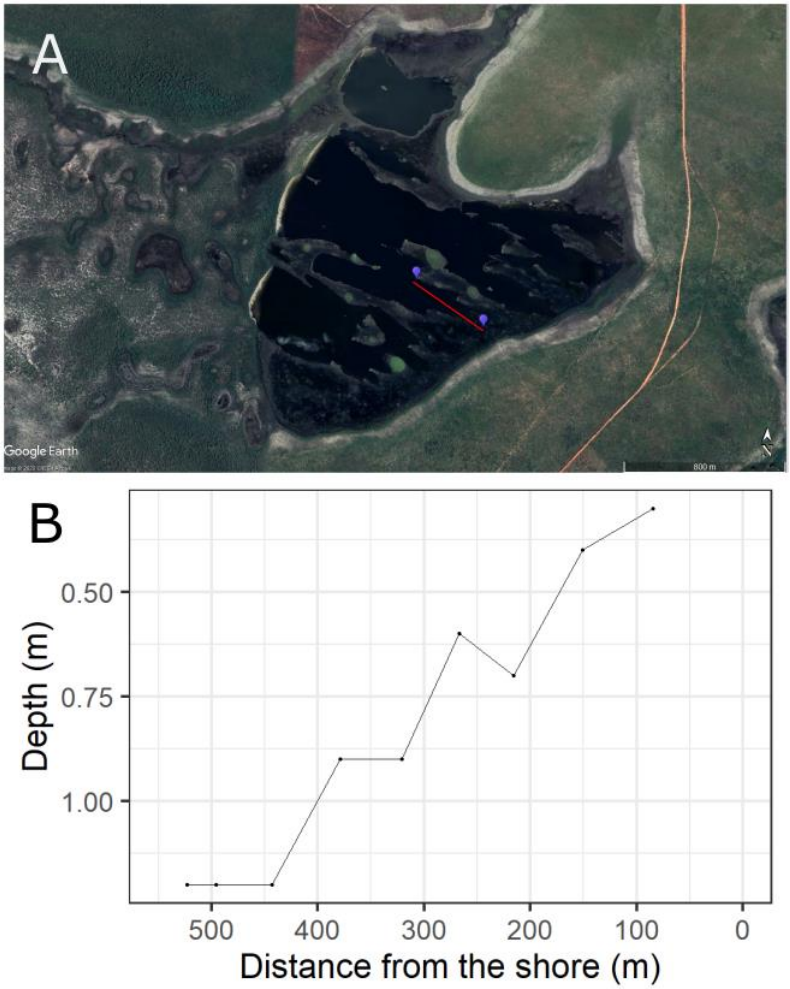

Figure 3.2. A) Satellite image of Sanamere showing the transect of water depth, B) Cross section of depths across Sanamere Lagoon

3.2.2. **Basic physical parameters**

The physical parameters were calculated following standard guidelines according to Håkanson and Jansson (1983).

Water content

The water content was calculated as the ratio of the weight of water (W), Ww in g, to the dry weight of solids, Ws in g.

$$W = \frac{Ww}{Ws} = \frac{Wt - Ws}{Ws} * 100$$

where Wt = the total wet weight (in g)

Dry bulk density

Bulk density was determined by weighing the wet samples secured from known volumes, oven-drying the material, and re-weighing the sample, according to the following formulas (Taylor, Fujioka, and et al. 1992):

$$p = \frac{Ms}{V}$$

$$p = \frac{M - Mw}{V}$$

where M= total mass of soil, Ms = the mass of the dry sample (weight of the solid portion of the sample), Mw = mass of water and V = the total volume

Grain size

Forty-two sediment samples, with a sample interval of 4 cm were dispersed with sodium hexametaphosphate and sieved at < 1000 μm. The < 1000 μm fraction was subsequently pretreated with 30 % hydrogen peroxide to remove organics and finally with 1 M NaOH to dissolve biogenic silica, leaving a clastic particulate residue for particle size determination. All pretreated samples were analysed using a Malvern Mastersizer 2000 laser diffraction spectrophotometer. The median grain size and the percentages of clay (< 2 μm), silt (> 2 μm and < 63 μm) and sand (> 63 μm) were obtained for each sample (Gee and Bauder 1986). Additionally, the percentage of coarse sand (> 275 μm, < 1000 μm) was also calculated. A correlation matrix between grain size and elemental concentrations was calculated to explore the relationships between these variables. Variability in grain size can indicate changing transport energy, lake levels, and/or the amount and energy of runoff into a sedimentary basin. The presence of larger grains in the sediment record indicates either increased precipitation (especially in closed-basin lake catchments) (Chen et al. 2004; Conroy et al. 2008) or lower lake levels resulting from higher accumulation of the nearshore components and/or weaker monsoon circulation in tropical settings (Xiao et al. 2009).

3.2.3. **Basic chemical parameters**

Carbon

A representative aliquot (~ 1 g) (making sure the bag where each individual sample was stored was mixed well enough) of each freeze-dried sample was homogenized using a mortar and pestle. An aliquot of each sample (1–10 mg) was weighed into a tin capsule and crimped. The presence of carbonates was checked by comparing the measurements (carbon stable isotope measurements) of a batch of 30 samples where carbonates were removed by acid with the results from the untreated batch. No differences were found between the two batches. Total organic carbon and nitrogen abundance and isotope composition of an aliquot of each (1–10 mg) were determined using a Costech elemental analyser fitted with a zero-blank auto-sampler coupled via a ConFloIV to a ThermoFinnigan DeltaV PLUS using continuous-flow isotope ratio mass spectrometry (EA-CF-IRMS) at James Cook University's Cairns Analytical Unit. Stable isotope results are reported as per mil (‰) deviations from the VPDB and AIR reference standard scale for δ^{13}C and δ^{15}N values respectively. Uncertainty on internal standards ('Low Organic Carbon' δ^{13}C −26.54 ‰, δ^{15}N 7.46 ‰; 'Taipan' δ^{13}C-11.65 ‰, δ^{15}N 11.64 ‰; and 'Chitin' δ^{13}C −19.16 ‰, δ^{15}N 2.20 ‰) was better than ± 0.1 ‰. Repeated measurements on samples showed that C and N concentrations were generally reproducible to ± 1 % (1σ).

Silicon, Titanium, Iron

XRF elemental profiles were completed for the four sections of the divided core (0-50, 50-100, 100-150, 150-172 cm), for a total of 172 cm, using the second-generation ITRAX core scanner (Cox Analytical, Gothenberg, Sweden) located at the Australian Nuclear Science and Engineering Organisation. Operating conditions for XRF were 40 kV and 30 mA, step size 1000 um and 10 seconds count time. The XRF scans produced data for a total of 25 elements and were performed using a chromium (to optimise the lighter elements Al, Si, P, S, Cl, K, Ca, Sc, Ti, V, Cr) and molybdenum tube set (to optimise the heavier elements Mn, Fe, Ni, Cu, Zn, Br, Rb, Sr, Y, Zr, Pd, Ba, La, Ce, Pb) (Table 3.1). Further information and statistical analyses are included in chapter 5. Optical and radiographic images were also taken of each core using the ITRAX scanner, during XRF scanning. Processing of ITRAX data was completed by ANSTO Facility Officer Dr. Patricia Gadd. ITRAX elemental counts were normalized using the procedure

outlined by Rothwell and Rack (2006) and Weltje et al. (2015). In brief, elements of interest were selected their counts were divided by the total number of counts for that depth. More details about the methodology are available in chapter 5.

In this chapter the results of only three elements (Ti, Fe, Si) are shown, for the purposes of introducing the core stratigraphy.

3.3. **Results**

Core description

The sedimentary sequence for the Sanamere Lagoon is shown in Figure 3.3 and Table 3.1. Four initial stratigraphic zones were identified based on variations in the basic physical and chemical parameters along the core. The core description will follow a sequence starting at the bottom of the core, with the last section referring to the top of the core. The first layer (172 cm - 140 cm) consists of a dark brown colour (5 YR 5/8), with carbon content below 0.5 %. Over the interval from 140 to 65 cm mineral content gradually decreases and the colour is light brown (7.5 YR 4/3). A series of three orange (7.5 YR 6/8) 1-cm thick bands are evident over 71 cm - 65 cm (Figure 3.4). Beginning at 65 cm, there is a marked decrease in organic content to values of 0.5 and 1 % over 43 cm and the sediment colour changes to reddish brown (5 YR 4/4). The upper 43 cm of the core consists of black (10YR 2/1), organic (5 % - 40 % carbon) sediments, including the presence of decomposed organic debris.

Table 3.1. Layers and units for the Sanamere core

Depth (cm)	Description	Layer
0-43	2.5 YR 4/6 Dark silty peat	4
43-65	5 YR 4/4 Silty clay	3
65-140	7.5 YR 4/3 Silty clay	2
140-172	5YR 5/8 Silty clay with gravel	1

3.3.2. **Physical parameters**

Water content

The water percentage in the sediment column varies between 70.5 % and 24.4 %. For the first three stratigraphic units (172 - 43 cm) the percentage stays between 24.4 % and 36 %. Starting at 43 cm (46 %) and until 26 cm, (63 %) there is a steep increase in water content, from which point it starts to drop to reach 36 % at 11.5 cm (Figure 3.3).

Dry bulk density

Dry bulk density varies between 0.02 and 1.1 g cm^{-3}. Between 172 cm and 43 cm values remained between 1.1 and 0.71 g cm^{-3}, starting to drop abruptly at 43 cm decreasing to the surface (Figure 3.3).

Grain size

Clastic material of less than 35 μm dominates most of the Sanamere sequence. Between 172 cm and 140 cm, very fine silt (6 - 10 μm) dominates the sequence. An abrupt increment in clay occurs at 136 cm, where clay (<2 µm) increases to 45 %, while silt drops to 55 %. Between 140 cm and 43 cm, the sand percentage fluctuates between 2 % and 18 %, with the only exception at 65 cm, where it increases to 32 %. At 43 cm, the median grain size, sand and silt percentages increase, and the clay percentage decreases. Sand surpasses clay at 38 cm and keeps increasing to the top of the core (Figure 3.3).

3.3.3. **Chemical parameters**

Carbon and Nitrogen

The abundance of carbon percentage varies between 0.3 % and 41 % along the entire core (Figure 3.3). Values fluctuate between 0.32 % and 1.10 % between 172 cm and 43 cm, from where they start to increase until they reach 41 % at 26 cm. From 26 cm, they decrease gradually until the top of the core. The nitrogen percentage values range between 0.03 % and 1.5 %. Between 172 cm and 44 cm, they fluctuate between 0.03 % and 0.2 %, to then increase gradually to 1.1 % at 37 cm, where they gradually decrease to 0.3 % at 5.5 cm, with the exceptions of two high values (1.5 %) at 4 cm and

4.5 cm (Figure 3.3). Nitrogen and isotope (carbon and nitrogen) abundances will be discussed in chapters 5 and 6.

Silicon, Titanium, Iron

Complete analysis and interpretation of the ITRAX record is performed in chapter 5. High water content and low elemental counts prevented the use of the XRF scanning results from 7 cm to the top of the core. The description of Si, Ti and Fe is included in this section to support interpretation in chapter 4. Between 172 cm - 71 cm, the Ti counts stayed relatively constant with minor fluctuations (0.68 - 0.80). After 65 cm, the Ti counts fluctuate and decrease abruptly to 0.01 at 31 cm. From 31 cm, counts increase steadily again to the top of core (Figure 3.5).

Between 172 cm and 140 cm there is minor fluctuations in the Si counts, with low values (0 - 0.07) dominating until 43 cm. Si values start to fluctuate between 0 and 0.32 until the end of the core. They increase rapidly to reach 0.32 at 26 cm (the highest value), to then decrease gradually to reach 0 counts at 18 cm. Finally, counts increase to 0.1 at 8 cm.

The Fe counts are highly consistent (0.95) until 43 cm from where they drop abruptly. Between 43 cm and 22 cm, they fluctuate (0.76 - 0.95). After this period, they increase and keep fluctuating between 0.41 and 1 between 18 cm and 9 cm.

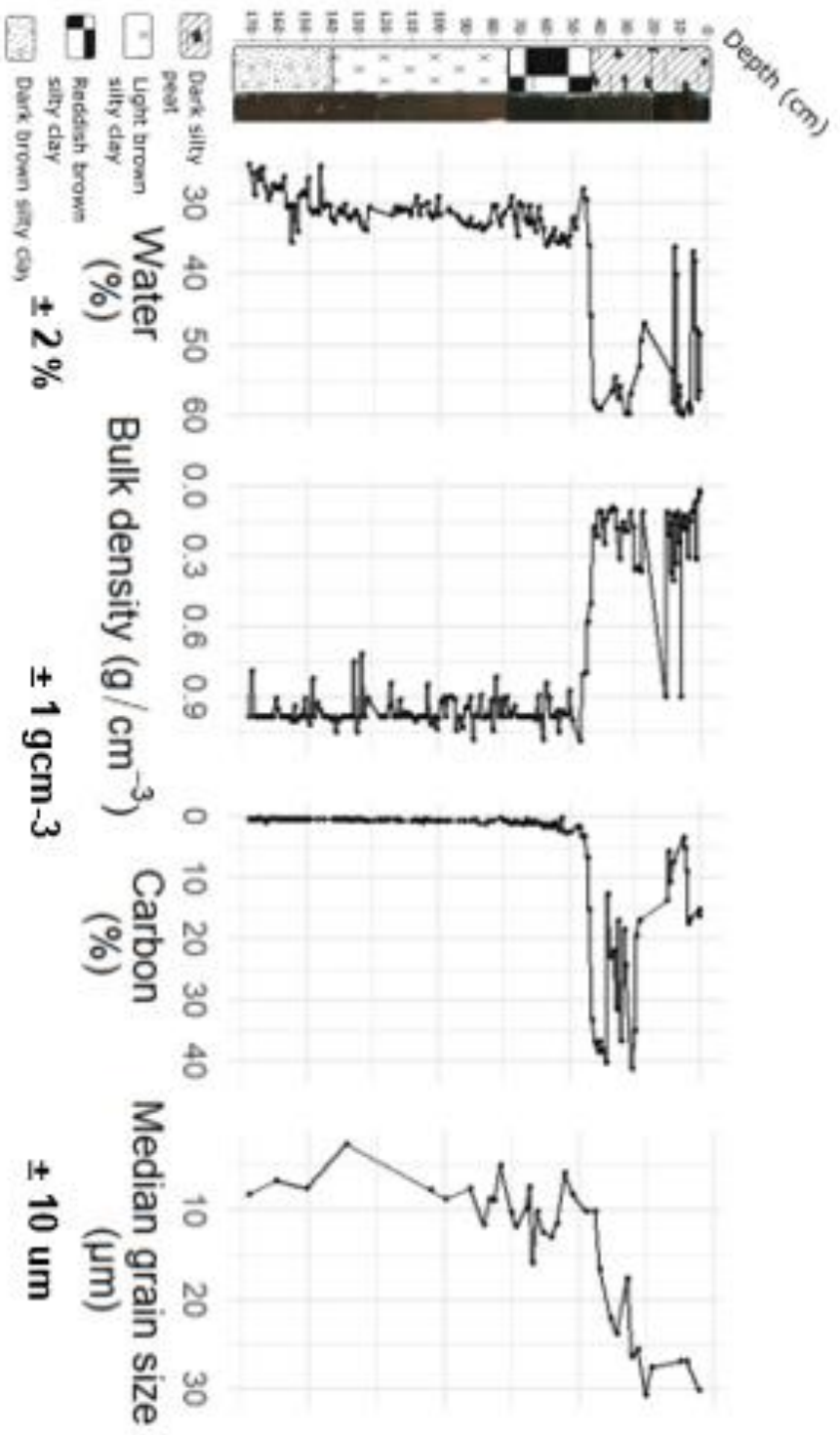

Figure 3.3. Stratigraphy of the Sanamere sediment core

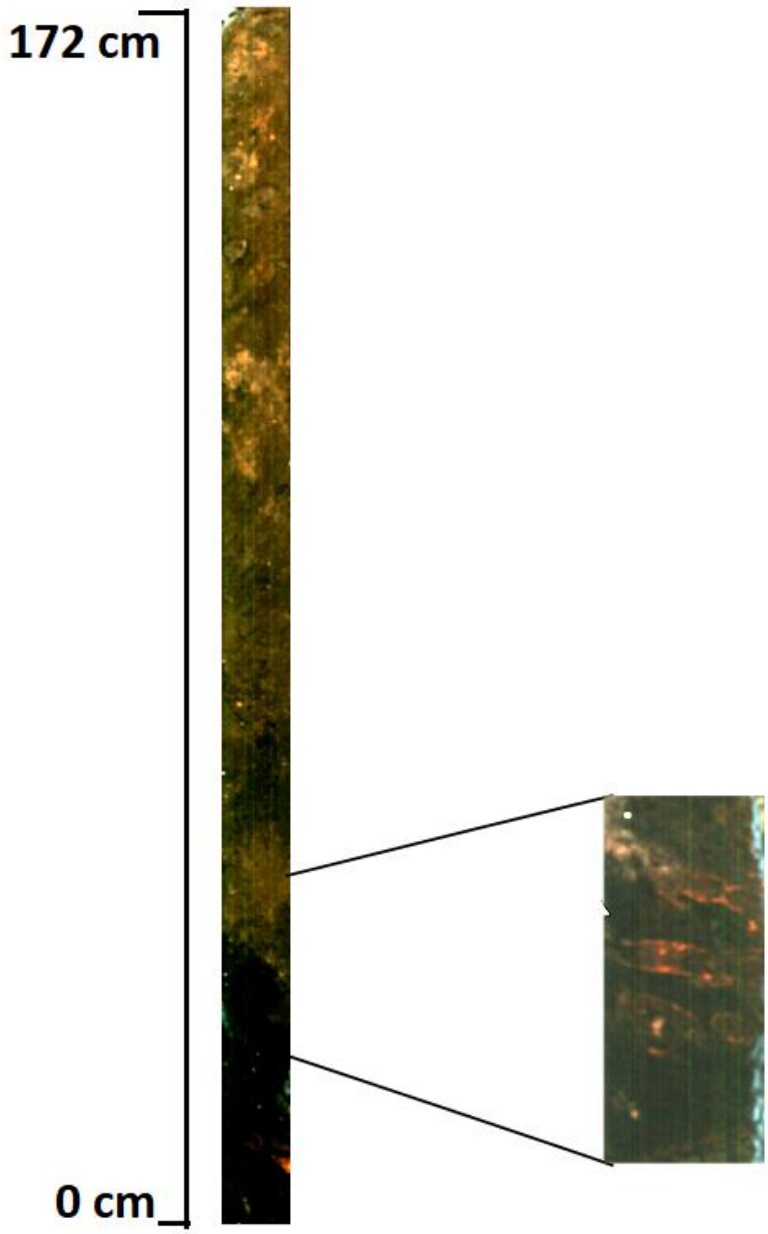

Figure 3.4. Orange bands in the Sanamere core

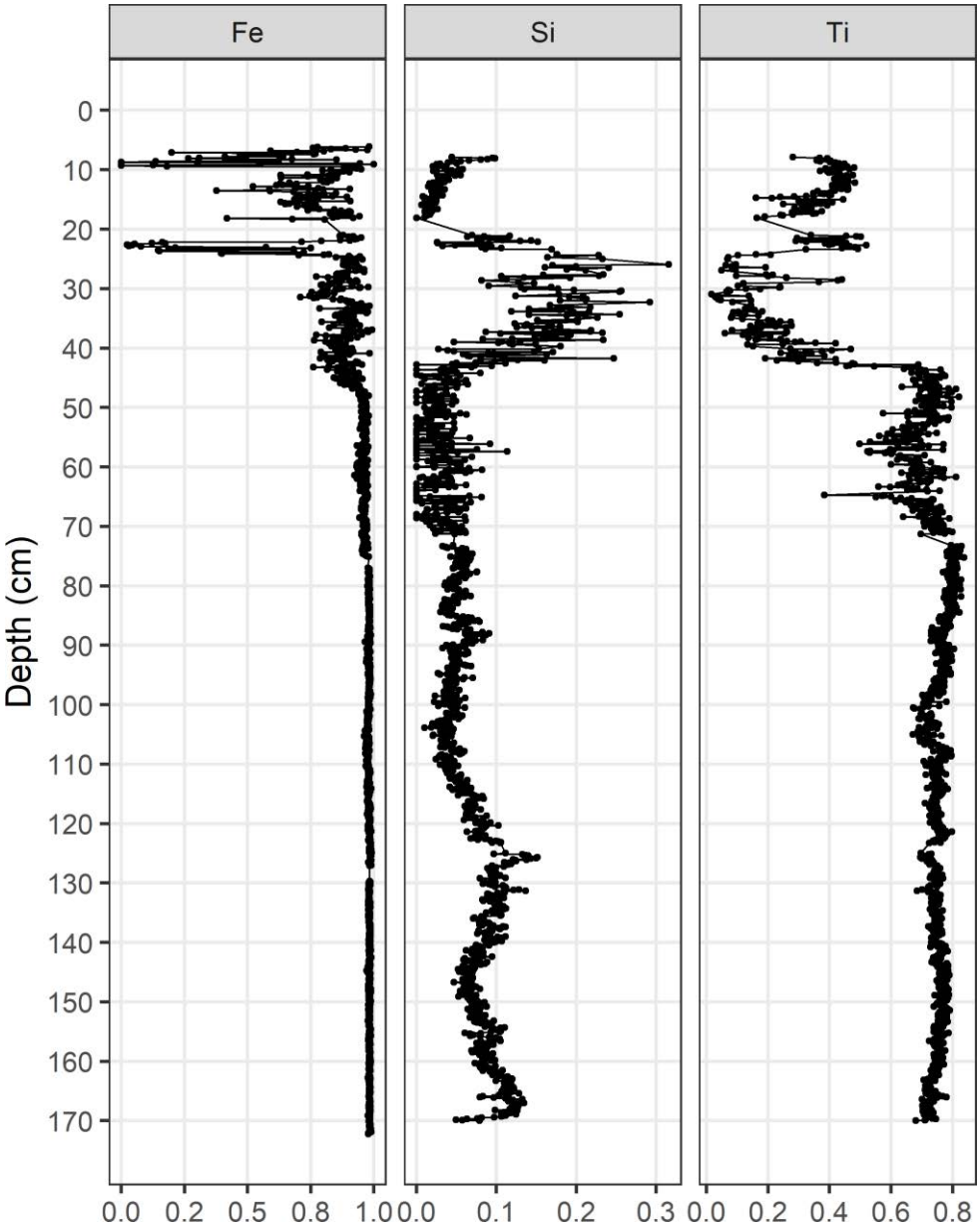

Figure 3.5. Elemental counts in the Sanamere sequence

3.4. **Chapter 3 summary**

The Sanamere core consists of a 1.72 m continuous sediment sequence with no evidence that the lake has dried out during the time-span represented by the core. The first layer (172 cm - 140 cm), is organic poor and very fined grained with moderate bulk density transitioning to an interval from 140 cm to 65 cm that is similar to the previous

one unit, with lighter-coloured sediment and slightly coarser grains. This layer contains three orange bands between 71 and 65 cm. The unit between 65 - 43 cm changes to a reddish-brown color, with increased organic content. The unit between 43 - 0 cm is organic rich, with low bulk density as well as increased grain size and higher water content. High counts of Ti and Fe and low counts of Si dominated the core between 172 - 43 cm and a reverse trend is apparent for the top 43 cm. The following chapter deals with the dating of the sediment core.

Chapter 4. **Developing a radiocarbon chronology for the Sanamere Lagoon sediment core**

4.1. **Introduction**

Obtaining an accurate chronology is fundamental to placing any reconstruction of past environmental change within a robust temporal framework. Selecting a reliable carbon fraction and a pre-treatment that removes all or most of the contaminants are key to obtaining reliable radiocarbon dates (Pettitt et al. 2003; Bronk Ramsey 2008). This selection becomes particularly challenging in the tropics where high annual temperatures negatively and differentially influence the preservation of different organic fractions. Furthermore, the seasonal nature of the tropical hydrological cycle in northern Australia results in high rates of weathering and variable pH and redox conditions, in turn altering carbon cycling and preservation in lake sediment columns (Bird et al. 2002; Higham et al. 2009). Collectively, these conditions limit the availability of those organic components considered more reliable and the dating of other fractions can result in aberrant radiocarbon results that are linked to, for example, poorly preserved or degraded charcoal, identifiable when the combustion yields are lower than usually expected (50–60 % carbon by weight) (Higham et al. 2009). Although there is currently no agreement about which is the most reliable fraction to avoid these issues, short-lived plant macrofossils and charcoal (Cohen 2003; Martin et al. 2019) tend to be among the most favoured materials for dating.

Despite the importance of choosing a reliable carbon fraction that represents the age of contemporaneous sediment deposition, few studies have focused on sediments in the tropics. Comparative studies based on multiple organic fractions in the tropics have focused on swamps (May et al. 2018), peats (Wüst et al. 2008) and organic springs (Field, Marx, et al. 2018), with no studies having been undertaken using lake sediments and no studies in any tropical environment compare more than four fractions. Results from the available studies (as mentioned above) are contradictory regarding the reliability of macro-charcoal and pollen concentrates (yielding anomalously older or younger ages compared to other fractions). Studies in temperate areas have also

reported significant discrepancies between radiocarbon ages for different, supposedly contemporaneous carbon fractions in lake sediments from the same depth. For example, in boreal and Arctic lake sediments wood and charcoal were found to be older than other organic materials such as conifer and deciduous periderms, usually by several hundred years (Oswald et al. 2005). These anomalies are probably the consequence of Inbuilt age of the wood and charcoal.

Discrepancies in age have likewise been found within different types of macrofossils, with some more prone to an apparent 'reservoir effect' (Turney et al. 2000). For instance, pollen, charcoal and bulk sediment are recognized to be highly mobile, porous and heterogeneously sourced, all of which complicates their reliability for radiocarbon dating. Additionally, several studies have demonstrated that there are significant uncertainties associated with simply dating bulk sediment, regardless of the geographical location from where the sample was collected (Björck et al. 1998; Wüst et al. 2008; Xu and Zheng 2003). Extensive research has shown how the effect of contamination depends on the age of the sample (Pettitt et al. 2003; Higham et al. 2011; Wood 2015). Dating beyond 10 ka becomes considerably more problematic as even minimal percentages of contamination can cause hundreds to thousands of years of offset (Aitken 1990; Wood 2015). In fact, offsets of up to 16,000 years between radiocarbon ages from bark and pollen from a tropical peat were obtained in a previous study, with pollen extracts resulting in older dates (Wüst et al. 2008).

Pre-treatment procedures are also fundamental to the generation of accurate radiocarbon ages. While acid-base-acid (ABA treatment) is routinely employed to remove contaminants, it is not always effective (Chappell, Head, and Magee 1996; Gillespie et al. 1992). Notably, the determination of when decontamination is complete is technically challenging (Wood 2015). The base treatment during ABA can further remove charcoal by solubilizing it to 'humic acid', resulting in considerable sample loss. As an alternative to ABA, acid-base-wet oxidation (ABOX) has been found to be more appropriate and an effective method to remove contamination, especially for old samples (Bird et al. 1999, 2014). However, the harshness of the technique can remove excessive carbon and this may limit the application of the technique in the tropics where macroremains are scarce (Bird et al. 1999). Recent studies have shown that ABA- and hypy-treated pairs can produce comparable results to each other in some contexts (Bird et al. 2014; Alex et al. 2017; David et al. 2019). Hydropyrolysis (hypy) (to isolate stable

polycyclic aromatic carbon: SPAC) has shown promising results in mound spring deposits, where the technique appeared to remove the effects of post-depositional modification to the ages obtained from different organic fractions from the sediment (Field, Marx, et al. 2018). Given this promising result, hypy pretreatment might be expected to be similarly effective in lake sediments.

Given the fact that most studies rely on the dates from one organic fraction over the entire sequence, it is imperative to test whether alternative protocols using different carbon fractions, pre-treatments would yield more accurate results across a range of depositional ages. This chapter examines six carbon fractions in samples from Sanamere Lagoon (Figure 4.1) sediment core to determine which fraction and technique pre-treatment is most appropriate to obtain reliable radiocarbon dating results.

4.2. Methodology

Details about the site, field work and core processing can be found in chapter 3. Samples for ^{14}C AMS dating were obtained for six different carbon fractions (hypy, microcharcoal, macrocharcoal, pollen concentrate, 'cellulose' and bulk organics) for six depths spread along the core (Table 4.1, Figure 4.2 and Figure 4.3). These depths were chosen by consideration of the stratigraphic changes (see chapter 3) observed along the sequence (texture, color, elemental abundance). Although attempts to extract all fractions from the same depth were made, this was not achieved as samples from some depths yielded insufficient amounts of carbon after pretreatment to be processed for radiocarbon dating (Appendix 1). In order to address this issue, samples from additional depths were analysed to complete the age-depth model.

4.2.1. Pre-treatment

Pre-treatment of radiocarbon samples for pollen, cellulose, macrocharcoal, microcharcoal and bulk organics (standard method) followed the ANSTO protocols detailed below.

Pollen

Extraction of pollen was adapted from Bennett and Willis (2002). Three sediment samples were washed with 10 % HCl and then passed through a 150 μm sieve. The

smaller fraction was retained and then washed with 10 % NaOH several times until the supernatant was clear. Subsequently, 20 mL of 40 % HF was added and the sample left overnight. Following HF, samples were first washed two times with 2 M HCl and finally with Milli-Q water, until neutral. Lithium heteropolytungstate (LST) with a specific gravity of 1.8 was used for density separation, with the floating fraction retained for examination under the microscope. The resultant pollen concentrate was dried overnight at 60°C.

Bulk organics (standard method)

Five sediment samples were processed at ANSTO following the ABA pre-treatment detailed in Hatte et al. (2001). First, visible contaminants (roots, rocks) were removed and then a wash with 2 M HCl was performed (to remove carbonates), followed by sequential washes of 0.5 %, 1 %, 2 % and 4 % NaOH, until the supernatant liquid was clear (to remove fulvic and humic acids). A wash with 2 M HCl to remove any atmospheric carbon dioxide (CO_2) absorbed during alkali treatment was performed, followed by three washes with Milli-Q water, and the samples were finally oven-dried at 60 °C overnight.

Bulk organics (modified method)

The pretreatment with hydrogen peroxide has proven to be effective in removing contaminant organic matter in radiocarbon dating samples (Chiu et al. 2005). In order to further test the success in removing exogenous organic matter, two additional sediment samples were first pretreated with 30 % hydrogen peroxide overnight at the Advanced Analytical Centre at James Cook University Cairns, freeze dried and then sent for standard ABA pre-treatment at the Waikato Radiocarbon Dating Laboratory. This procedure involved the removal of visible contaminants, following with the samples washed with hot HCl, then rinsed and treated with multiple hot NaOH washes. The NaOH insoluble fraction was treated with hot HCl, filtered, rinsed, and dried.

Macro and microcharcoal

Charcoal samples at 6 cm were pre-treated with 30 % hydrogen peroxide for 2 h and then passed through 250 μm and 63 μm sieves. These two fractions were then examined under the microscope, and pieces of charcoal were recovered using tweezers (in the case of the >250 μm fraction) and an Eppendorf InjectMan® 4 micromanipulator (for the 63 - 250 μm fraction). Samples were then washed with 0.5 % NaOH and 2 M HCl. Samples at 3 and 82 cm were pre-treated with 10 % hydrogen peroxide and the pre-treatment followed as above.

Cellulose

Extraction of cellulose was adapted from Gillespie (2019). Three sediment samples were pre-treated with 1 M NaOCl/NaOH for 2 hours and washed with 1 M HCl. The samples were then reacted with 1 M $NaClO_2$/HCl for another 2 hours and then washed with 1 M HCl. This procedure was then repeated, and the samples were washed with water three times. Finally, samples were oven-dried at 60°C overnight.

Hypy fraction

Fourteen sediment samples were pretreated using hypy to isolate the pyrogenic carbon (PyC) (Ascough et al. 2009; Meredith et al. 2012). First, 30 % hydrogen peroxide was added to the samples. The samples were left overnight then washed with 2 M HCl and freeze dried. Aliquots of each sample were then loaded with a catalyst (0.2M ammonium dioxydithiomolybdate [(NH4)2MoO2S2]) and 20 % MeOH/H_2O solution, sonicated for 15 min and dried over a hotplate at 60 °C. These samples were placed in the HyPy reactor, pressurized with hydrogen (H_2) to 150 bar with a gas flow of 4 L/minute over 40 minutes. Finally, samples were washed for 2 hours with 6 M HCl at 60 °C.

4.2.2. **Graphitization and measurement**

Samples were combusted at 900 °C to convert them to CO_2, followed by graphitisation using the H_2/Fe method (Hua et al. 2001). Carbon-14 measurement of all samples was undertaken by Accelerator Mass Spectrometry (AMS) on the VEGA and ANTARES accelerators at ANSTO (Fink et al. 2004) except for samples Wk50327 and Wk50328, which were sent for standard ABA pre-treatment at the University of Waikato Radiocarbon Dating Laboratory. The process involves pre-baking tubes, CuO and silver (added to the tube to capture any sulphur that might be present in the sample) in the oxygen stream before loading to remove any traces of surface carbon contamination. Samples went through standard sealed quartz tube combustion with CuO and silver wire. In parallel with actual samples a blank is used (or a few of them) – same tube(s) with same reagents but the source of carbon is dead geological graphite – to determine the level of inadvertent contamination in the process of combustion transfer and graphitisation. Final results are corrected for this, though usually it is a very small quantity.

4.2.3. **Calibration**

All samples were calibrated using the Oxcal Program and the IntCal13 calibration curve (Reimer et al. 2013) with 0 calibrated years before present representing 1950 AD. IntCal13 was used rather than SHCal13. IntCal13 was used due to the influence of Northern Hemisphere air masses on the Tropical North of Australia, when the Inter Tropical Convergence Zone moves southwards during the Australian-Indonesian summer monsoons (Hogg et al. 2013). The rbacon R package (Blaauw and Christen 2019) was used to create the age models for the core.

Figure 4.1 Sanamere Lagoon on Cape York Peninsula

4.3. **Results**

A total of 27 radiocarbon dates were obtained for 17 different depths along the core (Table 4.1). Overall, the calibrated ages ranged from 2,067 - 2,466 cal BP at 3 cm (hypy fraction) to 30,889 - 31,304 cal BP at 162 cm (hypy fraction), spanning 29,237 years in total. As discussed above, ages were obtained for more than one fraction from six depths. Table 4.1 shows the results from the radiocarbon dating measurements and the calibrated results. From the bottom of the core to 82 cm, the availability of fractions to compare was reduced to bulk organics, the hypy fraction and pollen concentrates, as these were the only fractions to yield sufficient carbon to be analysed by AMS. Therefore, charcoal fractions > 63 μm and cellulose could not be analysed below 82 cm. From the three depths originally processed with the cellulose pre-treatment method only one sample (OZY419) retained enough carbon to be measured, given the aggressiveness of the pretreatment.

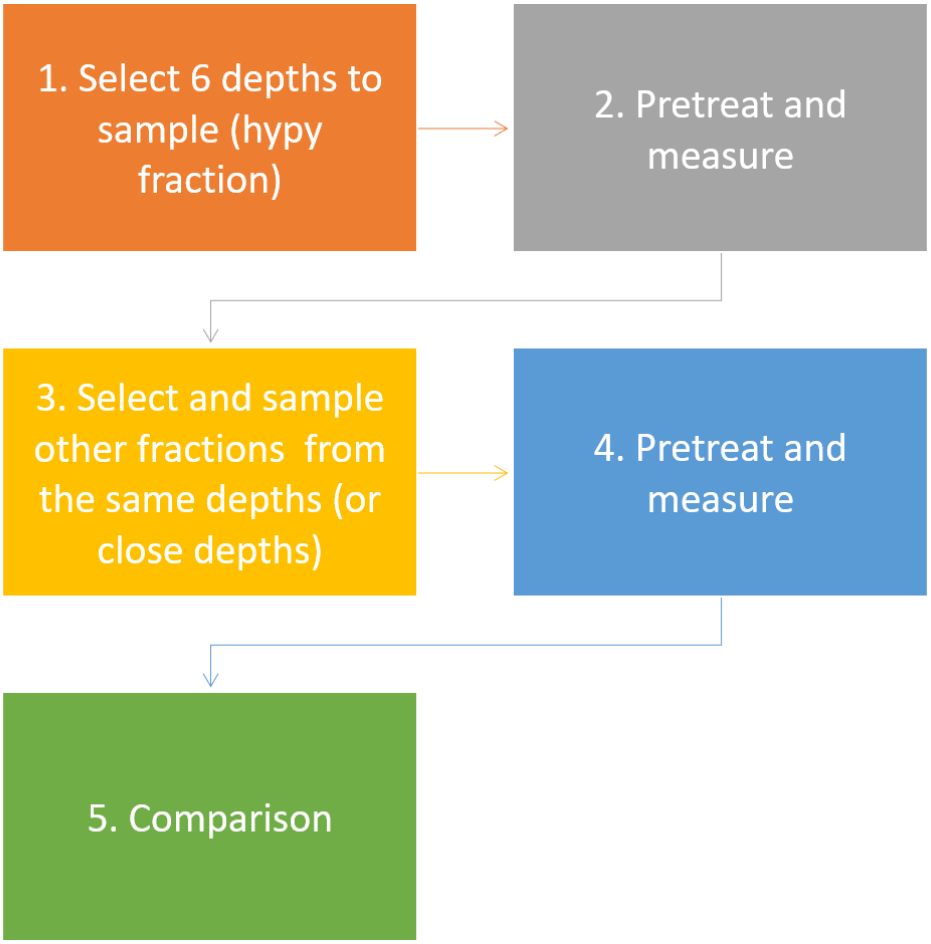

Figure:4.2. Summary of methods

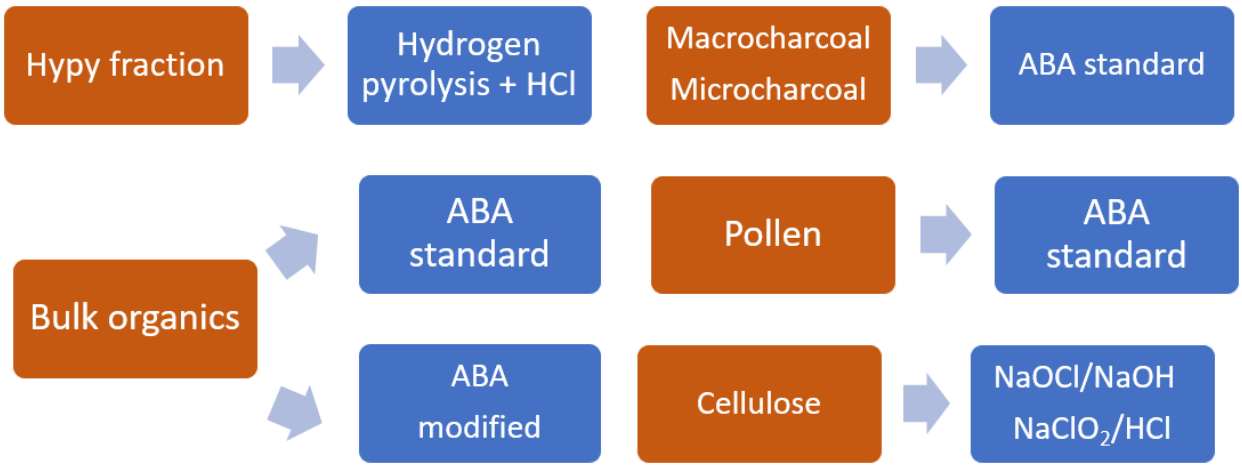

Figure 4.3. Carbon fractions and corresponding pretreatment techniques

The micro-charcoal result at 3 cm showed the largest age reversal overall, 8,990 cal years older than the hypy date at the same depth (Figure 4.4). Two pairs of hypy ages also showed age reversals, with the smallest (a difference of 705 cal years) between the dates at 23 and 32 cm and the largest between the dates 90 and 105 cm (a difference of ~1,100 cal years). The only cellulose sample yielded a younger date in comparison to what was expected for that depth based on the other results (Table 4.1, Figure 4.4).

The difference between the ages from different fractions generally increased with depth (Table 4.2). The only section of the core where all dating results overlap (except for the pollen concentrate) is at 6 cm, while the other five depths showed large differences between the results from different fractions, with the largest offset at 146 cm (a difference of ~16,500 years), between hypy and pollen. The bulk organic fractions pretreated with standard ABA procedures also differed significantly from the hypy fraction (being up to ~9,500 years younger than the former). Although not from the same depths (but within 10 cm), the modified ABA pretreatment (samples Wk50327 and Wk50328) yielded results that aligned closely with the hypy results at the two depths they could be compared.

In four out of six cases (the deepest samples), hypy yielded the oldest age from those available at that depth, and in two cases (the shallowest samples), hypy yielded the youngest results. Bulk organics (standard ABA) yielded the youngest result for four depths (43, 67, 137 and 146 cm). The pollen results were inconsistent, yielding the oldest and youngest dates at 6 cm and 146 cm, respectively (Table 4.2).

4.4. **Discussion**

4.4.1. **Assessment of reliability**

The hypy dates yielded the oldest dates and the most consistent internal chronology with only two minor age reversals (at 23 and 90 cm). Although previous studies suggest that hypy dates could be biased to older ages due to potential for reservoir effects (Field, Marx, et al. 2018), this study found this pre-treatment and its resulting carbon fraction (SPAC) to be the most reliable.

All ages returned (except at 6 cm) following hypy pre-treatment are considerably older than dates from comparable levels for other carbon fractions. This finding is consistent with the results obtained from the radiocarbon dates from organic spring deposits in northwest Australia, where hypy ages were found to be older than other fractions, but also considered more reliable based on their more consistent age-depth relationship within each core (Field, Marx, et al. 2018). Hypy reduces labile organic matter to volatile products (Ascough et al. 2009) and potentially removes > 92 % of all labile carbon (Bird et al. 2014). Hypy represents the carbon fixed by pyrolysis at the time of a burning event, therefore the 'indigenous' or core component of the original charcoal (Ascough et al. 2009, 2010).

Table 4.1. Conventional and calibrated dates from all samples tested in the study

Laboratory Code	Depth (cm)	Conventional radiocarbon ages (1 sigma)	Calibrated age range (95 %)	Carbon fraction dated	Pretreatment method
OZY416	3.0	2,270 ± 70	2067 – 2466	SPAC	Hypy
OZY423	3.0	11,260 ± 160	12742 - 13368.5	Charcoal >63 um	ABA
OZX672	6.0	3,840 ± 45	4099.5 – 4412	SPAC	Hypy
OZY131	6.0	4,450 ± 30	4894 - 5284.5	Pollen	ABA
OZX765U2	6.0	4,180 ± 140	4243 – 5040	Charcoal >63 um	ABA
OZX765U1	6.0	4,120 ± 100	4296.5 – 4845	Charcoal >250 um	ABA
OZX765	6.0	4,165 ± 35	4580 - 4830.5	Bulk organics	ABA
OZY417	12.5	4,230 ± 70	4535 – 4960	SPAC	Hypy
OZY418	23.0	7,140 ± 80	7798 – 8162	SPAC	Hypy

Laboratory Code	Depth (cm)	Conventional radiocarbon ages (1 sigma)	Calibrated age range (95 %)	Carbon fraction dated	Pretreatment method
OZY333	32.0	6,435 ± 30	7292.5 – 7425	SPAC	Hypy
OZY419	42.0	6,150 ± 80	6754.5 - 7239.5	Cellulose	Gillespie
OZX673	43.0	8,660 ± 40	9774 - 10164.5	SPAC	Hypy
OZX766	43.0	7,750 ± 35	8435 - 8594.5	Bulk organics	ABA
OZX674	67.0	15,240 ± 60	18344 - 18670.5	SPAC	Hypy
OZX767	67.0	9,900 ± 50	11208 - 11599.5	Bulk organics	ABA
OZY420	76.0	17,670 ± 160	20929 - 21825.5	SPAC	Hypy
OZY758	82.0	10,940 ± 110	12665.5 – 13036	Charcoal >63 um	ABA
OZY421	90.0	19,450 ± 80	23101.5 – 23685	SPAC	Hypy
OZY422	105.0	18,350 ± 170	21815 – 22540	SPAC	Hypy
Wk50327	114.0	23,549 ± 126	27470 - 27889.5	Bulk organics	H2O2 + ABA
OZX675	137.0	24,340 ± 190	27932.5 – 28765	SPAC	Hypy
OZX768	137.0	15,560 ± 90	18620.5 – 18996	Bulk organics	ABA

Laboratory Code	Depth (cm)	Conventional radiocarbon ages (1 sigma)	Calibrated age range (95 %)	Carbon fraction dated	Pretreatment method
OZX676	146.0	26,290 ± 260	29870 – 31010	SPAC	Hypy
OZY132	146.0	11,920 ± 40	13567 – 13944	Pollen	ABA
OZX769	146.0	16,270 ± 70	19449 – 19905	Bulk organics	ABA
Wk50328	150.0	25,931 ± 167	29655 – 30683	Bulk organics	H2O2 + ABA
OZX677	162.0	27,100 ± 140	30889.5 – 31304	SPAC	Hypy

Table 4.2. Offset, minimum and maximum calibrated ages by depth

Depth (cm)	Minimum age	Carbon fraction (min)	Maximum age	Carbon fraction (max)	Offset	Number of dates
3	2067.0	Hypy	13368.5	Charcoal >63 um	10788.75	2
6	4099.5	Hypy	5284.5	Pollen	833.50	5
43	8435.0	Bulk organics	10164.5	Hypy	1454.50	2
67	11208.0	Bulk organics	18670.5	Hypy	7103.50	2
137	18620.5	Bulk organics	28765.0	Hypy	9540.50	2
146	13567.0	Pollen	31010.0	Hypy	16684.50	3

The hypy dates at 23 cm (~7,800 - 8,200 cal yr BP) and 32 cm (7,300 - 7,400 cal yr BP) show an age reversal of 506 - 870 years (Figure 4.4). These dates are from the section of the core that has high organic content, high pyrogenic carbon mass accumulation rates (refer to chapter 6) and large fluctuations in the normalized titanium counts (range 0.02 - 0.45). Both changes in erosion (as evidenced by clastic input) and high organic input at this time suggest that some reworking could have happened during this period, which coincides in timing with the flooding of the adjacent continental shelf in response to an increase in sea level during the early Holocene in north Australia (Sloss et al. 2018; Chivas et al. 2001; Yokoyama et al. 2001; Reeves et al. 2013), and therefore to a period of wetter climate, with potentially more intense seasonal rainfall events. More overland transport of soil material from the catchment, may well have transported ‘old’ charcoal into the lake at this time. A second age reversal is present between results at 90 cm and 105 cm (1,100 years) in the hypy results, with the only apparent sedimentological indication of change being a slight decrease in the titanium counts down-core between these two depths. It is possible that the date at 105 cm exhibits an incomplete removal of exogenous carbon, the main issue identified when applying hypy pre-treatment to charcoal formed at 400°C or below (Bird et al. 2014).

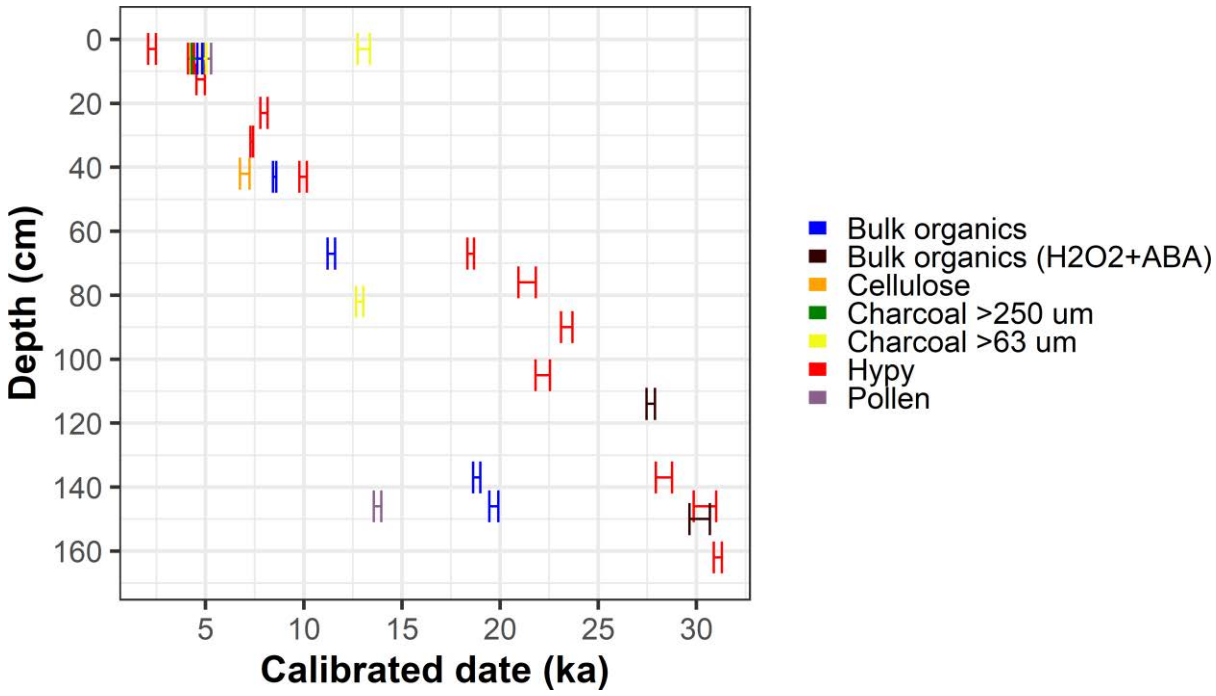

Figure 4.4. Calibrated ages by depth and carbon fraction along the Sanamere sediment core

The results from fractions other than hypy at the same or comparable depths (except at 6 cm) were uniformly younger than the hypy results. Besides the possibility of the physical mobility of material in the sediment columns, it is likely that the differences between the ages of fractions at 43, 67, 137 and 146 cm are the result of unremoved contamination by carbon of a different, generally younger age in the bulk organics (standard treatment) and pollen fractions. The mobilization of materials and therefore, the contamination of samples with exogenous carbon is made more likely in the Sanamere sequence because the entire 31,000 years of accumulation is represented in only 172 cm of sediment. The top 43 cm contains high proportions of water, which also facilitates the mixing of materials by physical translocation and/or solubilization.

The results suggest that, for most samples in this study, the standard ABA pretreatment was ineffective in removing modern contamination from the bulk organic fraction. An inbuilt ‘reservoir’ age associated with a period of storage in the lake catchment may have biased the hypy results to older ages by an unknown amount. However, it is unlikely that this could cause such large offsets between the hypy ages and ages from the other fractions. If there was a reservoir offset relating to a period of storage of up to ~ 9,500 years in the catchment, this would manifest itself in the hypy

dates throughout the sequence, whereas what is observed is a generally smaller offset up the core. Indeed, the uppermost hypy date is younger than that of the other fractions, implying the circulation of carbon of an apparent age representative of all carbon in the sediment through the relatively thin sediment pile, such that dates high in the sequence are biased old and dates deeper in the sequence are biased young.

Further evidence that there is no substantial reservoir effect on the hypy dates is provided by the observation that the two samples subject to the modified bulk organic pretreatment, where peroxide was used before standard ABA yielded results close to those obtained from the hypy fraction. Except for the anomalous charcoal result at 3 cm, and the slightly old pollen age at 6 cm, all ages from all fractions and pretreatments before 23 cm overlapped (when they belonged to the same depth) and did not show any age reversals. Below 23 cm, large offsets between samples from the same depth and age reversals were observed (Figure 4.4).

The increasing magnitude of the difference between hypy and the other fractions ages with depth/age is consistent with what would be expected for the younger samples having between 2 and 5 % unremoved modern contamination (Wood 2015), or more contamination of an older aggregate apparent age.

The results strongly indicate the presence of unremoved exogenous carbon contamination in some of the fractions. For example, the largest offset between two fractions was found at 146 cm (~16,700 years) between pollen and hypy, which suggests that pollen from higher depths mobilized down the core and/or the concentrate contained exogenous younger materials. The two pollen concentrate samples available show inconsistent results, as has been found in previous studies (younger (Field, Marx, et al. 2018; May et al. 2018) or older (Neulieb 2013; Fletcher et al. 2017)), with the sample at 6 cm having the oldest age compared with the other fractions at the same depth, while the sample at 146 cm is the youngest compared to the bulk organics and hypy results. When inspected under the microscope, these samples appeared to be composed by around 50 % pollen, with the rest of material being plant material and charcoal. This addition of heterogeneously sourced materials could have added exogenous carbon contamination resulting in the aberrant results. Other studies also have identified anomalous, generally younger ages derived from pollen concentrates (May et al. 2018; Clymo and Mackay 1987) due to the high physical mobility of small

particles but also the high porosity of the pollen walls, which can sorb and accumulate exogenous carbon (Kilian et al. 2002). The existence of clearly anomalously young pollen dates strongly suggests that there is potential for contamination by young carbon in all the organic fractions.

Large offsets (up to ~ 9,500 years) were also found between bulk organics and hypy, with the former showing younger ages. This finding is consistent with previous studies which found that bulk organics pretreated with standard ABA can yield anomalously young dates (Wang, Amundson, and Trumbore 1996; Wüst et al. 2008; Pessenda, Gouveia, and Aravena 2001). Although measured at 42 cm (not 43 cm as the other two fractions), the cellulose extraction yielded an age younger compared to what was expected from the bulk organics and hypy age-depth relationship.

While the results from micro and macro charcoal were expected to be tested along the entire core to better understand differences in their sources, their availability was limited below 82 cm. As the age ranges obtained for both overlapped at 6 cm, the possibility that they represent different sources is low. The charcoal samples (>63 μm fraction) at 3 cm and 82 cm showed older and younger dates (respectively), compared to the age/depth relationships expected from the relationship determined by samples treated by hypy or modified ABA. It is possible that the incomplete removal of organic contaminants by the standard ABA method caused this offset. Given its large surface area and porosity, charcoal is known for absorbing exogenous carbon, which can undergo irreversible reactions with the charcoal surface. Charcoal is also suitable for microbial colonization, and microbial carbon cycling could also lead to the incorporation of exogenous carbon (Bird, 2007).

4.4.2. **Developing a robust chronology**

While two age-depth models were built with the results from bulk organics (ABA) and hypy ages (Figure 4.5), the model including only the hypy ages was the most consistent with the stratigraphic and sedimentologic changes identified in the Sanamere sequence (chapter 3), and is preferred over what also appears to be a reliable chronology based on the bulk organic ages based on the discussion above. This model included 13 hypy samples (Table 4.1), with all but two ages (23 cm and 105 cm) fitting within the 95 % confidence interval. The modelled ages ranged between 0.4 (3 cm) and

33,000 cal yr BP (162 cm). The peroxide+ABA pretreated bulk organics samples also agree reasonably well with the hypy-only model, including one of the dates fitting within the error range, and the other yielding a slightly older date (by 314 years). This further supports the reliability of the hypy results and bolsters the conclusion that old contamination has not affected the hypy results to any significant degree.

The timing of changes in sedimentation rate inferred using the hypy model is consistent with the observed changes in sedimentology observed at 43 cm and 71 cm, which are the upper and lower bounds of two of the stratigraphic units observed in the Sanamere sequence (chapter 3, Figure 4.5). Between 71 and 172 cm, there are no major sedimentological changes, (other than the inclusion of more coarse clastic debris at 140 cm down-core). The charcoal samples (both sizes) were consistent with hypy ages at 6 cm, but not down-core. This inconsistency suggests that dates from pieces of charcoal pre-treated only by ABA could lead to biased results. Again, the hypy samples appear more reliable, as total pyrogenic carbon content measured using the hypy technique is less likely to be biased by individual charcoal fragments, each of which may have some (unknown) residence time prior to deposition in the lake sediment and/or degree of unremoved contamination.

Although the age-depth model built with the standard ABA-pretreated bulk organics samples had no age-reversals, and a range between 4,100 to 22,300 cal yr BP, the modelled ages were not consistent with the stratigraphic changes in the Sanamere sequence (in contrast with the hypy model). Additionally, none of the pollen and cellulose samples fit within the age-model derived from the organics or bore any relationship to the observed stratigraphic units in the sequence, regardless of depth. These inconsistencies between pollen, cellulose and bulk organics ages suggest that results from any of these fractions are likely biased by unremoved contamination or physical translocation to a variable degree.

Additional evidence to support the choice of the hypy model is its consistency with the timing of environmental events. For instance, the layer 65 - 71 cm matches the time period 18,000 – 20,000 cal yr BP, identified as a period of environmental change in regional studies (Reeves et al. 2013). Strong evidence from paleoenvironmental studies has been found to support the dominance of cooler and drier conditions during this period in tropical Australasia (Reeves et al. 2013; Turney et al. 2006; Burrows et al.

2016). In contrast, this layer was modelled as 11,000 – 11,600 cal yr BP based on the age model derived from the bulk organics (ABA) curve. Moreover, the hypy chronology is consistent with the most likely timing for the formation of the lake ca. 33,000 cal yr BP. In this instance, a collapse in laterite karst formed a depression, as a result of lowered water tables that would accompany the rapid drop in sea level and drier conditions moving from MIS3 into MIS2 (Xu, Lai, and Li 2019).

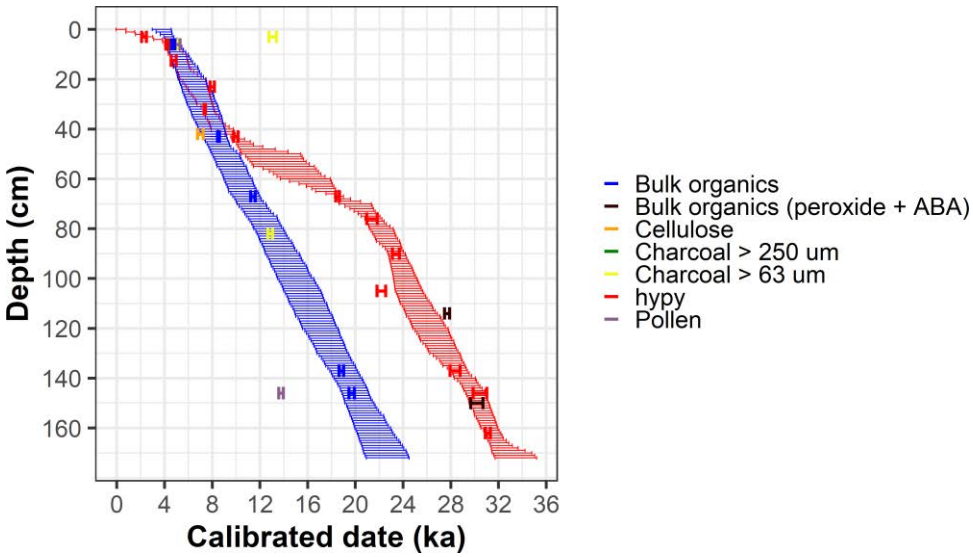

Figure 4.5. Age-depth models (95 % confidence error bars) constructed using Bayesian age modelling with rbacon package in R. Chronology based on Hypy is represented in red and chronology based on bulk organics in blue, along with the calibrated ages from additional carbon fractions, none used in the construction of either chronology.

Finally, the results from this study highlight the importance of comparing the results from different fractions (when using radiocarbon dating) or contrasting the ages from multiple dating methods when building to support the construction of palaeoenvironmental proxy records and comparing results those derived from other dating methods. Caution should be exercised when interpreting chronologies derived from bulk organics carbon fractions. Although the chronology obtained using bulk organics with the standard ABA-pretreatment method appeared to be consistent and with no age reversals, hypy provides the most robust chronology for the Sanamere Lagoon sequence and indicate the bulk organics chronology to be incorrect.

4.5. Chapter 4 summary

The selection and pre-treatment of a reliable organic fraction from which to acquire radiocarbon ages is fundamental to the development of accurate and precise chronologies. Sampling from tropical lakes is particularly challenging given the adverse preservation conditions and diagenesis in these environments. This chapter examines and quantifies the differences between the radiocarbon date results and reliability from different carbon fractions and pretreatments from the same depths from Sanamere Lagoon, a tropical lake sediment core (1.72 m long) located in north Australia. Six different organic fractions (bulk organics, pollen concentrate, cellulose, stable polycyclic aromatic carbon (SPAC), charcoal >250 um and charcoal >63 um), for a total of 27 radiocarbon dates, were compared in six different depths along the core. Acid-base-acid (ABA), modified ABA (30 % hydrogen peroxide + ABA), 2chlorOx (a novel cellulose pre-treatment method) and hydrogen pyrolysis (hypy) were used to pre-treat the correspondent organic fractions.

The oldest age is 31,300 cal yr BP ka and the youngest is 2,500 cal yr BP, spanning 29,247 years. The smallest offset between the minimum and the maximum age in a given depth was found to be 975 years (between SPAC and charcoal >63 um) and the largest ~16,500 years (between pollen concentrate and SPAC). The SPAC fractions pre-treated with hypy yielded older ages compared to all other fraction in most cases, while bulk organics consistently yielded younger ages. The magnitude and consistency of the offsets and the physical and chemical properties of the tested organic fractions suggest that SPAC is the most reliable fraction to date in tropical lake sediments and that hypy successfully removes contamination sourced from exogenous carbon.

The Sanamere Lagoon chronology was built exclusively using samples pretreated with hypy. Hypy outperforms the other procedures to pretreat samples for radiocarbon dating, and it was the most consistent with the stratigraphical changes found in the core.

Chapter 5. **The palaeohydrological record of Sanamere Lagoon**

5.1. **Introduction**

This chapter presents a continuous terrestrial record of hydrological change covering the last ~ 33 ka of Sanamere Lagoon located in an under-studied region of northeast Australia. I present a lake sediment record, combining geochemical (micro X-ray fluorescence [μXRF] scanning, carbon and nitrogen content and associated stable isotopes), physical (grain size) and biological (diatoms) proxy data sets. Three main sections guide this chapter. The first section describes the methodology used to reconstruct fire and vegetation; the second section presents the results, and the last section discusses the results in terms of the broad temporal and regional trends.

5.2. **Methodology**

Details about the site (chapter 2), fieldwork (chapter 3), core processing (chapter 3), and chronology (chapter 4) can be found in previous chapters.

5.2.1. **Sedimentation rates**

The radiocarbon dating and the age model results are presented in Figure 5.1. Ages were interpolated for each depth point using the age-depth model (built in chapter 4), and sedimentation rates were calculated over 1 cm intervals using the number of years covered by that interval according to the age-depth model using only the Hypy dates.

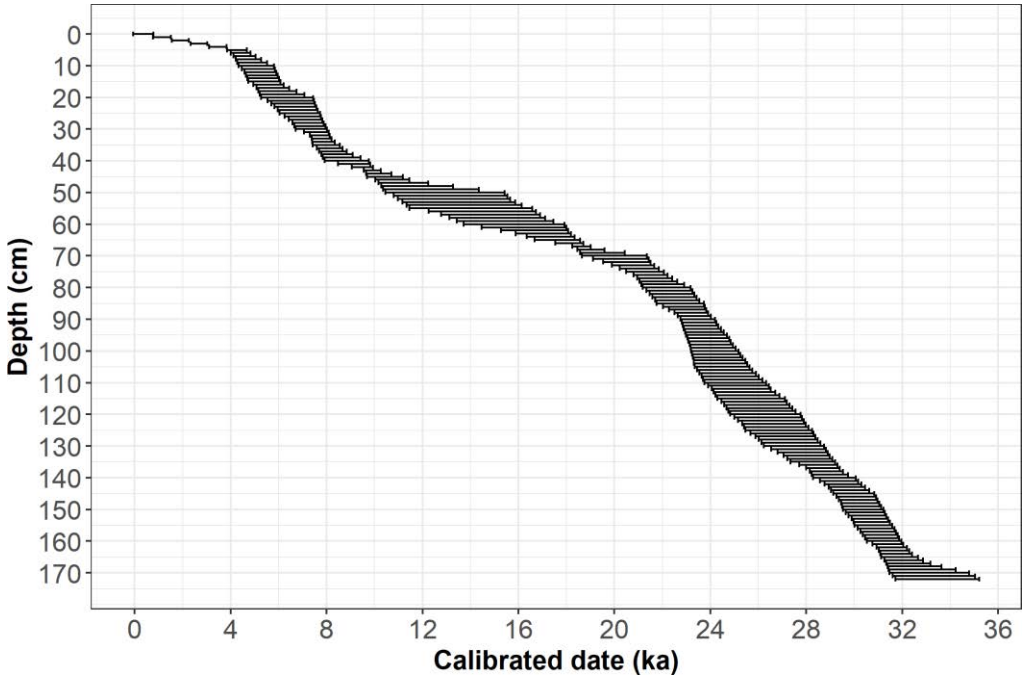

Figure 5.1. Age-depth model

5.2.2. **Grain size**

Grain size analyses followed the procedure in section 3.2.2.3.

5.2.3. **Elemental abundance**

X-ray fluorescence (μXRF) elemental profiles were completed for the four sections of the core (0-50, 50-100, 100-150, 150-172 cm), for the total of 172 cm, using the second-generation ITRAX core scanner located at the Australian Nuclear Science and Engineering Organisation (ANSTO). Although the scanner produced data for a total of 25 elements (Al, Si, S, Cl, Ar, K, Ca, Ti, V, Cr, Mn, Fe, Ni, Cu, Zn, Br, Rb, Sr, Y, Zr, Pd, Ba, La, Ce, Pb), only those elements that produced valid and above background counts were selected for comparative and statistical analyses. To determine if a measurement was valid, the sample surface, argon and total counts were analysed for anomalous and/or inconsistent behavior. For example, out of range values were removed from the corresponding dataset. The selected elements were normalized by calculating the proportion of counts of each element per total counts at each depth (Rothwell and Rack 2006), resulting in a dimensionless value. A ten-point running mean

was calculated for the normalized ratios, which gave an effective sample interval of 1 cm. High abundances of lithogenic elements such as iron (Fe), titanium (Ti), aluminum (Al), and calcium (Ca) in lake sediments can indicate times of low lake level or greater material transport under conditions of higher precipitation and consequent runoff (Douglas, Brenner, and Curtis 2016). Ti is often used as a proxy for erosion and transport of silt and fine sand and it is often associated with Fe. Potassium (K) is used as an indicator of detrital input, and strontium (Sr) is associated with terrigenous sources such a as feldspars and clays. Si:Ti ratios are interpreted as a measure of biogenic silica (Davies, Lamb, and Roberts 2015). The use of Si:Al ratios as proxies for grain size (Turner et al. 2015) was validated by comparing the results with the grain size measurements obtained by laser diffraction (section 3.2.2.3). The ratio of incoherent (inc) to coherent (coh) dispersion depends on the average atomic number of the sediment material (Rothwell and Rack 2006). Generally, it correlates with organic carbon content (Burnett et al. 2011), since the organic elements have average atomic weights smaller than aluminosilicates or quartz. The ratio of inc/coh was also validated as a proxy of organic content using the carbon abundance data (section 5.2.5).

Stratigraphic units, based on the ITRAX results, were delineated using hierarchical clustering and a broken stick model using the packages vegan (Oksanen et al. 2019) and rioja (Juggins 2017), with Euclidean distance and constrained cluster analysis by the incremental sum of squares (CONISS) as the clustering method. The broken stick model separates the data into intervals and fits a separate line segment to each interval. The stratigraphic units defined using ITRAX were compared to the ones defined visually (chapter 3).

The μXRF core scanning results were also summarized using a principal curve (PC). A PC is a smooth one-dimensional curve that passes through the middle of a p dimensional dataset, providing a nonlinear summary of the data. The PC takes the form of a curve, after being fitted through multiple dimensions (Simpson and Birks 2012).

5.2.4. **Diatoms**

The core was sampled for diatom analysis every second centimeter between 1 cm and 43 cm and every three centimeters there-after. Sample processing followed standard techniques (Morley et al. 2004), including sample deflocculation, oxidation of

organic matter by adding 30 % hydrogen peroxide, isolation of diatom frustules by floatation in heavy liquid (Sodium Polytungstate, s.g. = 2.15 g/cm^3), centrifuging for 15 minutes at 1500 rpm and then transferring the light fraction by pipette to a clean tube. The concentrate thus obtained was diluted to 4 mL and an aliquot was transferred to a microscope slide to be counted using a Nikon Eclipse TE300 microscope. The volume in the tube and the volume pipetted in the slide were recorded, so the concentration of diatoms per sample could be calculated. This procedure was chosen, instead of Battarbee (2002), given the low concentration of diatoms in some of the core sections, along with the interference of clay. Cautious interpretations were made following the limitations of the used procedure. Each sample was counted until at least a total of 300 complete valves were identified or a maximum of 10 transects were counted from each slide. Diatoms were identified using various taxonomic guides (Gell, 1999; Sonneman 1999; Krammer and Lange-Bertalot, 1999). The relative abundance of each species was calculated as a proportion of the total. Raw diatom counts were converted to relative abundance before statistical analysis. Diatom autecology was established using published studies and databases (Whitmore 1989; Carter and Flower 1988; Spaulding and Edlund 2010; Dam, Mertens, and Sinkeldam 1994; Potapova et al. 2020).

Diatoms are widely established indicators of palaeoenvironmental conditions, demonstrating specific preferences for aquatic habitat types and water quality conditions (Battarbee et al. 2002; Stoermer and Smol 2001). On Cape York Penninsula, diatom species composition has been previously correlated with total alkalinity, bicarbonate concentration, pH, electrical conductivity (EC) and latitude (Negus et al. 2019). This correlation confirms the potential for using these organisms as palaeoclimate proxies in this area.

5.2.5. **Carbon and nitrogen abundances and isotopes**

Section 3.2.3 details the methods for elemental and isotopic abundance analyses.

The composition of organic matter in lake sediments depends on the amount and type of allocthonous and autochthonous material deposited at different times in the history of a lake (Meyers 1997). The source of organic matter in the Sanamere Lagoon sediments was assessed using bulk sedimentary nitrogen and organic carbon isotope

values, as well as carbon to nitrogen (C:N) ratio. C:N ratios have often been used to distinguish the origins of sedimentary organic matter, with algae demonstrating ratios between 5 and 8, and vascular plants > 20. Ratios of ~10–20 mark the transition from primarily aquatic (< 10) to primarily terrestrial (> 20) organic matter (Meyers and Ishiwatari 1993, 1995).

Carbon isotopes in terrestrial organic matter can be used to track variations in the proportion of C_3 and C_4 plants in the lake catchment, generally interpreted in the tropics as indicating changes in moisture availability (Rao et al. 2017; Stewart et al. 1995). Carbon isotopes of algal organic matter also reflect the availability of dissolved CO_2 (Fogel and Cifuentes 1993). They can respond to the amount of CO_2, but proportional to the growth rate (Laws et al. 1995). There is expected to be Rayleigh fractionation as CO_2 is taken up during photosynthesis, and effects of differences in DIC speciation, which can result from changes in groundwater but also as a consequence of photosynthetic uptake, change in pH.

Nitrogen isotopes are associated with several processes (organic matter sources, past mixing regimes, history of nutrient loading) (Brodie et al. 2011; Talbot 2002), including a possible inverse relationship between nitrogen isotope values and moisture availability (in the savannas in Northern Australia) (Bird et al. 2019).

5.3. **Results**

A detailed description of the stratigraphy is available in chapter 3, section 3.3.1. In general, physical characteristics, colour and structure are very homogenous along the 172 cm of the core (Figure 5.2). Silty, dark brown sediments dominate the whole sequence.

5.3.1. **Sedimentation rates**

Sedimentation rates change from 0.05 to 0.17 mm/year (Figure 5.2) between 33 ka and 23.5 ka and range from 0.09 to 0.01 mm/year between 23.4 ka and 7.6 ka (Figure 5.2). Higher rates (0.09 to 0.15 mm/yr) are maintained towards the surface, until they drop abruptly at 4.9 ka, staying low until the end of the sequence (~ 0.01 to 0.09 mm/yr).

5.3.2. **Grain size**

Particles less than 35 μm dominate most of the Sanamere record (Figure 5.2). Between 33 ka and 19 ka, percentages of sand are higher (up to 32 % at 28.6 ka) compared to the rest of the sequence, where the percentage stayed below 10 %. Percentages of clay stay around 20 % between 33 ka and 30 ka and decrease to values below 5 % until 24 ka. These values then increase to 20 % until the top of the sequence. The clay percentage broadly corresponds to the general trends seen in Ti counts (Figure 5.5). For example, elevated clay percentages correspond with high counts of Ti. This correlation is most likely explained from the anatase (metastable mineral form of titanium dioxide) derived from lateritic deep weathering, which comprises the fine fraction according to the geology of the area (Eggleton et al. 2008). Percentages of coarse sand stay below 10 % through the entire sequence, except for one observation at 19 ka (26 %).

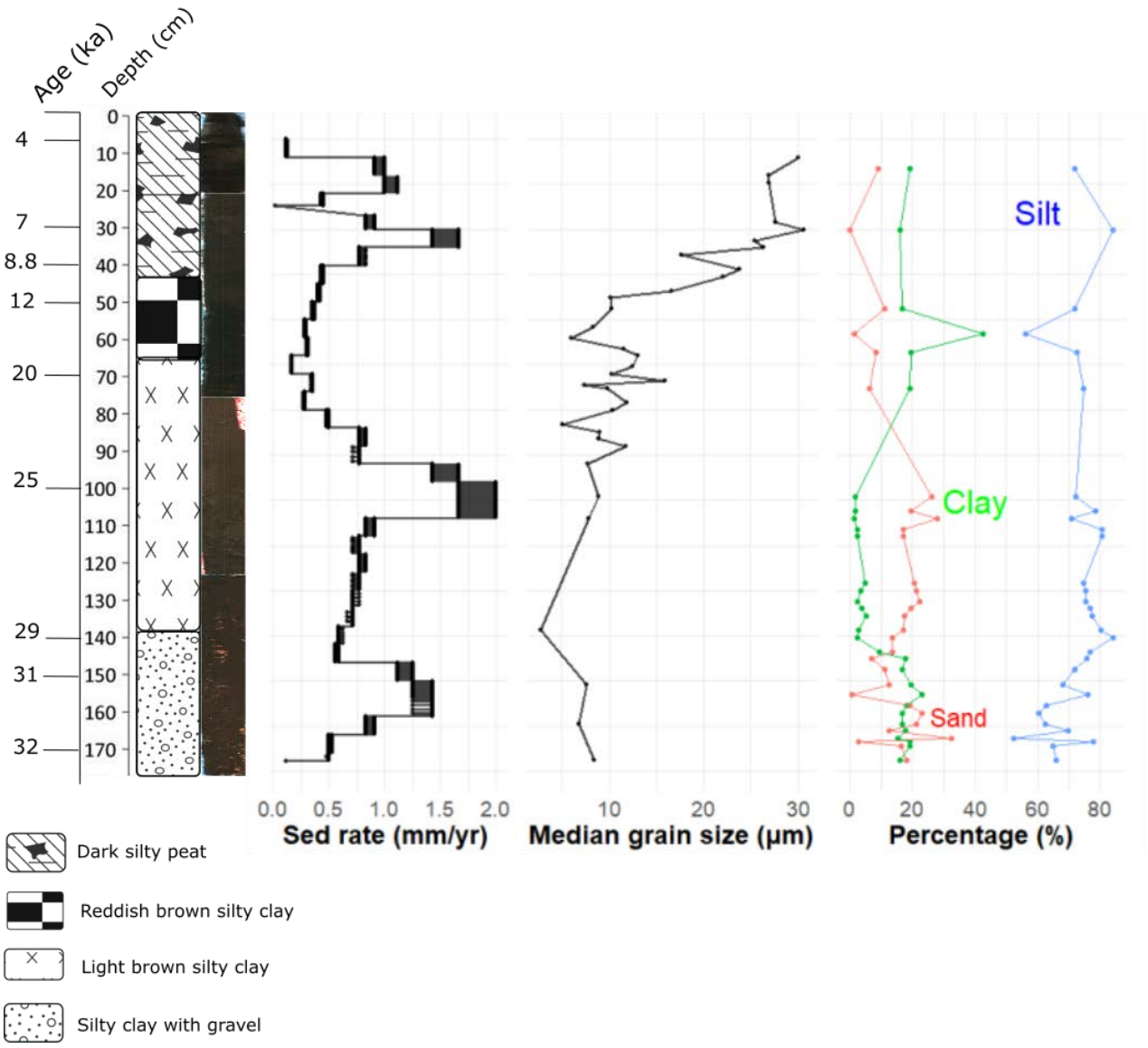

Figure 5.2. Sedimentation rates and grain size measured in the Sanamere sequence

5.3.3. **Elemental abundance**

High water content and low elemental counts prevented the use of the XRF scanning results between 0 – 7 cm (present to ~ 4.2 ka). Cluster analysis (broken-stick) identified 9 zones throughout the combined Sanamere profile (Figure 5.3, Figure 5.4 and Table 5.1). However, the Silhouette and Elbow methods suggested the optimal number of clusters to be 2 – 4. Therefore, four zones were selected, following the changes already observed in stratigraphy (Figure 5.2). Fe has the highest amount of relative

counts in the spectra, followed by Ti. Fe counts are stable and high until 10.8 ka from where they drop slightly (from 0.97 to 0.86). These counts fluctuate between 0.76 and 0.95 until they decrease abruptly to low values at 5.8 ka. After this, they increase again and fluctuate between 0.41 and 1 until they reach their lowest value at 4.8 ka, from which they peak again at 4.5 ka (Figure 5.3).

From the beginning of the sequence (bottom of the core) until 17.6 ka, Ti counts are high and exhibit only minor fluctuations (values between 0.68 and 0.80). At 17.6 ka, a decreasing trend is evident, with two major exceptions at 16.6 ka and 5.9 ka. Ti counts are also negatively correlated with Al counts.

Both Al and Si counts stay low until 9 ka, thereafter increasing to reach a peak around 7.5 ka, followed by an equally abrupt decrease around 5 ka. Sr, Rb and Al show the highest positive correlation with the PC, whereas Ti and Fe display a significant negative correlation with this curve (r = -0.69) (Figure 5.4). The μXRF data PC explained approximately 96 % of the total variance in the data set. Al and Si show a strong positive correlation with the PC; while Ti and Fe suggest a strong negative correlation.

Si:Ti values show a peak at 8 ka, from where they decrease to reach previous values (Figure 5.6). The inc/coh ratio increases at 11 ka and stay high until the end (top) of the sequence. Higher values of Si:Al are evident from the bottom of the sequence until ca. 20 ka, where these values drop abruptly. Increased values are also evident at ca. 4.7 ka (Figure 5.6).

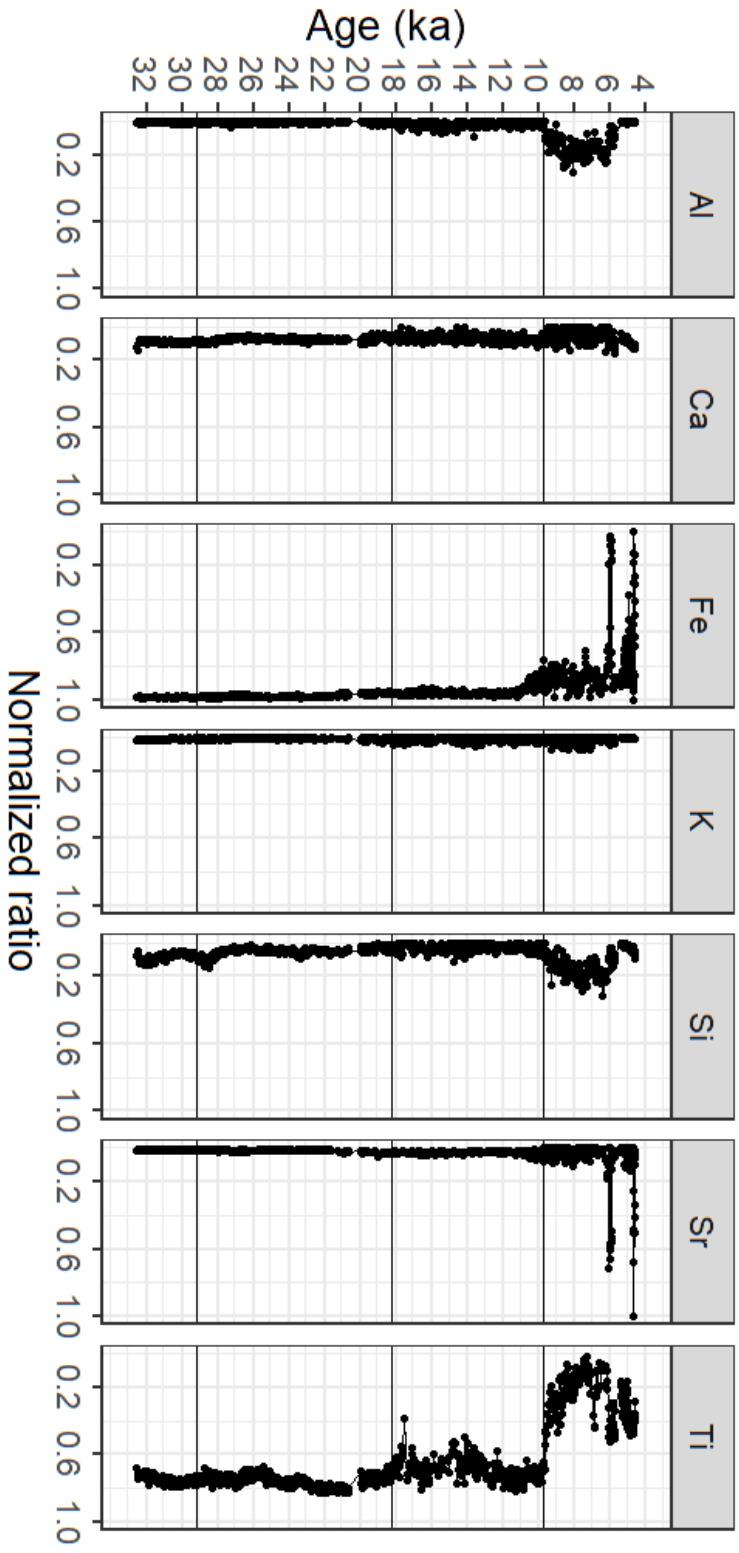

Figure 5.3. Identified zones using hierarchical cluster analysis throughout the sedimentary profile

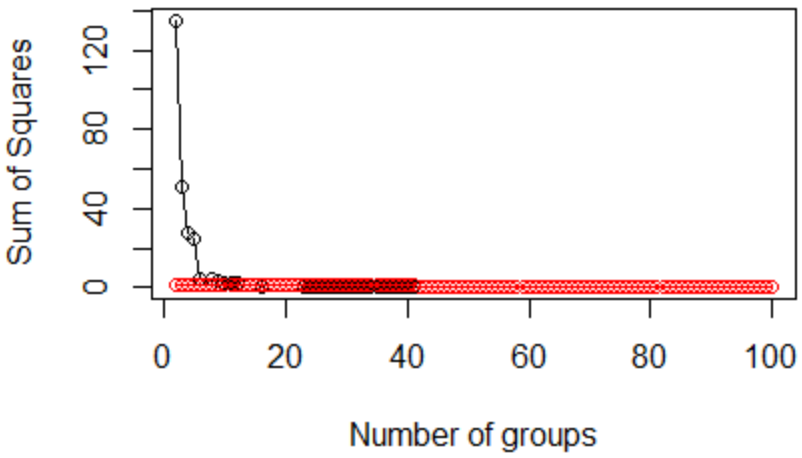

Figure 5.4. Group by sum of squares graph comparing the dispersion of the classification at different fusion levels to a null model. Red line: broken stick model

Table 5.1. Stratigraphic layers and units for the core as identified by cluster analysis of ITRAX data

Depth (cm)	Description	Layer	Age (ka)
0-43	10 YR 2/1 Dark silty peat	4	9.7- Present
43-71	5 YR 4/4 Silty clay, with 7.5 YR 4/3 thinly stratified lenses (reddish bands) between 65 and 71 cm	3	18.2- 9.7
71-140	7.5 YR 4/3 Silty clay	2	29.1 - 18.2
140-172	5YR 5/8 Silty clay	1	33 - 29.1

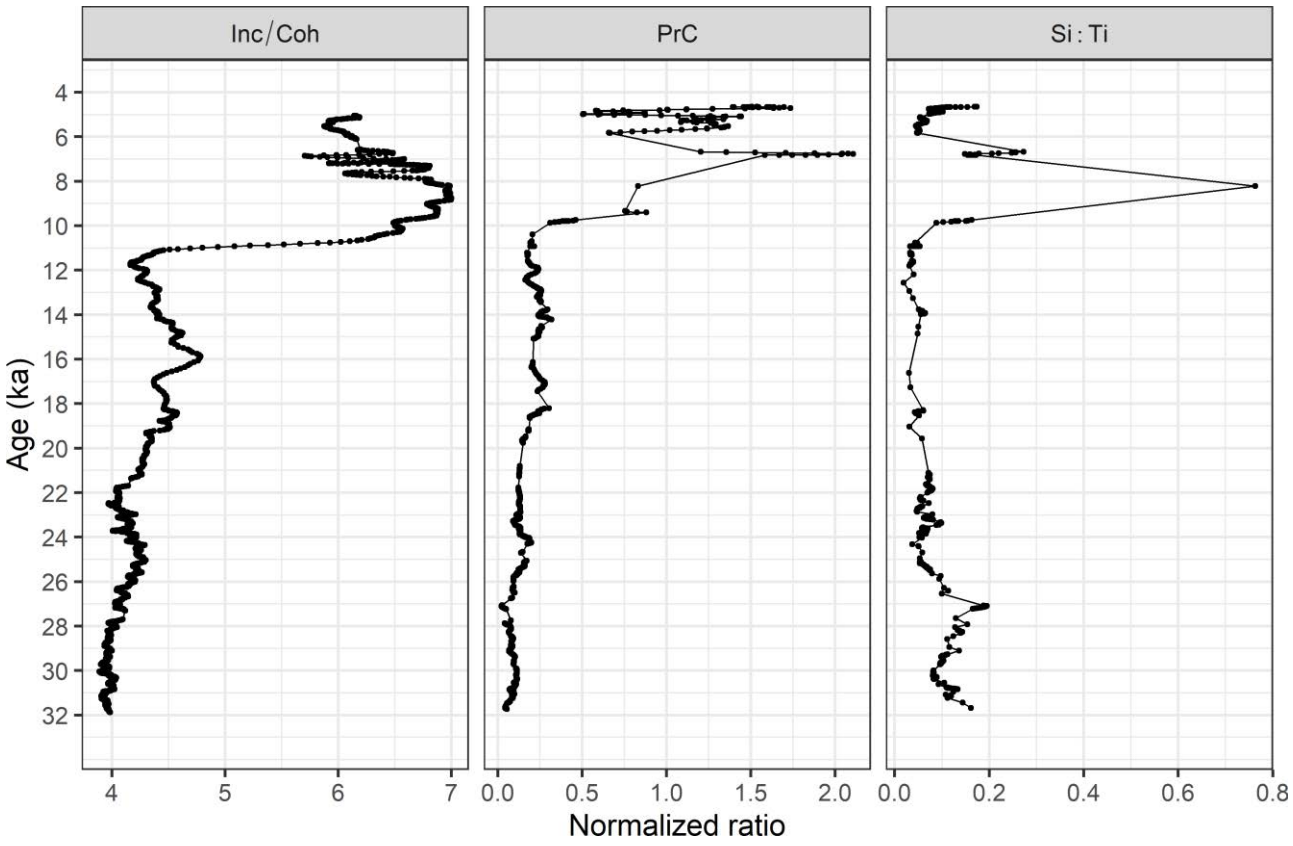

Figure 5.5. Coherent and incoherent dispersion (Inc/Coh), principal curve and Si:Ti (rolling mean with window width = 10)

Figure 5.6. Correlation matrix between elemental counts, XRF principal curve (PrC) and grain size percentages

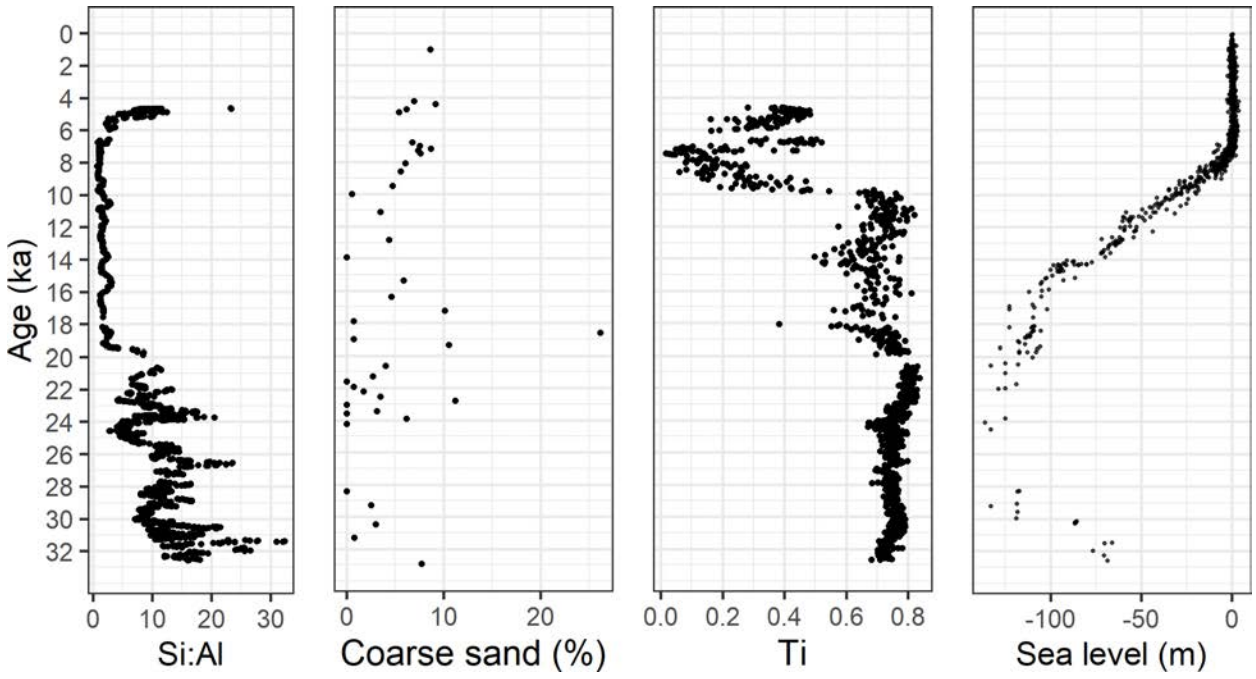

Figure 5.7. Si:Al ratios, coarse sand (> 275 □m; < 1000 □m), Ti and sea level (relative to modern sea level). Sea level data extracted from Lambeck et al. (2014)

5.3.4. **Diatoms**

The abundance of diatoms is low between the beginning of the sequence (850 - 1424 diatoms/g of sediment) and 21.2 ka, followed by a sustained increase in abundance from 10.9 ka. A peak in concentration is evident at 7 ka (~3 e5 diatoms/g), after which point the concentration decreased abruptly. Values increase and return to early Holocene proportions at the top of the core (Figure 5.7 and Figure 5.9). Although samples were extracted every 2 or 3 cm, some of them did not yield enough diatoms to comply with the minimum required to derive relevant conclusions.

A total of 19 diatom species were identified, with the assemblage dominated by benthic diatoms with a preference for acidic environments. Cluster analysis suggests the presence of three zones: ~ 33 ka – 18.2 ka, 18.2 ka – 7.3 ka and 7.3 ka – present. Before 18.2 ka, the sequence is mostly dominated by *Pinnularia viridiformis* and *Pinnularia stomatophora*, with *Stauroneis phoenicetron* and *Eunotia arcus* as secondary species. Around 18.4 ka, the proportion of additional species (such as *Brachysira brebissonii* and *Pinnularia sp.*) increases, while *P. viridiformis* becomes less abundant. The diversity of species starts to increase around 11 ka, and particularly after 9.8 ka,

when *Encyo-nema neomuelleri* and *Eunotia muscicola* appear. At 7.3 ka, the abundance of *B. brebissonii* increases from values below 6 % to values above 30 %, while *Pinnularia sp.* decreases to values below 10 % for the rest of the sequence. From 4.3 ka, the relative abundance of *B. brebissonii* declined from 54 % to values below 17 %, while *Frustulia rhomboides* increase, and species such as *Eunotia diodon* and *Stenop-teoribia intermedia* appear for the first time. A summary of the diatoms found in the core and the associated autecology is presented in Table 5.2. Selected photographs are available in Appendix 2.

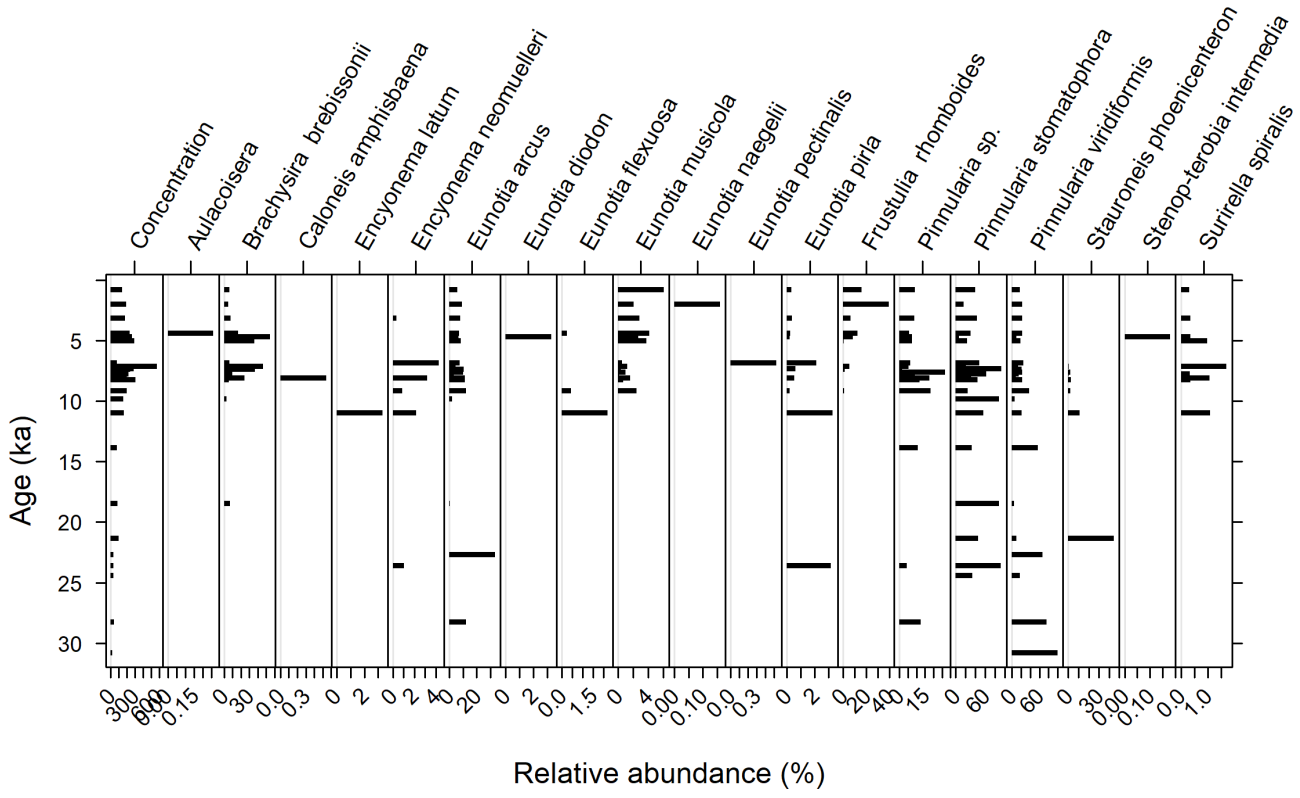

Figure 5.8. Diatom assemblage and concentration data

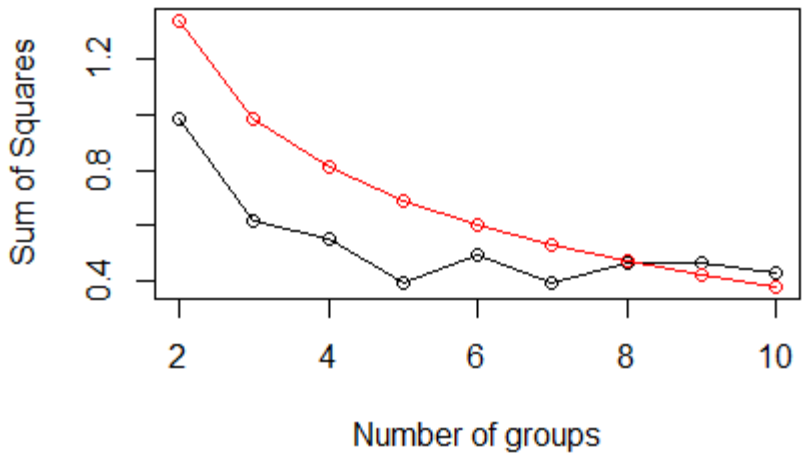

Figure 5.9. Group by sum of squares graph comparing the dispersion of the classification at different fusion levels to a null model. Red line: broken stick model

5.3.5. **Carbon and nitrogen**

A total of 134 samples were analyzed for carbon and nitrogen percentages and isotopes (δ^{13}C, and δ^{15}N).

The percentage of carbon ranges between 0.2 % and 41 % across the record. It is consistent and low (0.3 % – 1 %) during the period 33 ka to 18.2 ka (Figure 5.10). The period between 18.2 ka – 9.7 ka shows a sustained increase from 1 % to 2.2 %, from where it gradually increases to 40 % at 8.1 ka. From here, brief intervals of low abundance are evident until 4.3 ka, from where values increase again. Nitrogen percentages range between 0.03 and 1.52 % and follow a similar trend compared to carbon.

The C:N ratio shows a gradual, but substantial, increase up the sequence, changing from a value of 4 at 32 ka to 13 at 10 ka. At 6.9 ka the highest ratio is reached (44). From this date, the ratio declines to 11 at the end of the sequence (Figure 5.8).

δ^{13}C values broadly decrease from the base of the record (-27 ‰) to 4 ka (~ -22 ‰) (with inter-interval fluctuations of usually ~ ± 0.5 ‰, but with individual short, larger

excursions to individual values as high as -18 ‰ and as low as -29 ‰. From 4 ka to the present values increase slightly to ~ -22 ‰ and remained constant. Nitrogen isotopes exhibit the same trends, except variability between samples is generally larger (± 1 ‰ or more) (Figure 5.8).

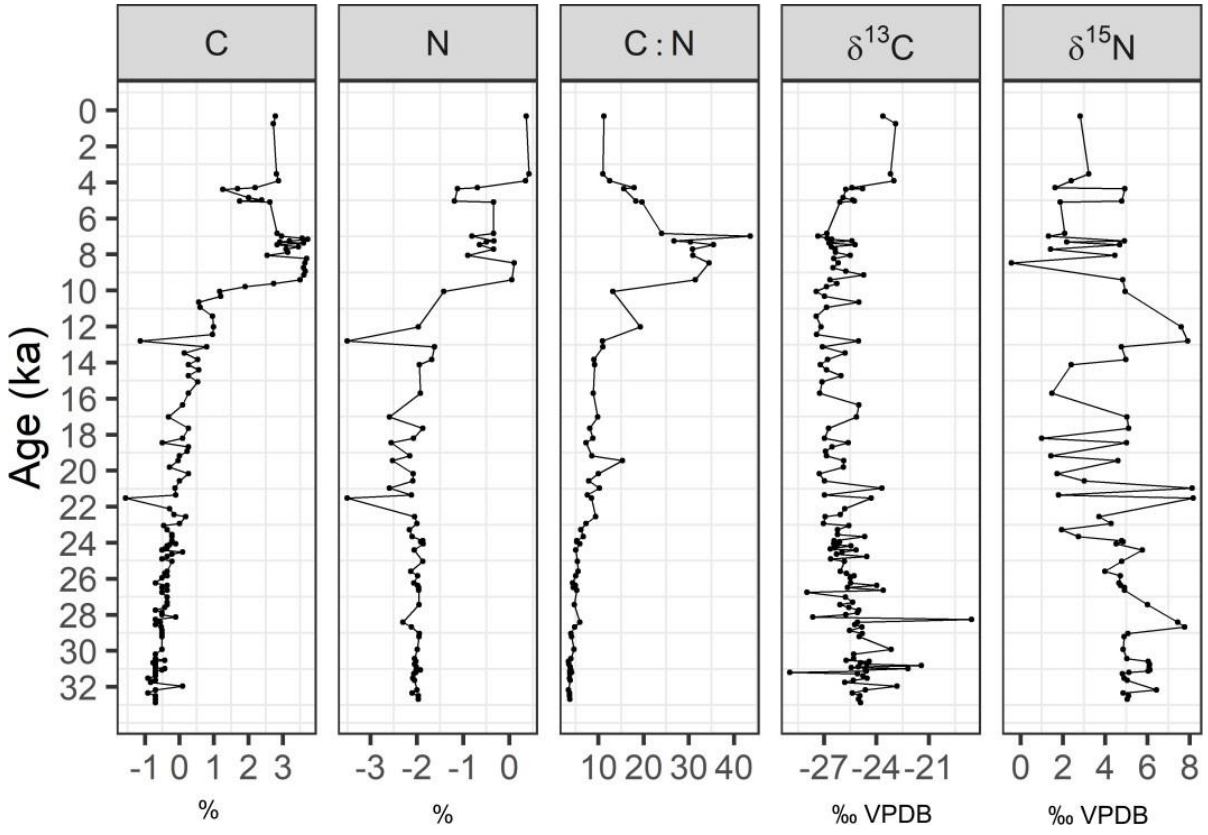

Figure 5.10. Total carbon, nitrogen and isotopic abundance for the Sanamere sequence. Note that % C and % N are presented as log-transformed values.

5.4. **Discussion**

5.4.1. **Unit A (33 - 29.2 ka)**

The age-depth model (Figure 5.1) indicates sediments in Sanamere Lagoon started to accumulate around ca. 33 ka, in the depression formed by collapse of the underlying laterite karst. This section of the core represents the bottom of the sequence, and this section is compared to present climatic conditions. This depression was then located below regional groundwater level, supporting initial water accumulation. The accumulation is likely to have occurred under dry climate conditions, and before major

sea level drop at 30 ka, even as water table reduced further into the LGM (Brooke et al. 2017) (Figure 5.6). Between 33 ka - 30.1 ka, a possible wetter phase is suggested by the high sedimentation rates (Figure 5.2) associated with possible enhanced runoff of clastic sediment, with the highest percentage of clay in the sequence and an average particle size of 2.7 μm. Overall, climatic reconstructions in the region suggest drier and colder conditions, with the monsoon considered to be inactive, or greatly weakened at this time (Reeves et al. 2013). However, regional variations are starting to be demonstrated as more research is completed. Previous studies have suggested a major latitudinal shift of the ITCZ in southerly tropical regions (south Papua New Guinea) during Heinrich Stadial 3 (ca. 30 ka), associated with intense rainfall (Bayon et al. 2017; Jacobel et al. 2016; Lewis et al. 2011). Other studies have also proposed the presence of wet periods during the Glacial (30 – 18 ka) in the wet tropics of Australia in Broomfield swamp (Burrows et al. 2016) and Lynch's Crater (Muller et al. 2008). Noting with caution that these ages are potentially overestimated (May, Preusser, and Gliganic 2015), extreme floods have been also identified during this period (Nott, Bryant, and Price 1999), for example those recorded in Wangi waterfall in the Northern Territory (Nott, Price, and Bryant 1996; Nott and Price 1994).

The ITRAX/grain size analyses indicate the presence of coarser quartz grains (higher Si:Al), and high concentration of Ti, both in accordance with the expected lithology after the lagoon formation and arid conditions during this period (Lambeck et al. 2014; Brooke et al. 2017; Ishiwa et al. 2019). Enriched values of δ^{15}N suggest decreased rainfall, according to the significant correlation between rainfall and δ^{15}N found by Bird et al. (2019) in northern Australia. Bird et al. (2019) concluded that δ^{15}N values at Girraween Lagoon in the Northern Territory were associated with precipitation and this thesis suggests the same for north Queensland, base on the results from Sanamere Lagoon.

It is likely that during this time the site formed a shallow pond or swamp with low nutrient availability. These conditions likely support the aquatic plants that dominated the lagoon during this period (chapter 6). The low concentration and autecology of the diatoms at the base of the column support this finding. For instance, *P. viridiformis*, an aerophilous diatom, is the single dominant species during this period and is commonly found in neutral or acidic water. Aerophilous species commonly occur in subaerial environments such as moist or temporarily dry places, to the point of surviving nearly

exclusively outside water bodies (Johansen 2010). The lagoon was probably dominated by emergent macrophytes, or it was only intermittently inundated. The C:N ratio values (< 20) and δ^{13}C (< -25 ‰) suggest the input of aquatic plants or lacustrine algae, predominantly.

The end of this period is associated with an abrupt decrease in sea level (from -83 m to -126 m) that started ca. 30 ka (Lambeck 2014). However, there are no apparent effects of this decrease in the Sanamere Lagoon sediments.

5.4.2. **Unit B (29.2 - 18.2 ka)**

Site conditions appear to be relatively arid over the period between 29.2 ka – 18.2 ka (corresponding to the beginning of MIS 2). δ^{15}N values suggest decreased regional rainfall (increased aridity), a trend that continues from the previous period. Coarse grains, represented by high values of Si:Al characterise this period, along with an increase in median grain size (from 2 to 11 μm). Diatoms continue to appear in low concentrations, although species additional to *P.viridiformis* and *E.arcus* appear for the first time, including *E.arcus* and *S. phoenicentron*. These are all acidophilous species recorded in habitats with running water (such as rivers and streams) (van Dam, Mertens, and Sinkeldam 1994). Diatoms from these habitats could indicate the presence of shallow and unstable environments (van Dam, Mertens, and Sinkeldam 1994). Carbon and nitrogen concentrations continued to be low, indicating low production of biomass within the lagoon and the catchment around.

Increased coarse sand percentages (Figure 5.6) also agree with the episodes of sand deposition (aeolian or fluvial origin) at 26 ka, 24 ka, 21.5 ka at Lake Carpentaria. These events were reported during a dry and cool period with large fluctuations of the Carpentaria lake level (Devriendt 2011) (section 2.3.3). Furthermore, the sedimentary record at Lake Carpentaria indicates a temporary contraction of the lake to around the -63 m contour (23 ka – 19 ka), when the sea was at the lowest level (approximately − 125 m) (Brooke et al. 2017; Yokoyama et al. 2001), and the Sahul shelf was fully exposed. The contraction of Lake Carpentaria probably increased aridity and reduced vegetation cover. The availability of sand and larger grains to be transported to the lagoon also increased, along with the formation of possible wind-blown features. Further evidence comes from dust records across several sites in east and north Australia. These records

have documented increased aeolian sedimentation during this period (Petherick, McGowan, and Kamber 2009; Lewis et al. 2020). Fluctuating water depths may have induced periodic deflation of exposed sediments on the lake shore, though the lake did not dry at the core location. During this time, dune formation and increased aeolian sedimentation took place in other locations in north and east Australia (section 2.3.3).

These episodes of sand deposition are coincident with periods of elevated IASM rainfall at Ball Gown Cave in Western Australia. These synchronous changes also link the responses of sites in western Kimberley and the Gulf of Carpentaria during the Last Glacial period (Denniston, Wyrwoll, Asmerom, et al. 2013).

In the broader tropical Australasian region, most studies agree on evidence of drier, cooler conditions during the late MIS 3 and LGM (ca. 33 ka and 18 ka) (Denniston, Wyrwoll, Asmerom, et al. 2013; Denniston et al. 2017; DiNezio and Tierney 2013; Reeves et al. 2013) (section 2.3.2.1 and section 2.3.3). Studies in the wet tropics of Australia also suggest drier and cooler conditions (33 – 18 ka) (Petherick, McGowan, and Kamber 2009). Lowered sea level and the exposure of the Sunda and Sahul shelves initiated changes in atmospheric circulation over the Indo-Pacific warm pool (IPWP). These two factors contributed to the large-scale regional drying during the LGM (Nezio et al. 2016).

Although studies in the region have proposed the LGM to be a particularly dry phase, with an irregular monsoon (Hanebuth 2000; Hesse, Magee, and van der Kaars 2004; Reeves et al. 2013; Wyrwoll and Miller 2001), the Sanamere Lagoon record does not suggest this period to be particularly dry (according to the geochemical and biological evidence), suggesting that the exposure of the shelves did not have a significant impact on the hydroclimate of the site, and therefore by extension, the northern-most part of Cape York Peninsula. In fact, recent modelling studies suggest there was still an effective monsoon rainfall regime across the northern Australian region (Yan et al. 2018). The results from Sanamere Lagoon contribute to document the effects documented by this study.

A mild LGM climatic impact for northern Cape York Peninsula may be explained by the position of the coastline during the LGM, 900 km northwest of Sanamere Lagoon (Ishiwa et al. 2019). Yan et al. (2018) conclude that changes in land-sea distribution and

east-west gradients in sea surface temperature resulted in a modest lowering of total rainfall but an increase in rainfall seasonality across northern Australia. The change in coastline position probably decreased precipitation at any terrestrial site given the strong rainfall gradient into the interior.

This pattern of not extreme, dry climate is consistent with other studies from the area (Yan et al. 2018; Denniston et al. 2017; Jiang et al. 2015). Furthermore, the only terrestrial vegetation and fire record available from northern Australia (Girraween, Northern Territory) during this period also suggest dry, cool conditions with low CO_2 concentrations during the LGM (Rowe et al. 2020).

5.4.3. **Unit C (18.2 – 9.7 ka)**

The Ti counts show increased magnitude fluctuations starting at 20 ka, indicating changes in the erosion activity derived from precipitation around the lagoon. The sedimentation rate reached its lowest rate, the median grain maintained the same size (11 μm), and the diatom concentration remained as in the previous period. Diatom species diversity did however decrease, with only three species present: *P.stomatophora*, *P. viridiformis* and *B. brebissonii*.

Between 17.6 ka and 12.8 ka, the lagoon records the reactivation of the monsoon and increased moisture availability derived from the rise in post glacial sea level as recorded by wetter conditions and increased lake level at Lake Carpentaria (Devriendt, 2011). The decrease in Ti counts at 14 ka and the decrease in grain size (Si:Al) during this time may be reflecting a substantial relative increase in the area of Lake Carpentaria area, which may be limiting the accumulation of clastic sediments in the center of the lake, remote from sources of sediment supply. The increase in the C:N ratio at ~ 12 ka suggests an increase in terrigenous organic input into the lagoon. These results are consistent with previously published studies indicating that the monsoon became active in the region somewhere between 19 ka – 12 ka (Hanebuth 2000; Hesse, Magee, and van der Kaars 2004; Reeves et al. 2013; Wyrwoll and Miller 2001; Field, Tyler, et al. 2018; Rowe et al. 2019).

Between 12.8 ka and 9.7 ka, the trends in the biological and geochemical indicators suggest the existence of episodic wet events derived from an increase in

rainfall associated with a stronger monsoon. During this period (in particular 12 ka - 9.7 ka), enriched δ^{15}N values may be recording the input of nitrogen (inorganic and organic) from different sources around the catchment, compared to previous periods described for Sanamere Lagoon. For example, at 10.8 ka the increase in diatom concentration and the appearance of new diatom species (*E.flexuosa*, *E. latum*, *E. neollimueri*, *E. pirla*, *Surirella spiralis*), also indicate a change towards higher productivity and further lake deepening, with some of these species preferring stagnant water to grow (*E.flexuosa*, *E. latum*) (Proske et al., 2015). The C:N ratios (> 20) and the δ^{13}C values (< -25 ‰) record the input of terrestrial C_3 plants. Increased δ^{15}N values were probably driven by the further filling of the basin, as large amounts of nutrients were released to the lagoon (Talbot 2002). These changes in the lagoon are consistent with the increases in sea level (from ca. 12 ka) in Lake Carpentaria and the South Wellesley Archipelago (Sloss et al. 2018). For instance, from 12 ka, oceanic waters transgressed the Arafura Sill, and by 10.7 ka, the Lake Carpentaria region had become marine (De Deckker et al. 1988; McCulloch, De Deckker, and Chivas 1989; Chivas et al. 2001). Sloss et al. (2018) found that sea-level rose from −53 m (depth of the Arafura Sill) (Reeves et al. 2008; Harris et al. 2008) at ca. 11.7 ka to ca. –25 m by 9.8 ka (Sloss et al. 2018).

The Sanamere record is consistent with the increase in monsoon activity at ca. 12 ka suggested by several studies in the surrounding area (Wende, Nanson, and Price 1997; Kuhnt et al. 2015; Field, Tyler, et al. 2018). The rise in sea level facilitated increased moisture advection and tropical convection over Cape York. Warmer waters in parts of the IPWP region also contributed to amplify this effect, as a result of Northern Hemisphere insolation-induced heating (Griffiths et al. 2009). However, the Sanamere record does not agree with the evidence of a strengthened Indonesian-Australian summer monsoon (IASM) at ca. 14 ka, as other studies have noted (Reeves et al. 2013). Likewise, the Sanamere results do not indicate the initiation of wet conditions recorded in Lake Carpentaria during the immediate deglacial period (ca. 18 ka) (Reeves et al. 2008). In contrast, the Sanamere record agrees with records from the western equatorial Pacific, which suggest that dry conditions terminated after the main period of sea level rise had occurred (ca. 12 ka). As an example, a record from the western tip of Western Australia (De Deckker, Barrows, and Rogers 2014) proposes that prior to 13 ka, rainfall was low. By 13 ka, the Indo-Australian monsoon commenced in and offshore northwestern Western Australia. SST and land temperature increased dramatically, and

ocean alkalinity changed due to the formation of a “barrier layer” (a low salinity cap), over the Indo Pacific Warm Pool (De Deckker, Barrows, and Rogers 2014).

5.4.4. **Unit D (9.7 ka – Present)**

Starting around 9.7 ka, there is an abrupt change in the geochemical and biological composition of the lagoon, which coincides with the “big swamp phase” identified in previous studies in northern Australia (Prebble et al. 2005; Luly, Grindrod, and Penny 2006; Proske et al. 2017). The increases in the carbon and nitrogen abundance, C:N ratios (> 20) suggest a change in the origin of the organic input in the lake towards a dominance of terrestrial plants. The proportion of sand increases at 9.5 ka and stays at higher values until the top of the sequence. This increase indicates stronger allochthonous input into the lagoon. Furthermore, this change is probably a result of higher rainfall or enhanced seasonality (drier phases to expose the sand, wetter phases to wash it in) and enhanced transport of material from the catchment. The arrival of new diatom species such as *E. flexuosa*, *E. muscicola*, *E. latum* and *E. neomuelleri* suggest the further expansion and deepening of the lagoon. The Ti counts and the abundance of coarse grains (Si:Al) dropped abruptly as the swamp expanded. Several sites across the Australian tropics have identified a period of increased precipitation around 7.9 ka (Shulmeister 1992; Haberle 2005), linked to increased monsoon activity between 11 ka and 7.5 ka (Field, Tyler et al. 2018). Increasingly depleted δ^{15}N values are also consistent with increased rainfall. The results from Sanamere Lagoon are consistent with interpretations of wetter, less seasonal climatic conditions during this time. The Sanamere record is also synchronous with the timing of monsoon intensification at Flores (southeast Indonesia) ca. 9.5 ka, a product of the sudden increase in ocean surface area and/or temperature in the monsoon source region as the Sunda Shelf flooded during deglaciation (ca. 9.7 ka)(Griffiths et al. 2013). These results also agree with the conclusion that dry conditions may have been maintained until flooding of the Sunda–Sahul shelf, at the end of the deglaciation, according to De Deckker, Tapper, and van der Kaars (2003).

Indicators of relatively higher precipitation continue after 7 ka and sedimentation rates, carbon percentages, and Si:Ti ratios keep increasing. C:N ratios, median grain size and diatom concentrations also reached their highest values at 7 ka. Additionally, the increase in *B. brebissonii* at 7.3 ka suggests a shift towards water with lower pH

(Proske et al. 2015). The timing of these events is consistent with the initiation of the a mid-Holocene sea-level highstand (7.7 ka – 4 ka) and a corresponding period of increased precipitation and temperature during the Holocene (Sloss et al. 2018).

From 6.9 ka, a decline in precipitation is suggested by the decreased values (compared to the early Holocene) in diatom concentration, C:N ratios and carbon percentages. This change implies changing environmental conditions. Other records in the area inferred the occurrence of wetter conditions during the mid-Holocene (Haberle 2005; Shulmeister 1992), including a peak in precipitation. However, records from northwest of the region support decreased precipitation during the mid-Holocene (Denniston, Wyrwoll, Polyak, et al. 2013; Field, Tyler, et al. 2018), suggesting a northward shift of the ITCZ (Reeves et al. 2013). Evidence for a northward shift of the ITCZ at this time comes from the Pacific, Indian and Atlantic Oceans (Haug et al. 2001).

This drier trend continued until 4.9 ka, where C:N ratios declined to values below 20, indicating greater input from algae. The progressive increase in the relative abundance of *F.rhomboides* started at 4.9 ka, along with the decrease in carbon percentage, and high sedimentation rates (between 4.9 and 4.2 ka). These changes indicate a more permanent expansion and deepening of the lake body, probably as a consequence of an increased precipitation phase (and warmer temperatures) during this period, which resulted in an increase in available nutrients (Hembrow et al. 2014). After 4.2 ka, decreased sedimentation rates and C:N ratios indicate stable conditions at Sanamere Lagoon and probably decreased rainfall, with a limited contribution of terrestrial vegetation. This interpretation should be taken with caution, given the chronological and interpretive complexities of the Sanamere Lagoon record during this period. The changes in sedimentation rate at ca. 4.9 ka - 4.2 ka broadly corresponds with the global “4.2 ka event”, which has been associated with intense climatic variability in several locations around the globe (Marchant and Hooghiemstra 2004; Perry and Hsu 2000). In tropical Australia, possible expressions of this event have been found in the Kimberley region (Denniston, Wyrwoll, Polyak, et al. 2013; Field, Marx, et al. 2018) and the Gulf of Carpentaria (Shulmeister 1992). These results agree with previous studies that have identified reduced summer monsoon activity and less effective precipitation during this phase (Denniston, Wyrwoll, Polyak, et al. 2013; Reeves et al. 2013; Lough et al. 2014; Field, Tyler, et al. 2018), including the trend seen at Big Willum in Weipa, with a very low sedimentation rate during this time period (Proske et al. 2017).

Starting at 4.2 ka, a significant decline in Sanamere's sedimentation rate suggests decreased transport of material from the catchment to the lake, and further stabilisation. However, no information is available for changes in these processes as the ITRAX elemental abundance record is not reliable after this period. While the decrease in C:N ratios implies a higher contribution of algae/aquatic plants into the lake, the diatom assemblage does not show any change during this period compared to the previous phase. In fact, the Sanamere Lagoon results do not reflect the climatic variability found at other sites in the area (Stevenson et al. 2015; Haberle 2005; Shulmeister 1992). This climatic variability has been linked to the increase in frequency and amplitude of El Niño from 5 ka in several climate models and records (Gagan et al. 2004; Conroy et al. 2008).

5.5. **Chapter 5 summary**

The Sanamere sequence is one of a handful of sediment sequences older than 14 ka available for the dry tropics of Australia (Denniston et al. 2017; Denniston, Wyrwoll, Asmerom, et al. 2013; De Deckker 2001; Reeves et al. 2008), and the only one for Cape York Peninsula. Four stratigraphic layers were identified using physical and chemical evidence. The geochemical evidence (μXRF) allowed the division of each layer into subunits. The collapse of the underlying laterite karst formed a depression below regional groundwater level, allowing the infilling of the lagoon around ca. 33 ka during low sea levels. Broadly speaking, higher percentages of coarse sand, low organic content, and enriched δ^{15}N values suggest that the climate during 33 ka - 29.1 ka was arid and the lagoon was shallow according to the abundance and presence of indicator diatom species. This period records the initial infilling of the lagoon, also evidenced by the increased sedimentation rates.

During the period 29.1 ka - 18.2 ka, sea was at the lowest level, and dry conditions dominated, allowing the formation of wind-blown features, given the increased availability of sand to be transported. From 18.2 ka - 9.7 ka, an abrupt decrease in the percentage of coarse grains and Ti counts suggest the lagoon expanded, with limited sediment reaching the center of the lake, forming a shallow and small lake, but deeper and larger than before. The lagoon also records the reactivation of the monsoon and increased moisture availability derived from the rise in post-glacial sea level. For

instance, starting at 12.4 ka, the addition of increased terrestrial input derived from higher rainfall is recorded. Around 10.8 ka new diatom species indicate further lake deepening, as some of these species prefer stagnant water to grow (*E.flexuosa*, *E. latum*). Terrestrial input peaked at 7 ka and dropped abruptly as the lagoon further expanded in depth and area. From ca. 4.7 ka organic matter and terrestrial input decreased, following the stabilisation of sea to current levels and a period of climatic fluctuations related to ENSO cyclicity.

In summary, the timing of the proposed changes suggests that sea level was the most significant factor that influenced regional climate and the consequent evolution of Sanamere Lagoon. Monsoon activity and the position of the ITCZ were also relevant features.

Table 5.2. Autecology of diatoms found in the study

Species	Habitat	pH	Additional information	References
B. brebissonii	Freshwater	moderately acidic	Present in coastal lakes	Hamilton (2010)
Encyonema	freshwater	6.5 – 7.5	Periphytic (attached to surfaces) and most common in stagnant or almost stagnant water but also in running creeks	Foged (1978); Gell (1999)
Eunotia sp.	freshwater	acidic	Principally epiphytic (i.e. growing on other plants), strongly dislike high concentrations of salts (Ca, Mg, Na, K)	Gell (1999)
E. arcus	freshwater	4.5–6.5 (also 6.5-7.5)	In rivers and creeks with running water, halophobous, acidophilous	Foged (1978)
E. flexuosa	freshwater	4.5 – 6.5	Most common in stagnant or almost stagnant water but also in ponds and pools, cosmopolitan, oligohalobous (indifferent), acidophilous	Foged (1978)

Species	Habitat	pH	Additional information	References
E. musicola	freshwater	Circumneutral to weakly acidic	In springs and swampy areas but not in peats or swamps/peats	Krammer and Lange-Bertalot (2000):
E. pectinalis var undulata	freshwater	6.5 – 7.5	Creeks and rivers with running water, cosmopolitan, acid most common in stagnant or almost stagnant water but also in halophobous	Foged (1978):
E. pirla	freshwater	acidic		Carter (1988)
E. subgibba	freshwater	pH 7 (potentially circumneutral)	Oligohalobous	Foged (1978)

Species	Habitat	pH	Additional information	References
F. rhomboides	freshwater	4.5 – 6.5 but also pH 6.5 – 7.5 (pH circumneutral)	Intolerant of saline habitats, cosmopolitan, high sulphate levels. Most common in stagnant or almost stagnant water but also in ponds and lakes, cosmopolitan, halophobous. Most typical in acid conditions with pH lower than 3, grows on the surface of sediments, clays, and silt (i.e., residing at the water/sediment interface). Widespread in acidic waters (can be abundant there), mostly found in epipelic and epilithic assemblages, water low in total phosphorous and conductivity, pH 1-2	Foged (1978); Gell et al. (1999); Sonneman et al. (2000)

Species	Habitat	pH	Additional information	References
Gomphonema	freshwater to fresh brackish	7	Sensitive to pollution, nearly every habitat type within near neutral lakes and streams, establish late on new substrate – often as last genus of all diatoms in the specific habitat	Dam (1994)

Species	Habitat	pH	Additional information	References
G. gracile	freshwater	6.5 – 7.5 but also pH 4.5 – 6.5 and 2-3	Recorded to occur in more or less neutral water but has been found in acidic water in the NT, can be rel. abundant in weakly acidic water. Most common on rivers with running water but also in rivers and creeks with stagnant, near stagnant or slowly running water, oligohalobous (indifferent), alkaliphilous, cosmopolitan. Widespread but rarely abundant, mostly found attached to epiphytes but can be found in epilithic and epipelic assemblages, low total phosphorous and electrical conductivity	Foged (1978); Sonneman et al. (2000)

Species	Habitat	pH	Additional information	References
Pinnularia sp.	freshwater	slightly acidic	Grow on the surface of sediments, clays, and silt (i.e., residing at the water/sediment interface)	Dam (1994)
P. gibba	freshwater	pH 4.5 – 6.5, optimum above 6	Tolerant to pH fluctuations and moderate oxygen deficiencies, can occur in very acid water (NT); most common on rivers with running water but also in rivers and creeks with stagnant or near stagnant water or in ponds; cosmopolitan and very adaptable to a range of habitats – stagnant to running water, variable conductivities	Foged (1978); Krammer and Lange-Bertalot (2000)

Species	Habitat	pH	Additional information	References
P. major	freshwater	pH indifferent to circumneutral	Widely distributed in water of fairly low mineral content, can be found in a wide range of habitats; very shallow water; oligohalobous (indifferent); optimum in waters with low electrical conductivity	Foged (1978); Krammer and Lange-Bertalot (2000); Prebble (2005)
P. stomatophora	freshwater	4.5 – 6.5 but also pH 6.5 – 7.5	Most common on rivers with running water but also in rivers and creeks with stagnant or near stagnant water or in ponds, halophobous; also observed on wet mosses	Foged (1978); Krammer and Lange-Bertalot (2000)
P. viridiformis	freshwater-brackish	pH circum neutral	Widespread but rarely abundant, in epipelic and epilithic assemblages, can be aerophilous, pH1-3, low total phosphorous	Sonneman et al. (2000)

Species	Habitat	pH	Additional information	References
S. phoenicenteron	freshwater	pH 4.5 – 6.5 but also pH 6.5 – 7.5, pH circumneutral	Oligohalobous (indifferent), most common on rivers with running water but also in rivers and creeks with stagnant or near stagnant water or in ponds; Stauroneis as genus often living on (or in) fine sediment, exclusively in freshwater	Foged (1978); Gell (1999)
S. intermedia	freshwater	pH 4.5 – 6.5	Most common on rivers with running water but also in rivers and creeks with stagnant or near stagnant water, halophobous, acidophilous	Foged (1978)

Chapter 6. **Vegetation change and fire dynamics around Sanamere Lagoon over the last 33,000 years**

6.1. **Introduction**

This chapter contributes to refining the vegetation and fire records for the savannas of tropical Australia using phytolith, carbon isotope and pyrogenic carbon-based reconstructions from the Sanamere Lagoon sedimentary record. Three main sections guide this chapter. The first section describes the methodology used to reconstruct fire and vegetation; the second section presents the results, and the last section discusses the results in terms of the broad temporal and regional trends.

6.2. **Methodology**

6.2.1. **Vegetation inventory and analysis of modern reference material**

A vegetation survey was carried out at 50 m intervals along a 450 m transect south from the lake shore (Figure 6.1 and Figure 6.2). The 450 m transect extended to the ridgeline and wider regional woodland boundary, so that the survey concentrated on the immediate catchment heathland surroundings. A group of 17 species collected during the survey was selected for the extraction of phytoliths to build a local modern reference collection. Selection was based on previously reported phytolith presence in a species (e.g. Wallis (2003); Wallis (2001); Albert and Marean (2012)), and their dominance along the transect. Where possible, the two main parts of each plant (stems, leaves) were subjected to dry-ashing to extract phytoliths and analysed separately following the procedures detailed in Pearsall (2015) and Piperno (2006) (Figure 6.3). All morphological descriptions followed the guidelines provided by the International Code for Phytolith Nomenclature 2.0 (Neumann et al. 2019).

Figure 6.1. Transect pathway southeast of Sanamere Lagoon

Figure 6.2. Specimen collection in transects around Sanamere Lagoon

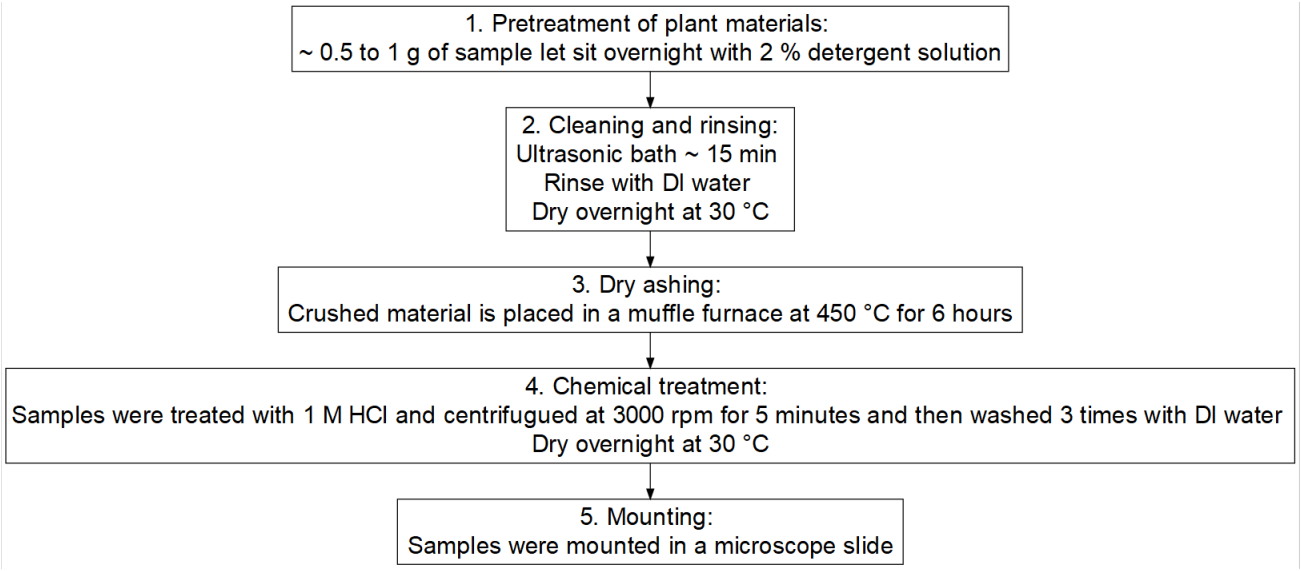

Figure 6.3. Dry-ashing procedure for the extraction of modern phytoliths following Pearsall (2015) and Piperno (2006)

6.2.2. **Fossil phytolith extraction, identification, and classification**

The phytolith extraction for fossil samples followed the procedures described in previous studies (Aleman et al. 2013; Piperno 2006): (1) deflocculation of the sediment with $NaPO_3$, (2) oxidation of organic matter with H_2O_2, (3) removal of clay by gravity, and (4) densimetric separation of phytoliths in a dense solution of Sodium Polytungstate (specific gravity = 2.3).

A minimum of 200 diagnostic phytoliths were counted per sample when possible. In cases where the count of 200 diagnostic phytoliths was not possible, a minimum count of 50 diagnostic phytoliths was considered in the interpretation. The fossil phytolith taxonomic identification was carried out using published photographs and descriptions (Neumann et al. 2019), including notably, the Australian research on phytolith morphology by Wallis (2003) and Wallis (2001). More generalized taxonomic keys such as those published by (Piperno 1995, 2006) also served as reference.

Since phytoliths cannot provide detailed taxonomic information about trees, shrubs, and herbs that lack specialized unique phytoliths (Piperno, 2006), morphologies were grouped into four categories according to plant type following standard

classification schemes (Daniau et al. 2019; Neumann et al. 2019): Poaceae or grasses (saddle, bilobate, trapezoid oblong), Poaceae/Cyperaceae or grasses/sedges (bulliform, bulliform flabellate, elongate entire, elongate psilate, elongate blocky, elongate rugose, elogate facetated), woody dicotyledons (spheroid ornate) and non-diagnostic. Within the Poaceae group, morphologies representing both C_3 and C_4 species are not differentiated. The reason for this is that most of the short cells identified corresponded to the C_3 groups and very few can be assigned unequivocally to the C_4 (saddle, bilobate) (Albert and Marean 2012; Daniau et al. 2019). Phytolith counts were converted into relative abundances and their distribution analyzed according to the chronological zones determined previously using the climatic reconstruction for Sanamere Lagoon (chapter 5).

6.2.3. **Pyrogenic carbon analyses and geochemical indicators**

Hydrogen pyrolysis (hypy) was used to determine the stable polycyclic aromatic carbon content of the samples (Hypy fraction) (Bird et al. 2015). The Hypy fraction was used as a proxy for fire activity (section 2.4.4). Sediment samples (~ 1–15 mg) were loaded with a Mo catalyst (5 – 10 % of sample mass) using an aqueous/methanol solution of ammonium dioxydithiomolybdate [$(NH_4)_2MoO_2S_2$]. The dried catalyst-loaded samples were placed in the hypy reactor and pressurized to 150 MPa of hydrogen gas with a sweep gas flow of 5 L min^{-1}, then heated at 300 °C/min to 250 °C, then 8 °C/min until a final hold temperature of 550 °C. This final temperature was maintained for 2 min. The carbon content of the sample before and after hydrogen pyrolysis was used to calculate the PyC content as a fraction of total organic carbon with an error of ± 5 % (Meredith et al. 2012; Wurster et al. 2012). Hypy mass accumulation rates (Hypy MAR) were calculated using the formula below and the age-depth model developed for the Sanamere Lagoon core (chapter 4). The $\delta^{13}C$ value of pyrogenic carbon ($\delta^{13}C_{hypy}$) (after hydrogen pyrolysis) was calculated using the formula given in Wurster et al. (2012) and used to draw inferences about the vegetation being burnt. The $\delta^{13}C$ of total organic carbon ($\delta^{13}C_{TOC}$) was used as an indicator of the organic matter source and the photosynthetic pathway of the vegetation that surrounded the lake. Carbon (% C), nitrogen abundance (% N), C:N ratios and $\delta^{13}C$ value were measured according with the procedures described in chapter 5.

Mass accumulation rates (MAR) were calculated using the equation below, sedimentation rates using the methods detailed in (chapter 5), and dry bulk density in chapter 3.

MAR = sedimentation rates * dry bulk density

Hypy MAR = MAR * % PyC

where % PyC is the percentage of pyrogenic carbon in the sample

The interpretation of past vegetation is based on both the results from the phytolith classification as well as the $\delta^{13}C_{TOC}$ and $\delta^{13}C_{hypy}$ values (section 2.4.5). The phytolith morphology does not allow differentiation between grasses and sedges. However, the $\delta^{13}C_{TOC}$ values allow distinguishing between C_3 (sedges) and C_4 photosynthetic pathways (grasses), which can assist in identifying changes in the vegetation composition of the savanna. For instance, the $\delta^{13}C$ values for the C_3 end-member in tropical savannas are expected to be -24 ‰ or lower (Diefendorf et al. 2010), while values of - 15 ‰ or greater are indicative of a C_4 plants (grasses), with intermediate values representing a mixed source derived from both C_3 and C_4 biomass (O'Leary 1988; Saiz et al. 2018). Those $\delta^{13}C_{TOC}$ values above -24 ‰ unambiguously indicate either the presence of tropical grasses and that the hydroclimate was significantly drier and/or more seasonal than previous periods (Wurster et al. 2019). For example, *Eleocharis* sedges present at the site have been identified as C_3 plants, with a $\delta^{13}C$ of approximately -26 ‰ or lower (Boon and Bunn 1994; Bunn and Boon 1993).

6.3. **Results**

6.3.1. **Vegetation inventory, modern phytolith identification and classification**

A detailed description of the modern vegetation is given in section 2.2.2. In brief, sedges and heaths dominated the surroundings of Sanamere Lagoon between the edge and 300 m, beyond which point the vegetation transitions to woodland with grassy understorey. A total of 23 plant species from 16 families were identified in the vegetation survey. Table 6.1 presents the plant species distribution along this transect and their dominance. Table 6.2 shows the selected plants and corresponding phytolith

morphologies associated with each species after the dry-ashing procedure. The presence of phytoliths was identified in five species, with the elongated morphology (and variants) dominating the assemblage. Two of the species were from the Poaceae family, while the rest was composed by the Pandanaceae, Restionaceae and Arecaceae families.

Table 6.1. Vegetation inventory and modern reference material of Sanamere Lagoon catchment. Specimens collected in July 2017. Dominance within the community is based on visual representation and estimate.

Distance from lake (m)	Common name	Scientific name	Family	Dominance
0	Native Lasiandra	*Melastoma malabathricum*	Melastomataceae	minor
0	Pandanus	*Pandanus tectorius*	Pandanaceae	minor
0	Tassel cordrush	*Baloskion tetraphyllum*	Restionaceae	major
0	Thryptomene	*Thryptomene oligandra*	Myrtaceae	minor
0	Bulburu sedge	*Eleocharis sphacelata*	Cyperaceae	major
50	Tropical Banksia	*Banksia dentata*	Proteaceae	minor
50	Weeping Tea tree	*Leptospermum madidum*	Myrtaceae	minor
50	Bladderworts	*Utricularia*	Lentibulariaceae	minor
50	Woody Sun dew	*Drosera lanata*	Droseraceae	minor
50	Tassel cordrush	*Baloskion tetraphyllum*	Restionaceae	minor

Distance from lake (m)	Common name	Scientific name	Family	Dominance
50	Cape york heath plant	*Asteromyrtus lysicephala*	Myrtaceae	minor
50	Golden parrot tree (honey wattle)	*Grevillea pteridifolia*	Proteaceae	minor
100	Tropical Bankisia	*Banksia dentata*	Proteaceae	minor
100	Melaleuca		Myrtaceae	minor
100	Jacksonia	*Jacksonia thesioides*	Fabaceae	major
100	Cape york heath plant	*Asteromyrtus lysicephala*	Myrtaceae	minor
100	Golden parrot tree (honey wattle)	*Grevillea pteridifolia*	Proteaceae	minor
150	Tropical Bankisia	*Banksia dentata*	Proteaceae	minor
150	Ada-A Morinda (Mapoon)	*Morinda reticulata*	Rubiaceae	minor
150	Beach myrtella	*Lithomyrtus obtusa*	Myrtaceae	minor
200	Tropical Bankisia	*Banksia dentata*	Proteaceae	minor
200	Bushman's Clothes Pegs	*Grevillea glauca*	Proteaceae	minor
200	Boronia	*Boronia alulata*	Rutaceae	minor
200	Wedge Pea	*Gompholobium nitidum*	Fabaceae	minor

Distance from lake (m)	Common name	Scientific name	Family	Dominance
300	Ada-A Morinda (Mapoon)	*Morinda reticulata*	Rubiaceae	minor
300	Acacia		Fabaceae	minor
300	Northern Cabbage Tree Palm	*Livistona muelleri*	Arecaceae	minor
300	Bushman's Clothes Pegs	*Grevillea glauca*	Proteaceae	minor
350	Poaceae	*Isachne confusa*	Poaceae	major
350	Bushman's Clothes Pegs	*Grevillea glauca*	Proteaceae	minor
400	Hop Bush	*Dodonaea polyandra*	Sapindaceae	major
450	*Eucalyptus*		Myrtaceae	major
450	Quinine tree	*Petalostigma pubescens*	Picrodendraceae	minor
450	Poaceae	*Thaumastochloa major*	Poaceae	minor

Table 6.2. Phytolith morphologies of modern plants surrounding Sanamere Lagoon

Distance from lake (m)	Common name	Scientific name	Family	Morphology
0	Pandanus	*Pandanus tectorius*	Pandanaceae	Elongate sinuate
50	Tassel cordrush	*Baloskion tetraphyllum*	Restionaceae	Elongated
300	Northern Cabbage Tree Palm	*Livistona muelleri*	Arecaceae	Globular echinate
350	Poaceae	*Isachne confusa*	Poaceae	Elongate sinuate
450	Poaceae	*Thaumastochloa major*	Poaceae	Stomata

6.3.2. **Fossil phytolith identification and classification**

The diversity of fossil phytolith taxa is represented by 18 different morphotypes identified in the Sanamere Lagoon sediment sequence. Figure 6.4 presents the relative abundances with the 18 morphotypes associated to the corresponding group, along with the zone delineation derived from the stratigraphic divisions identified in chapter 5. Figure 6.5 presents the relative abundances summarised by plant group. Samples younger than 6.7 ka did not yield the ideal number of diagnostic phytoliths from which to infer reliable conclusions. However, because these samples were composed of a majority of spheroid ornate phytoliths suggestive of woody taxa (> 70 %), they were included in the diagram, as the main purpose of the analysis was to infer the relative vegetation composition of the samples.

Between the beginning of the sequence (33 ka) and 9.7 ka, the assemblage was dominated by phytoliths associated with species in the Poaceae/Cyperaceae families, especially the elongate rugose morphotype. After 9.7 ka, and especially from 7 ka, > 70 % of the phytolith assemblage was derived from woody taxa, especially spheroid ornate

forms. Poaceae morphotypes were identified in low relative abundances (less than 11 %), with the highest percentages found at 22.6 ka. Relative counts of non-diagnostic morphologies (acicular, elongate echinate, elongate sinuous, elongate sinuate, and tracheids) varied across the sequence, with the highest values at 23.7 ka (58 % of the total).

Phytolith concentration also varied widely across the sequence. The highest values were represented at the beginning of the record (30.8 ka) and between 21.4 and 20.4 ka (Figure 6.5). Concentrations decreased steadily from 21.4 ka, and low values were largely maintained, with the only exceptions being at 13.8 and 7 ka. Selected photographs of phytolith types are available in Appendix 2.

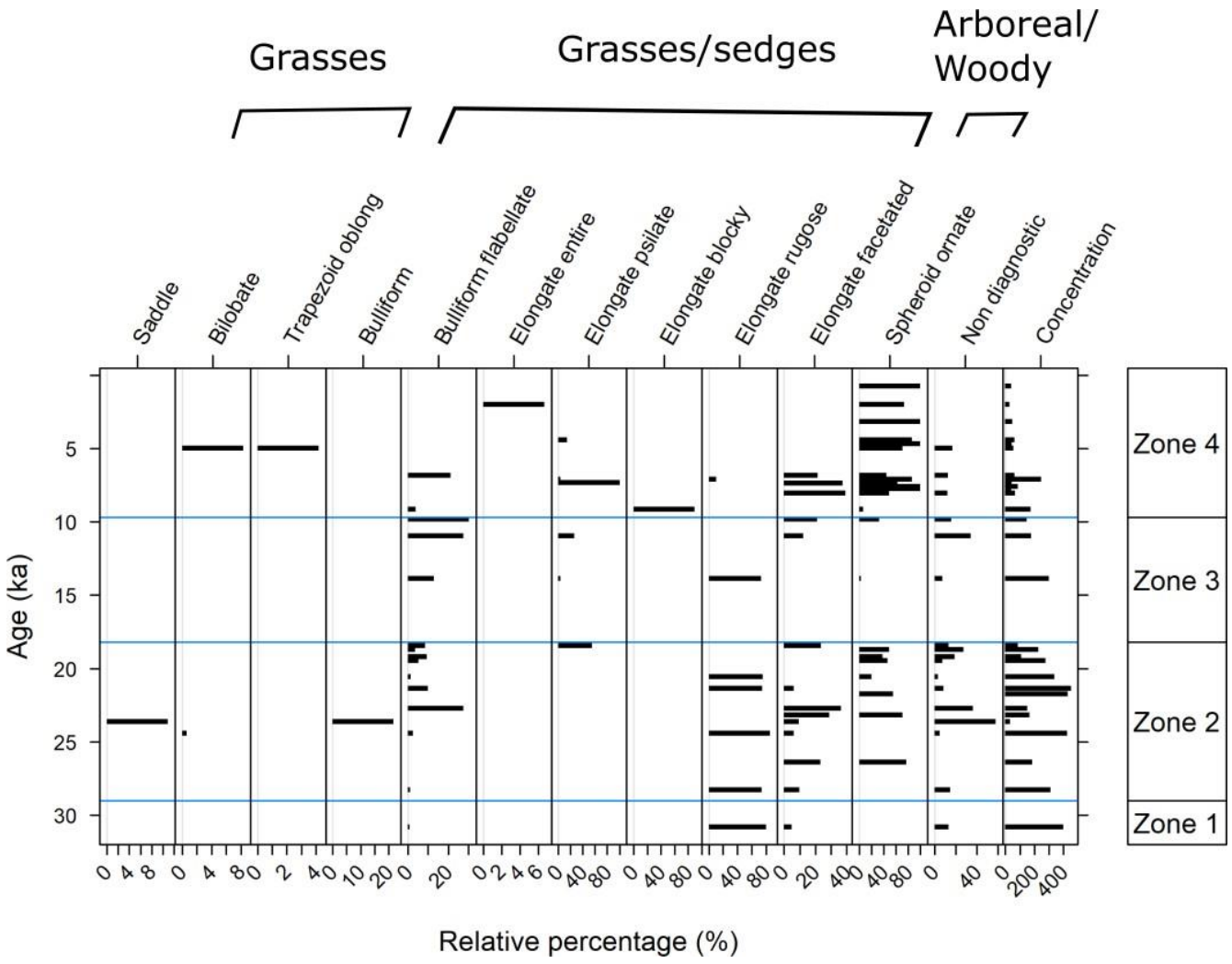

Figure 6.4. Relative abundances of phytolith morphologies and plant groups (concentration in phytoliths/g)

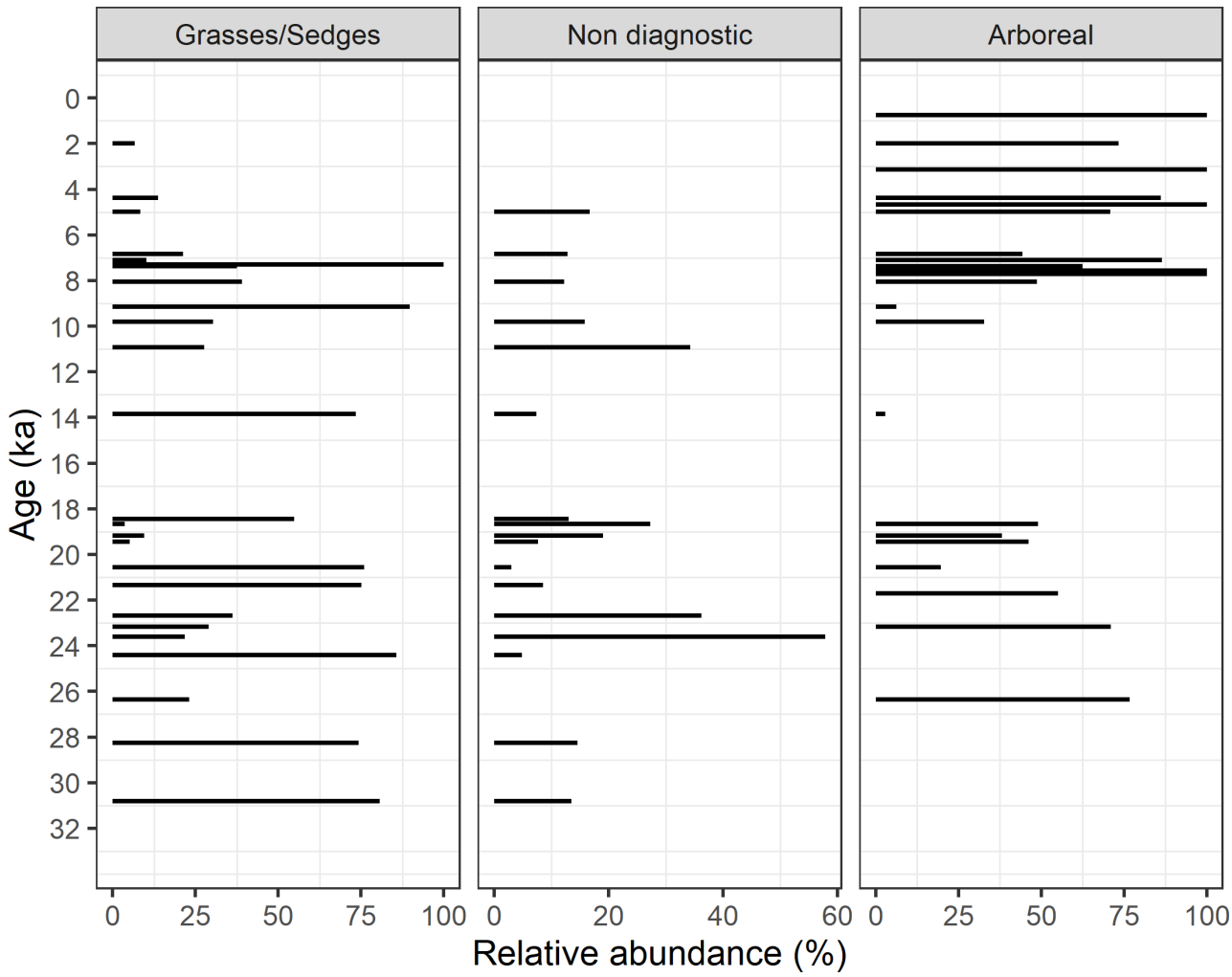

Figure 6.5. Relative abundances of plant groups and concentration of phytoliths

6.3.3. **Pyrogenic carbon and geochemical indicators**

Fire activity was recorded using pyrogenic carbon mass accumulation rates (Hypy MAR) as a proxy for changing fire regime (Figure 6.6). The results suggest periods of very low fire activity between 30.8 ka - 9.3 ka. Large fire increments were identified at 9.3 ka, 7.4 ka - 7.1 ka and 4.7 ka, while small events represented by increased PyC MAR were found at 31.4 ka, 24.9 ka and 15.8 ka.

The $\delta^{13}C_{hypy}$ ranged between -25.5 ‰ and -23.0 ‰ and were most enriched between 26.5 ka - 24 ka and at 9 ka, while the $\delta^{13}C_{TOC}$ values fluctuated between - 29.2

‰ and - 18.4 ‰. The highest values were found before 21 ka (ca. 28 ka). Overall, higher $\delta^{13}C_{TOC}$ values (generally >-24 ‰) dominated prior to the start of the LGM, with irregular values through the LGM and lower values continuing into the post glacial and Holocene periods (Figure 6.5). Only weak correlations were found between the carbon abundance and the isotopic values. For example, the correlation coefficient (r^2) between the abundance of TOC and the abundance of Hypy is 0.27, the r^2 between $\delta^{13}C_{TOC}$ and $\delta^{13}C_{hypy}$ is 0.15. This is the case even when calculated only for the period of time when terrestrial input was found to be dominant (4.7 - 10 ka) (r^2= 0.3) (Figure 6.7).

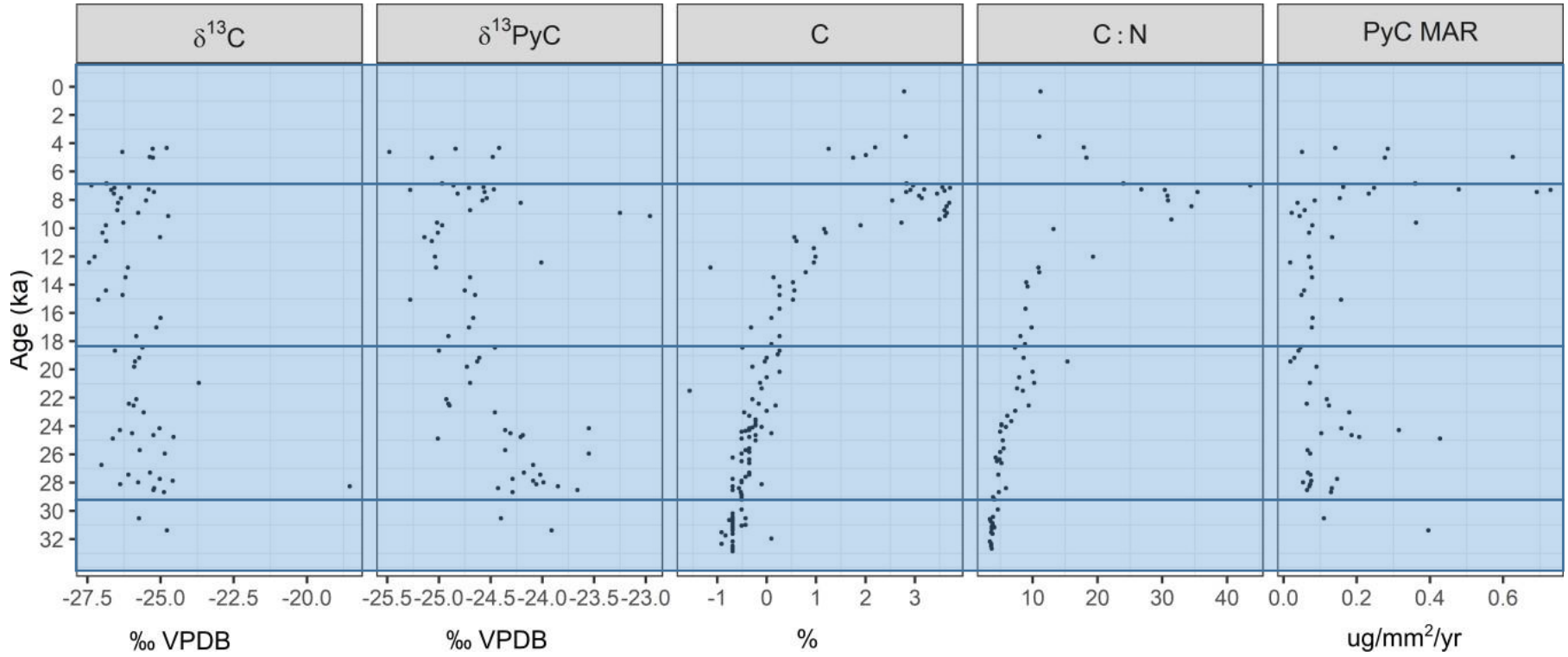

Figure 6.6. $\delta^{13}C_{TOC}$ value, $\delta^{13}C_{hypy}$, Carbon percentage, C:N ratio, and pyrogenic carbon mass accumulation rate (PyC MAR or Hypy MAR) ((ug mm^2/yr)

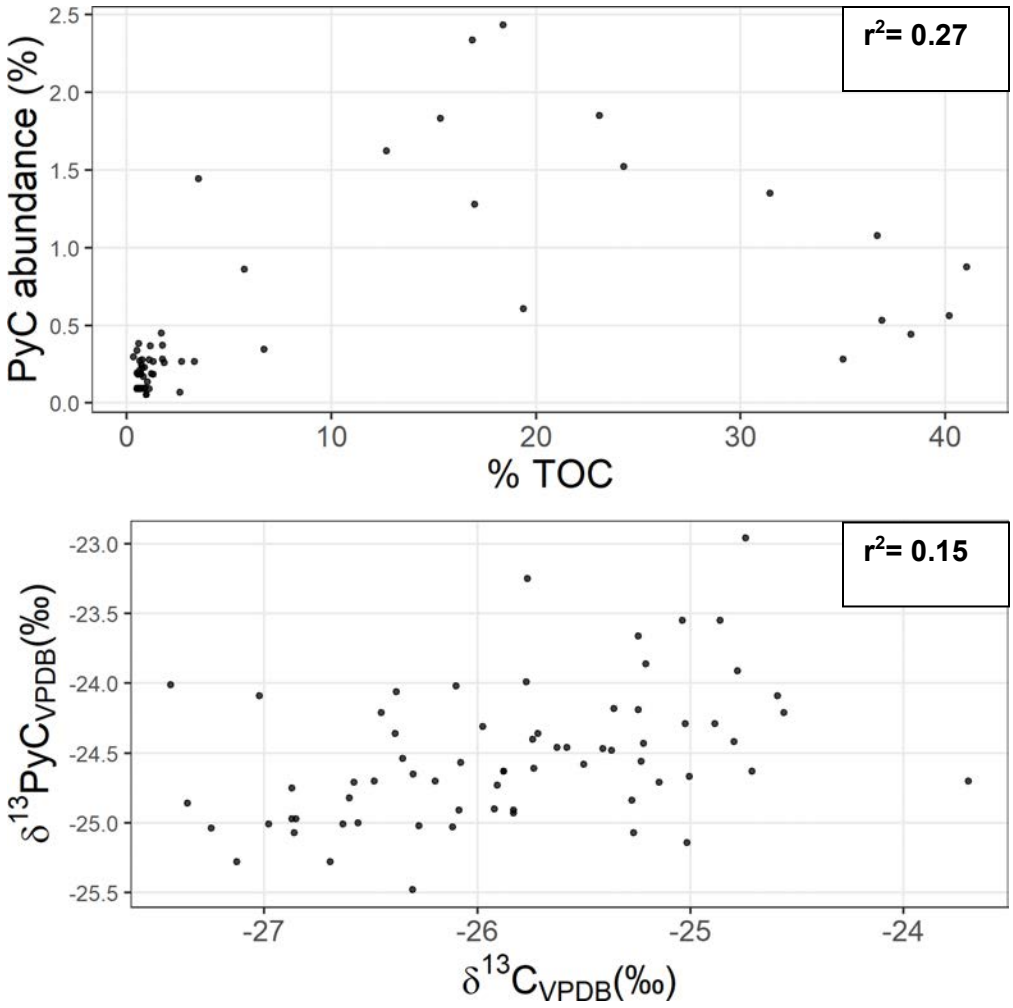

Figure 6.7. Relationships between (a) Hypy abundance and TOC and (b) $\delta^{13}C_{hypy}$ value and $\delta^{13}C_{TOC}$

6.4. **Discussion**

6.4.1. **Vegetation and fire change at Sanamere Lagoon**

This section discusses fire and vegetation changes reflected in the sedimentary record of Sanamere Lagoon spanning the last 33,000 years. The $\delta^{13}C_{TOC}$ (< -24 ‰) and C:N (< 15) values are consistent with the dominance of aquatic plants at the site, including the presence of a mixture of sedges, woody taxa (C_3) and minimal presence of grasses (C_4) during the Glacial and the LGM periods (33 – 18 ka). C_3 taxa (arboreal and

sedges) dominated during the Deglacial and the Holocene (18 ka – Present). The $\delta^{13}C_{hypy}$ also confirms the vegetation burnt in the lake catchment was predominantly C_3. The naming of the temporal periods follows the previous chapter (units A-D).

6.4.1.1 Units A and B (33 - 18.2 ka)

Aquatic plants were dominant in the sedimentary organic matter during this period according to the $\delta^{13}C_{TOC}$ values and the C:N ratios (fresh algal organic matter typically has C:N ratios between 4 and 10 (Meyers and Ishiwatari 1995)). The phytolith counts support the dominance of Cyperaceae species, with limited amounts of C_4 taxa ($\delta^{13}C_{TOC}$ < -24 ‰). The $\delta^{13}C_{hypy}$ values suggest that the pyrogenic carbon derived from fires came predominantly from C_3 species. At around 26 ka, arboreal taxa are first recorded. Low phytolith concentrations and Hypy MAR values also suggest minimal biomass availability to carry fires, with a small increase in fire activity recorded at 24.8 ka, so fire was not completely absent within the ecosystem. Fire patterns at Sanamere were similar to those found in other sites in northern Australia, where fire activity was low during the LGM, but small increases in fire were found between 26.2 - 24.5 ka (Rowe et al. 2019).

During 22 ka - 18.2 ka, vegetation in the immediate catchment of Sanamere continued to be dominated by sedgeland species, with very few grasses (C_4), according to the phytolith and $\delta^{13}C_{TOC}$ values. The C:N ratios started to record values between 10 and 20, as these samples probably contain elevated proportions of land-derived organic matter in comparison with older samples. This response is expected given that the site was probably receiving low precipitation under a drier, inactive monsoon and a mild LGM (chapter 5, section 5.4.2). According to the biological and geochemical indicators analysed from Sanamere (chapter 5), decreased precipitation dominated during this time period. Cape York had limited moisture sources to the north or west (Williams et al. 2018) as a result of low sea levels (-120 m) (Ishiwa et al. 2019; Brooke et al. 2017). The sediments at Sanamere record a slight decrease in woody taxa in favor of sedges during the LGM, compared to the previous period. This change agrees with modern studies that have determined that water stress decreases woody biomass and diversity (Cook et al. 2002; Cook and Heerdegen 2001). These results are consistent with the presence of mild LGM (not extremely dry) conditions at the site.

The Sanamere record for the LGM reflects a difference in the intensity of the LGM conditions recorded in the only terrestrial vegetation and fire record available from the savannas of northern Australia (Girraween Lagoon, Northern Territory). This record indicates the dominance of grasses as a response to dry, cool conditions (Rowe et al. 2020). Palynological investigations of sea cores between Australia and New Guinea also show an expansion of grassland at the LGM (Petherick, Moss, and McGowan 2011). Studies on the wet tropics (Lake Euramoo, ODP820) also suggest increased Poaceae during the LGM. Expansion of sclerophyll woodland at the expense of rainforest is seen at Lynch's Crater, Strenekoff's Crater (Kershaw 1994), Lake Euramoo (Haberle 2005) and ODP820 (Moss and Kershaw 2007), indicating a regional trend across the tropics.

Decreased CO_2 is likely to have decreased the competitiveness of woody C_3 biomass compared to grass dominated C_4 biomass (Prentice et al. 2017). Low CO_2 has also been shown to reduce or prevent reproduction in C_3 species, whereas growth and reproduction of C_4 species (e.g. tropical grasses) are generally unaffected (Rowe et al. 2019). However, decreased LGM temperature would decrease evaporation and therefore increase effective plant available moisture for a given mean annual rainfall (Liu, Jiang, and Lang 2018). These conditions would help to maintain C_3 species, such as sedges, at Sanamere Lagoon. Woody plants in the site may have occurred as scattered individuals above the grasses.

6.4.1.2 Unit C (18.2 - 9.7 ka)

Aquatic plants continued to dominate according to the isotopic values and both woody taxa and Poaceae decreased compared to the previous period. The $\delta^{13}C_{TOC}$ values (<-24 ‰) suggest the continued dominance of C_3 species, in particular sedges, according to the phytolith record. Both the isotope and phytolith records suggest that few grasses were present during this time. Black Springs in northwest Australia reports an increase in Cyperaceae, *Pandanus* and wetland taxa (Field, Tyler, et al. 2018) during the deglacial period, while Girraween indicates that grasses expanded during the early Holocene. Low fire activity continues from the previous period and was sustained by C_3 taxa at Sanamere. According to the $\delta^{13}C_{hypy}$ and $\delta^{13}C_{TOC}$ values, the vegetation being burnt at Sanamere was C_3, with no C_4 grass-derived pyrogenic carbon present. The sediments from Sanamere Lagoon are consistently ^{13}C-depleted, falling well within the range expected for C_3 plants (O'Leary 1988; Saiz et al. 2018). The presence of a grass

component would result in substantially more positive $\delta^{13}C_{TOC}$ values, with $\delta^{13}C_{TOC}$ values expected to fall between approximately -17 ‰ and -22 ‰ (assuming end members of -15 ‰ and -24 ‰ for C_4 and C_3 respectively; Saiz et al. (2018)).

The Sanamere record is also congruent with the low burning biomass activity recorded by the available studies for the Australian dry tropics for this period (Field, Tyler, et al. 2018; Rowe et al. 2019). At ca. 12.8 ka, a change towards a mixture of land- and aquatic plant-derived, with a dominance of sedges is evident at Sanamere, with C:N ratios between 10 and 20. These vegetation changes are consistent with a return to more humid conditions (ranging from 14 ka to 12 ka) resulting from the increase in sea level and enhanced monsoon activity at the site (chapter 5) and across the region (Denniston et al. 2017; Denniston, Wyrwoll, Asmerom, et al. 2013; De Deckker 2001). These changes were fueled by the return to marine conditions in the Gulf of Carpentaria (ca. 10.5 ka) after sea level rise. The differences in detail between sites may be explained by the spatially inconsistent redevelopment of the monsoon (Denniston, Wyrwoll, Polyak, et al. 2013). Other records from sites in the region record change in vegetation. For example, pollen sequences from Lynch's Crater (Turney et al. 2004) suggest that rainforest was established at 10.9 ka. Considerable intensification of the monsoon coincided with Southern Hemisphere warming and intensified greenhouse forcing over Australia during the atmospheric CO_2 rise at 12.9 ka – 10 ka (Kuhnt et al. 2015).

6.4.1.3 Unit D (9.7 ka – Present)

At 9.7 ka, most of the organic input to the lagoon came from terrestrial sources according to the C:N ratios (>20) at this time. Vegetation switched from dominant sedges to a dominance of C_3 woody/arboreal taxa ($\delta^{13}C_{TOC}$ <-24 ‰), with almost no contribution of Poaceae (C_4) species. The presence of Poaceae appears to be increase slightly only around 9 ka, where $\delta^{13}C_{hypy}$ values are higher indicating that grass, possibly remote from the lake edge, was contributing to the PyC. Wetter conditions and higher CO_2 encouraged vegetation change, facilitating the growth of woody taxa around Sanamere. Overall, pollen from the region also reflects woodland expansion at this time (Proske, Heslop, and Haberle 2014), when modern vegetation probably became established in the Sanamere Lagoon catchment. Around Big Willum, as open water developed, from around 7 ka - 5 ka, grass and sedge representation declined as the swampy basin

bottom became submerged. At Black Springs, there is a clear change in pollen assemblages at 6.8 ka because of the decreasing abundance of wetland taxa (particularly Cyperaceae) and increases in ferns. Girraween maintains a dominance of grasses. In contrast, extensive stable mangrove communities dominated coastal Torres Strait starting at 6 ka and 3 ka (Rowe 2007). The presence of woody taxa is also recorded at Walala in the Gulf of Carpentaria (Prebble et al. 2005). The changes at Sanamere are in agreement with the timing of transition to rainforest in the wet tropics of Australia at Lake Euramoo (Haberle 2005) and ODP820 (Moss and Kershaw 2007) ca. 9.5 ka, also interpreted to reflect an increase in rainfall. Vegetation at Girraween Lagoon also showed changes (taxa characteristic of a dampland-swamp environment to form a fringing zone) due to wetter climate (Rowe et al. 2019).

An increase in the quantity and diversity of biomass to burn is reflected in the record of fire activity at Sanamere, which remains high until 4.7 ka. A moderate peak exists at 9.5 ka, and the period between 7.7 and 7.1 ka presents the highest accumulation rates of the hypy fraction in the sequence. The C:N ratio also reflects the increased contribution of terrestrial plants to the sediments in the lake (Figure 6.5), reflecting increased runoff from the lake catchment (chapter 5). The increases in fire activity and vegetation followed the increment in precipitation suggested by the climatological changes identified at the site (section 5.4.4) and regionally (9 ka - 4 ka) (Field, Tyler, et al. 2018; Denniston, Wyrwoll, Polyak, et al. 2013; Proske et al. 2017; Nott, Price, and Bryant 1996). This period of increased fire is coincident with the early Holocene development of swamps records in the Gulf of Carpentaria, Cape York Peninsula and eastern tropical Queensland (Luly, Grindrod, and Penny 2006; Prebble et al. 2005; Rowe 2007; Shulmeister 1992; Stephens and Head 1995).

The early to middle Holocene is generally associated with greatest regional precipitation in northern Australia. These changes during the early and middle Holocene are also congruent with the sea-level rise from −53 m (depth of the Arafura Sill) ca. 11.7 ka to ca. –25 m by 9.8 ka and the culmination of the Holocene sea-level highstand (7.7 ka - 4 ka) and a corresponding period of increased precipitation and temperature during the Holocene. Coastal flooding facilitated increased moisture and heat transfer/transport, fueling monsoon activity (Sloss et al. 2018).

After 4.6 ka, woody taxa and sedges continue to dominate the assemblage, with the $\delta^{13}C_{TOC}$ and $\delta^{13}C_{hypy}$ values suggesting a minimal presence of grasses. Studies in Girraween Lagoon also suggest a peak in woody regrowth (Rowe et al. 2019) during this time, while at Black Springs the abundance of *Timonius timon* and *Terminalia* increased, suggesting that the monsoon was weaker than earlier in the Holocene section of the record, as these plants thrive during drier conditions (Field et al. 2017). After 4 ka, phytolith concentration, C:N ratios and Hypy MAR decrease, which indicate an expansion of the lagoon (less sediment supply able to reach the lake center). Short dry phases and more variable conditions has been identified at other sites in northern Australia after 4 ka, related to increased ENSO variability (Field, Tyler, et al. 2018; McGowan et al. 2012), and have been associated with falling sea-level (Sloss et al. 2018). These conditions resulted in a decrease in effective precipitation and temperature after ca. 5 ka (Shulmeister 1992, 1999). At Sanamere Lagoon these changes resulted in a decrease in terrigenous sediment supply into the lake and hence organic-rich sediments (section 5.4.4).

Although the vegetation composition remained unchanged at Sanamere, fire activity decreased, as result of a decline in available biomass. Continuing the trend seen in the previous period, the pyrogenic carbon signature is dominated by C_3 species. Rehn et al. (2020) also found that burning in the upper sediments of Sanamere Lagoon is dominated by C_3 species. The decrease in fire activity is in contrast to most other sites in northern Australia (Prebble et al. 2005; Rowe 2015, 2007), which show enhanced fire activity during the Late Holocene (Stevenson et al. 2015; Luly, Grindrod, and Penny 2006; Stephens and Head 1995). Generally, the late Holocene is characterized by climatic variability in most of the sites in the area. However, at Sanamere Lagoon there is not a clear evidence to suggest the presence of climatic variability at the site at this time (section 5.4.4). Therefore, these results suggest inconsistent monsoon intensity in the area, with areas north of Sanamere Lagoon recording higher intensity in monsoon activity.

6.4.2. **Phytoliths and pyrogenic carbon as environmental proxies**

Although the results presented in the chapter highlight the potential of phytoliths to reconstruct past vegetation, phytolith analysis is potentially biased given the production and taphonomic complications associated with the transport and preservation

of these microfossils (Bremond et al. 2004; Strömberg et al. 2018). Most of the species currently surrounding Sanamere do not produce phytoliths, and the same is expected for past vegetation. Also, phytoliths only allow the identification of general plant groups, with no data about families/species. Furthermore, the poorly resolved taxonomy associated with woody taxa and dicotyledonous herbs compared to grasses limit the inferences that can be derived from the record. Using alternative microfossil analyses such as pollen would increase the resolution of the identified vegetation taxa at Sanamere Lagoon.

The use of hypy saves considerable time when measuring pyrogenic carbon abundance. However, almost no PyC is produced by hydrogen pyrolysis at temperatures below ~ 350˚C, with ~ 50% of charred carbon being identified as PyC by 500˚C, and the majority of carbon present as PyC by ~ 700˚C (Wurster et al. 2013). Therefore, not all charred particles will be identified as PyC, and PyC could be biased against the recording of low intensity fires.

6.5. **Chapter 6 summary**

The combination of phytolith, pyrogenic carbon and $\delta^{13}C_{TOC}$ analysis increases the detail of our understanding of the vegetation and fire dynamics reflected in the Sanamere Lagoon sediments. While sedges are initially recorded as comprising the bulk of biomass at Sanamere Lagoon, the presence of arboreal taxa starts around 26 ka, at a time where dry and cool conditions prevailed in the Cape York region (Reeves et al. 2013). Poaceae species are also recorded for the first time during this phase. The redevelopment of the monsoon between 18.2 ka and 9.7 ka sustained the dominance of members of Cyperaceae at the site. Starting at 9.7 ka, wetter conditions sustained the development of more arboreal taxa over the course of the Holocene, compared to previous periods. This change is consistent with the development of a wetter phase through the late and middle Holocene, derived from sea level rise and wetter conditions associated with strengthening of the monsoon.

The use of phytolith, $\delta^{13}C_{TOC}$, and $\delta^{13}C_{hypy}$ values complement each other when reconstructing past vegetation. Although phytolith analysis provided ambiguous evidence of C_4 species, the results from the isotopic analyses confirmed the presence of some C_4 biomass at the site at different times, and the $\delta^{13}C_{hypy}$ values confirmed the vegetation being burnt included mostly C_3 species.

The Glacial and LGM periods were characterized by low fire activity, with small increases evident at 31.8, 24.9 and 16 ka. These peaks in fire activity are independent of phytolith concentration, which confirm these events reflect higher fire abundance. Peaks in Hypy abundance at 9.3 ka and 7.4 - 7.1 ka indicate increased fire activity (sustained by the availability of more biomass to burn) during the early and middle Holocene. This finding is consistent with the results from other studies in the region and the general trends indicated by the regional reconstructions.

Chapter 7. Synthesis and future research directions

The objective of the current chapter is to synthesize the central findings of the thesis and possibilities for future research. Therefore, the key findings from previous chapters are integrated in the context of past climate reconstruction.

Two main topics (geochronology and environmental change) guided the development of the project. For geochronology (aim 1, chapter 4), I built a reliable radiocarbon dating chronology by comparing the results from different carbon fractions. I concluded that the hypy fraction was the most consistent with the changes in stratigraphy and sedimentology observed in the core. For environmental change (aims 2 and 3), I then reconstructed changes in hydrology and sediment transport using diatoms and elemental concentrations (chapter 5). Finally, in the third aim, I reconstructed the vegetation and fire in the site (chapter 6) using phytoliths, stable isotope composition and pyrogenic carbon abundance derived from the hypy fraction.

7.1. Sanamere Lagoon climate, fire and vegetation over the last 33 ka

The Sanamere Lagoon sediments present a history of environmental change in the wet-dry tropics of northern Cape York for the last 33 ka. Table 7.1 and Figure 7.1 present a summary of the development of the lagoon and the associated climatic, vegetation and fire conditions. Sea level was a defining driver of local environmental change and development of the lagoon since its formation. Most of the vegetation burnt around Sanamere Lagoon was C_3, according to the isotopic values derived from the hypy fraction. The basis and evidence for the discussion and conclusions presented below is derived from the previous chapters and is not repeated here.

Table 7.1: Summary of environmental changes found at Sanamere Lagoon

Time (ka)	Hydroclimate	Vegetation and fire
33.1 - 29.2	Infilling of the lagoon, associated with wet event/ low sea levels, but not as low as during LGM/ shift of ITCZ	Low fire activity and limited availability of biomass to burn. Mostly aquatic plants, with limited contributions of C_3 (sedges) and C_4 (grasses) species
29.2-18.2	Small, shallow lagoon reflecting dry and cool conditions	Increased C_3 vegetation and low fire activity.
18.2-9.7	Wetter conditions, larger lake (increase in area)	Low fire activity continues. Mixture of land and aquatic plants, with dominance of sedges.
9.7-4.9	Expansion and deepening of the lagoon/sea level high stand and higher precipitation	Dominance of terrestrial plant input (C_3, sedges and arboreal) and peaks in fire activity between 9.3 ka and 7.1 ka. More availability of biomass to burn (C_3)
4.9 - Present	Present stabilization and deepening of the lagoon	Return to a mixture of aquatic and land derived plants, mostly sedges (C_4)

7.1.1. Unit A (33 - 29.2 ka) Initial formation

Low sea levels allowed the lagoon impoundment around ca. 33,000 years ago, through laterite karst collapse, as a result of regionally low water tables associated with progressive decline in sea level through MIS 3. This collapse allowed the emergence of a groundwater window that ensured that the site did not dry out since its formation, despite large changes in rainfall and a generally shallow depth. The water level in the shallow pond varied relatively little in response to changing hydroclimate but the low gradient basin meant that relatively small changes in groundwater level translated into large variations in the area and nature of the water present. Changes in rainfall, along with changes in water area exerted strong control on the transport of clastic material to the core site. After the lagoon formation, an initial interval of increased sedimentation rates (31.6 – 30.1 ka), and possibly initially relatively wet conditions, precedes a period of dryer hydroclimate (30.1 – 29.1 ka), that resulted in sparse vegetation cover, with aquatic plants and C_3 species (sedges) the only plants feeding into the core site deposition, and low fire activity.

7.1.2. Unit B (29 – 18.2 ka) Drier hydroclimate and reduced vegetation cover

The period 29.2 ka - 18.2 ka, before and into the Last Glacial Maximum was drier and cooler compared to the previous stage immediately following lake formation. Low rates of sediment transport and biological activity, including sparse vegetation cover and limited fire activity, with aquatic plants dominating the organic matter delivered to the lagoon floor the lagoon. The conditions reflected at Sanamere Lagoon are consistent with the regional records of dry and arid conditions during the Glacial period. The Sanamere Lagoon sediments (hydrology and vegetation) support evidence of increased aridity during the LGM, in contrast with the results proposed by some other regional studies. It is likely that at this time the lagoon was relatively small and shallow due to a reduction or cessation of monsoon rainfall. Reduced sea level meant that the nearest ocean was located several hundreds of kilometres from the lagoon. Extreme dry LGM conditions were not reflected on the Sanamere vegetation record, but analyses at the species level, through palynology, would provide more details regarding fine scale ecological changes at the site. However, dry conditions and a lower lagoon water level

could have supported the formation of several small sand bodies. Further geomorphological analyses would confirm this hypothesis.

7.1.3. **Unit C (18.2 – 9.7 ka) Sea level rise and reactivated monsoon**

During 18.2 ka - 9.7 ka Sanamere Lagoon expanded following the rise in sea level and reactivation of monsoon activity. Low sedimentation rates, along with decreased coarse grains and Ti counts suggest an expanded body of water after 19.8 ka. However, the most significant geochemical and biological changes are evident after the rapid increase in sea level ca. 11.2 ka recorded in the Gulf of Carpentaria. From 10.8 ka, increases in organic matter content and diatom diversity suggest increased terrigenous organic input, resulting from an increase in local biomass. Further strengthening of the monsoon (and wetter conditions) start at 12.8 ka. Low fire activity was consistent with low biomass availability during this period in the Sanamere Lagoon record. The vegetation being burnt was mostly C_3.

7.1.4. **Unit D (9.7 ka – 4.9 ka) Stabilizing sea levels and high lakes levels**

Wetter conditions compared to units A and B, continued during this phase. Strong evidence for a wetter phase along with higher rates of sediment transport and biological activity are consistent with the development of swamps in other areas in northern Australia (Prebble et al. 2005; Luly, Grindrod, and Penny 2006; Proske et al. 2017). The peaks in fire activity at Sanamere Lagoon at 9.5 ka, 7.7 ka - 7.1 ka and 4.9 ka suggest an increase in the availability of available biomass to burn, built by wetter and more humid conditions, but with seasonal drying to an extent that enabled fire to burn into the sedges surrounding the lake. A maximum in terrestrial sediment input, arboreal vegetation and fire activity is evident at ca. 7 ka. This period of increased precipitation is consistent with the records in Cape York and the Gulf of Carpentaria.

7.1.5. **Unit E (4.9 ka - Present) Stabilisation**

From ca. 4.9 ka organic matter, fire activity, vegetation and diatom concentrations decreased, a pattern that suggests decreased precipitation, or potentially greater variability in rainfall at interannual timescales. Between 4.9 ka - 4.2 ka, high

sedimentation rates and changes in the diatom assemblage and geochemical indicators indicate a deepening of the lake. The limited data after 4.2 ka reflects an absence of major additional transformations. Modern conditions approached as seasonally dry conditions supported low nutrient input and sedges around the edge, with savanna vegetation (heathland and *Eucalyptus*) developing further away from the lake edge.

33 - 29.1 ka

Changing climatic conditions

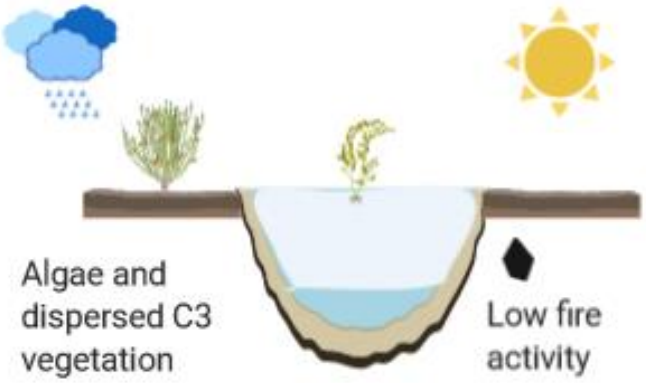

29.1 - 18.2 ka

Increased aridity

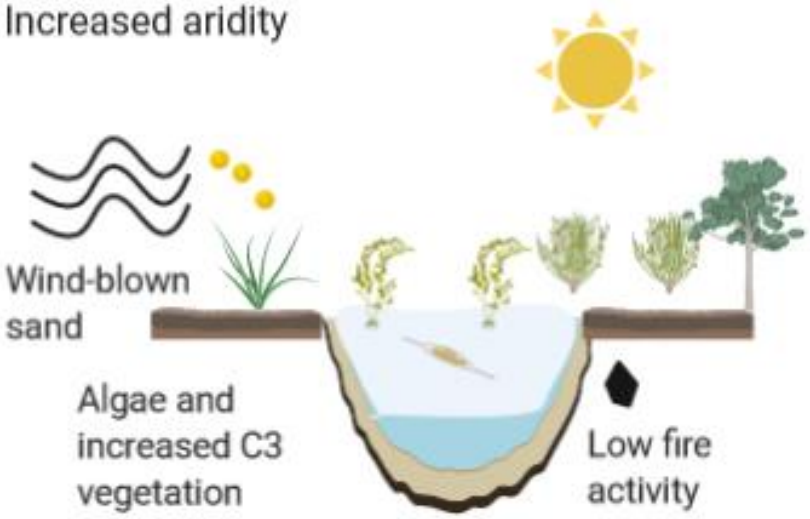

18.2 - 9.7 ka

Wetter conditions

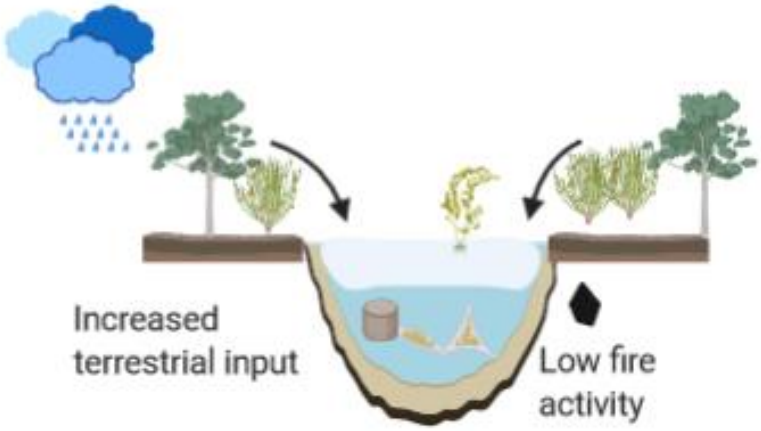

9.7 - 4.9 ka

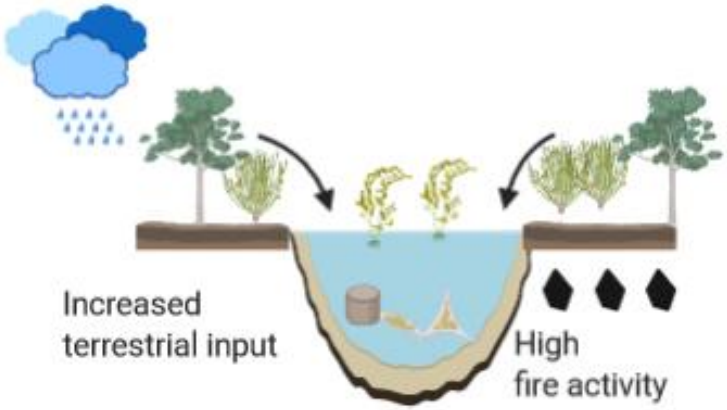

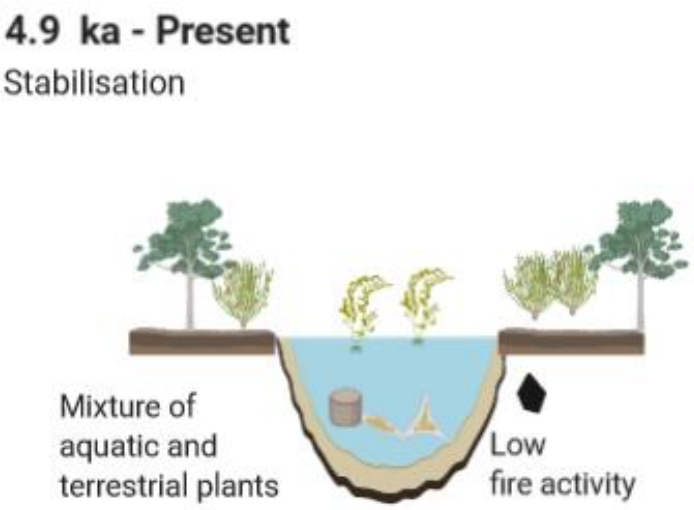

Figure 7.1. Summary of environmental changes at Sanamere Lagoon

7.2. Limitations of this study

The main limitations of this research are related to temporal resolution and the qualitative nature of the palaeoenvironmental interpretations.

First, the coarse temporal resolution (> 150 years per cm) obtained from the sampling of the sediment core limits the possibility of deriving centennial and sub-centennial scale inferences of environmental change. However, it was possible to compare with millennial-scale records from other sites in the area.

Second, the reconstruction of environmental data in this thesis was broadly described using comparative and qualitative terms referring to the preceding interval. This terminology was only able to provide a broad insight into the site's climate, rather than enabling quantitative assessments of environmental parameters such as temperature and rainfall amount.

7.3. **Future directions**

Future research has significant potential to complement the findings of this thesis. First, to validate the use of the hypy fraction as the most reliable to build radiocarbon chronologies, further tests in other lake sediment cores are required. I propose a similar approach to the one taken in this thesis, where I compare the results from several different carbon fractions from the same depth along the core and select the most reliable one based on the consistency between fractions and correspondence with observed stratigraphic changes. As a second step, I would suggest analysing the degree of agreement between the results from different cores, which will expand our understanding of the factors affecting different carbon fractions in lake sediments. Additionally, this methodology could be also tested using cores collected from outside tropical areas, where there is similar need for consistent, standardised protocols for selecting and pretreating carbon fractions for radiocarbon dating.

Although the extended use of radiocarbon and luminescence dating have facilitated the building of better age-depth correlation models in many studies, the establishment of a reliable and accurate chronology is still a challenge in the development of hydrological and palaeoenvironmental reconstructions. As mentioned above, the hot and wet conditions of some tropical areas influence the preservation state of the materials to be analyzed in these settings. For instance, aberrant radiocarbon results could be linked with poorly preserved or degraded charcoal, when the combustion yields are lower than usually expected (50–60 % C by weight) (Higham et al. 2009). Also, many materials used for radiocarbon dating are prone to contamination and reservoir effects, which are known to cause serious deviations in the obtained ages. Likewise, no matter the geographical location, reservoir and hard water effects compromise the reliability of radiocarbon dates.

Finally, the bioturbation caused by fauna is also a dominant mixing agent in the tropics (Johnson et al. 2014; Kristensen et al. 2015). This factor usually causes the disagreement between radiocarbon and optically stimulated luminescence results.

Another research priority will be the development of high-resolution palaeoenvironmental studies at the local level in the dry tropics of Australia. To date, few records span beyond the Holocene. Current and future studies can be integrated to

establish a detailed record of the local and regional changes in the area during the Pleistocene. Comparisons with the Kimberley area will be fundamental to understand the evolution of palaeoenvironmental differences at the regional level. This area preserves long and high-resolution records, such as speleothems, palaeochannels and springs, which are still to be found in Queensland

Although this study employed several geochemical and microfossil proxies, further information could be derived using additional proxies and analyses. For example, the use of pollen analysis would add higher resolution to the description of the long-term terrestrial vegetation present around Sanamere Lagoon. Pollen grains are the most widely used data source for describing past terrestrial vegetation and the recent development of modelling techniques such as the Landscape Reconstruction Algorithm with the purpose of improving understanding of past vegetation dynamics is increasing the ability to infer quantitative reconstructions (vegetation, temperature and precipitation) using palynology.

Further information can be provided by oxygen isotopes from diatoms. These isotopes have proven to be useful to infer past temperature and δ^{18}O of ambient water. Sponge spicules present in the Sanamere core, and in several lake sediment deposits across tropical areas, have also shown to be valuable sources of palaeoenvironmental information.

While the last decade has brought new technical advances to strengthen palaeohydrological research including the development of molecular level proxies such as *n*-alkanes and other biomarkers these techniques have been mostly applied in research carried out in temperate and artic areas. In the tropical Americas, their use is limited, while in tropical Australia they have not been applied with palaeohydrological purposes in mind. The use of biomarker techniques has been rapidly expanding in temperate areas, while their application in tropical areas is incipient. New analytical developments continue to be applied in mainly temperate areas that potentially have application in the tropics. For example, there have been some research efforts directed towards the use of the oxygen isotopic signal of biomarkers as indicators of the isotopic composition of lake water and thereby hydrology (Zech et al. 2014). These analyses could expand and complement those results retrieved in previous studies. Another important aspect to consider in the use of isotope measurements is their geographical

specificity. Some studies point out the complex factors that control isotopic values in rainfall in the tropics and highlight the importance of a better understanding of the variables affecting the observed composition of lake water and the proxy isotope signals derived from lake water (Bird et al. 2020; Douglas et al. 2012).

Furthermore, the development of quantitative palaeoclimate records for Cape York is essential to contribute to the understanding of the global climate and the monsoon systems across deep time scales. To accomplish this purpose, the development of modern analogues and transfer functions specific for the region will advance the efforts to increase the quantitative component available from palaeoenvironmental data in the region.

Finally, this study analysed vegetation and fire changes using phytoliths and pyrogenic carbon, which are proxies still in progress to become established. Further studies will compare the results from these proxies with pollen and charcoal counting, respectively, which are widely used in quaternary studies. These analyses and comparisons will expand the availability of proxies and the inferences derived from palaeoenvironmental studies.

References

Abrahams, H, M Mulvaney, D Glasco, and A Bugg. 1995. Areas of Conservation Significance on Cape York Peninsula. Canberra: Australian Heritage Commission.

Aitken, M. J. 1990. Science-Based Dating in Archaeology.Longman Archaeology Series London ; New York: Longman.

Albert, Rosa M., and Curtis W. Marean. 2012. "The Exploitation of Plant Resources by Early Homo Sapiens: The Phytolith Record from Pinnacle Point 13B Cave, South Africa: Phytoliths from Pinnacle Point 13B Cave, South Africa. Geoarchaeology 27 (4): 363–84. https://doi.org/10.1002/gea.21413.

Aleman, Julie C., Audrey Saint-Jean, Bérangère Leys, Christopher Carcaillet, Charly Favier, and Laurent Bremond. 2013. "Estimating Phytolith Influx in Lake Sediments." Quaternary Research 80 (02): 341–47. https://doi.org/10.1016/j.yqres.2013.05.008.

Alex, Bridget, Omry Barzilai, Israel Hershkovitz, Ofer Marder, Francesco Berna, Valentina Caracuta, Talia Abulafia, et al. 2017. "Radiocarbon Chronology of Manot Cave, Israel and Upper Paleolithic Dispersals." Science Advances 3 (11): e1701450. https://doi.org/10. 1126/sciadv.1701450.

Ali, Adam A., Philip E. Higuera, Yves Bergeron, and Christopher Carcaillet. 2009. "Comparing Fire-History Interpretations Based on Area, Number and Estimated Volume of Macroscopic Charcoal in Lake Sediments." Quaternary Research 72 (3): 462–68. https://doi.org/10. 1016/j.yqres.2009.07.002

Arnold, J. R., and W. F. Libby. 1949. "Age Determinations by Radiocarbon Content: Checks with Samples of Known Age." Science 110 (2869): 678–80. https://doi.org/10.1126/science.110.2869.678.

Ascough, P. L., Michael I. Bird, F. Brock, T. F. G. Higham, W. Meredith, C. E. Snape, and C. H. Vane. 2009. "Hydropyrolysis as a New Tool for Radiocarbon Pre-Treatment and the Quantification of Black Carbon." Quaternary Geochronology 4 (2): 140–47. https://doi.org/10.1016/j.quageo.2008.11.001.

Ascough, P. L., Michael I. Bird, W. Meredith, R. E. Wood, C. E. Snape, F. Brock, T. F.G. Higham, D. J. Large, and D. C. Apperley. 2010. “Hydropyrolysis: Implications for Radiocarbon Pretreatment and Characterization of Black Carbon.” Radiocarbon 52 (3): 1336–50. **Error! Bookmark not defined.**. Australian Geoscience Information Network. 2020. http://www.geoscience.gov.au/.

Barker, P. A., Jean-Charles Fontes, and Françoise Gasse. 1994. “Experimental Dissolution of Diatom Silica in Concentrated Salt Solutions and Implications for Paleoenvironmental Reconstruction.” Limnology and Oceanography 39 (1): 99–110. https://doi.org/10.4319/lo.1994.39.1.0099.

Battarbee, Richard W., Vivienne J. Jones, Roger J. Flower, Nigel G. Cameron, Helen Bennion, Laurence Carvalho, and Stephen Juggins. 2002. “Diatoms.” In Tracking Environmental Change Using Lake Sediments, edited by John P. Smol, H. John B. Birks, William M. Last, Raymond S. Bradley, and Keith Alverson, 3:155–202. Dordrecht: Kluwer Academic Publishers. https://doi.org/10.1007/0-306-47668-1_8.

Bayliss, Alex. 2009. “Rolling Out Revolution: Using Radiocarbon Dating in Archaeology.” Radiocarbon 51 (1): 123–47. https://doi.org/10.1017/S0033822200033750.

Bayon, Germain, Patrick De Deckker, John W. Magee, Yoan Germain, Sylvain Bermell, Kazuyo Tachikawa, and Marc D. Norman. 2017. “Extensive Wet Episodes in Late Glacial Australia Resulting from High-Latitude Forcings.” Scientific Reports 7 (1): 44054. https://doi.org/ 10.1038/srep44054.

Bennett, K. D., and K. J. Willis. 2002. “Pollen.” In Tracking Environmental Change Using Lake Sediments, edited by John P. Smol, H. John B. Birks, William M. Last, Raymond S. Bradley, and Keith Alverson, 3:5–32. Dordrecht: Kluwer Academic Publishers. https://doi.org/10.1007/0-306-47668-1_2.

Biggs, A. J. W., and S. R. Philip. 1995. “Soils of Cape York Peninsula.” Mareeba: Queensland Department of Primary Industries.

Bird, Michael I. 2007. “Charcoal.” Encyclopedia of Quaternary Science 4: 2950–8.

Bird, Michael I., and Philippa L. Ascough. 2012. “Isotopes in Pyrogenic Carbon: A Review.” Organic Geochemistry 42 (12): 1529–39. https://doi.org/10.1016/j.orggeochem.2010.09.005.

Bird, Michael I., L K Ayliffe, L K Fifield, Chris S. M. Turney, R G Cresswell, T T Barrows, and B David. 1999. “Radiocarbon Dating of ‘Old’ Charcoal Using a Wet Oxidation, Stepped-Combustion Procedure.” Radiocarbon 41 (02): 127–40. https://doi.org/10.1017/S0033822200019482.

Bird, Michael I., Michael Brand, Aaron F. Diefendorf, Jordahna L. Haig, Lindsay B. Hutley, Vladimir Levchenko, Peter V. Ridd, et al. 2019. “Identifying the ‘Savanna’ Signature in Lacustrine Sediments in Northern Australia.” Quaternary Science Reviews 203 (January): 233–47. https://doi.org/10.1016/j.quascirev.2018.11.002.

Bird, Michael I., Jordahna Haig, Xennephone Hadeen, Maria Rivera-Araya, Christopher M. Wurster, and Costijn Zwart. 2020. “Stable Isotope Proxy Records in Tropical Terrestrial Environments.” Palaeogeography, Palaeoclimatology, Palaeoecology 538 (January): 109445. https://doi.org/10.1016/j.palaeo.2019.109445.

Bird, Michael I., Vladimir Levchenko, Philippa L. Ascough, Will Meredith, ChristopherM. Wurster, Alan Williams, Emma L. Tilston, Colin E. Snape, and David C. Apperley. 2014. “The Efficiency of Charcoal Decontamination for Radiocarbon Dating by Three Pre-Treatments – ABOX, ABA and Hypy.” Quaternary Geochronology 22 (August): 25–32. https://doi.org/10.1016/j.quageo.2014.02.003.

Bird, Michael I., Jonathan G. Wynn, Gustavo Saiz, Christopher M. Wurster, and Anna McBeath. 2015. “The Pyrogenic Carbon Cycle.” Annual Review of Earth and Planetary Sciences 43 (1): 273–98. https://doi.org/10.1146/annurev-earth-060614-105038.

Bird, M. I., C. S. M. Turney, L. K. Fifield, R. Jones, L. K. Ayliffe, A. Palmer, R. Cresswell, and S. Robertson. 2002. “Radiocarbon Analysis of the Early Archaeological Site of Nauwalabila I, Arnhem Land, Australia: Implications for Sample Suitability and Stratigraphic Integrity.” Quaternary Science Reviews 21 (8-9): 1061–75. https://doi.org/10.1016/S0277-3791(01) 00058-0.

Björck, S., O. Bennike, G. Possnert, B. Wohlfarth, and G. Digerfeldt. 1998. “A High-Resolution 14C Dated Sediment Sequence from Southwest Sweden: Age Comparisons

Between Different Components of the Sediment." Journal of Quaternary Science 13 (1): 85–89. https://www.scopus.com/inward/record.uri?eid=2-s2.0-0031861218&partnerID=40&md5=4352aec2e4ad93d05a80ba39698f79a9.

Blaauw, Maarten, and J. Andres Christen. 2019. Rbacon: Age-Depth Modelling Using Bayesian Statistics. https://CRAN.R-project.org/package=rbacon.

BOM. 2010. "Australian Climate Influences." 2010. http://www.bom.gov.au/climate/about/australian-climate-influences.shtml#page-top.

———. 2018. "Monthly Climate Statistics: Horn Island." 2018. http://www.bom.gov.au/climate/averages/tables/cw_027058.shtml.

———. 2019. "Rose of Wind Direction Versus Wind Speed in Km/H." September 8, 2019. http://www.bom.gov.au/cgi-bin/climate/cgi_bin_scripts/windrose_selector.cgi?period=MaytoSep&type=9&location=27042.

Boon, Paul I., and Stuart E. Bunn. 1994. "Variations in the Stable Isotope Composition of Aquatic Plants and Their Implications for Food Web Analysis." Aquatic Botany 48 (2): 99–108. https://doi.org/10.1016/0304-3770(94)90077-9.

Bowman, David M. J. S., Jennifer K. Balch, Paulo Artaxo, William J. Bond, Jean M. Carlson, Mark A. Cochrane, Carla M. D'Antonio, et al. 2009. "Fire in the Earth System." Science 324 (5926): 481–84. https://doi.org/10.1126/science.1163886.

Bowman, D. M. J. S., G. K. Brown, M. F. Braby, J. R. Brown, L. G. Cook, M. D. Crisp, F. Ford, et al. 2010. "Biogeography of the Australian Monsoon Tropics." Journal of Biogeography 37 (2): 201–16. https://doi.org/10.1111/j.1365-2699.2009.02210.x.

Bremond, Laurent, Anne Alexandre, Errol Véla, and Joël Guiot. 2004. "Advantages and Disadvantages of Phytolith Analysis for the Reconstruction of Mediterranean Vegetation: An Assessment Based on Modern Phytolith, Pollen and Botanical Data (Luberon, France)." Review of Palaeobotany and Palynology 129 (4): 213–28. https://doi.org/10.1016/j.revpalbo.2004.02.002.

Brodie, Chris R., James S. L. Casford, Jeremy M. Lloyd, Melanie J. Leng, Tim. H. E. Heaton, Christopher P. Kendrick, and Zong Yongqiang. 2011. “Evidence for Bias in C/N, 13C and 15N Values of Bulk Organic Matter, and on Environmental Interpretation, from a Lake Sedimentary Sequence by Pre-Analysis Acid Treatment Methods.” Quaternary Science Reviews 30 (21): 3076–87. https://doi.org/10.1016/j.quascirev.2011.07.003.

Bronk Ramsey, C. 2008. “Radiocarbon Dating: Revolutions in Understanding.” Archaeometry 50 (2): 249–75. https://doi.org/10.1111/j.1475-4754.2008.00394.x.

Brooke, Brendan P., Scott L. Nichol, Zhi Huang, and Robin J. Beaman. 2017. “Palaeoshorelines on the Australian Continental Shelf: Morphology, Sea-Level Relationship and Applications to Environmental Management and Archaeology.” Continental Shelf Research 134 (February): 26–38. https://doi.org/10.1016/j.csr.2016.12.012.

Bunn, Stuart E., and Paul I. Boon. 1993. “What Sources of Organic Carbon Drive Food Webs in Billabongs? A Study Based on Stable Isotope Analysis.” Oecologia 96 (1): 85–94. https://doi.org/10.1007/BF00318034.

Burnett, Allison P., Michael J. Soreghan, Christopher A. Scholz, and Erik T. Brown. 2011. “Tropical East African Climate Change and Its Relation to Global Climate: A Record from Lake Tanganyika, Tropical East Africa, over the Past 90+kyr.” Palaeogeography, Palaeoclimatology, Palaeoecology 303 (1-4): 155–67. https://doi.org/10.1016/j.palaeo.2010.02.011.

Burrows, M. A., H. Heijnis, P. Gadd, and S. G. Haberle. 2016. “A New Late Quaternary Palaeohydrological Record from the Humid Tropics of Northeastern Australia.” Palaeogeography, Palaeoclimatology, Palaeoecology 451 (June): 164–82. https://doi.org/10.1016/j.palaeo.2016.03.003.

Carcaillet, Christopher, Martine Bouvier, Bianca Fréchette, Alayn C Larouche, and Pierre JH Richard. 2001. “Comparison of Pollen-Slide and Sieving Methods in Lacustrine Charcoal Analyses for Local and Regional Fire History.” The Holocene 11 (4): 467–76.

Carter, J. R., and R. J. Flower. 1988. “A new species of Eunotia, E. pirla sp. From Woolmer Pond, an acid pool in the southeast of England”. Diatom Research 3 (1): 1–8. https://doi.org/10.1080/0269249X.1988.9705013.

Catalan, Jordi, Sergi Pla-Rabés, Alexander P. Wolfe, John P. Smol, Kathleen M. Rühland, N. John Anderson, Jiři Kopáček, et al. 2013. “Global Change Revealed by Palaeolimnological Records from Remote Lakes: A Review.” Journal of Paleolimnology 49 (3): 513–35. https://doi.org/10.1007/s10933-013-9681-2.

Chappell, John, John Head, and John Magee. 1996. “Beyond the Radiocarbon Limit in Australian Archaeology and Quaternary Research.” Antiquity 70 (269): 543–52. https://doi.org/10.1017/S0003598X00083708.

Chellman, N. J., J. R. McConnell, A. Heyvaert, B. Vannière, M. M. Arienzo, and V. Wennrich. 2018. “Incandescence-Based Single-Particle Method for Black Carbon Quantification in Lake Sediment Cores: Black Carbon in Lake Sediments.” Limnology and Oceanography: Methods 16 (11): 711–21. https://doi.org/10.1002/lom3.10276.

Chen, Jing’an, Guojiang Wan, David Dian Zhang, Feng Zhang, and Ronggui Huang. 2004. “Environmental Records of Lacustrine Sediments in Different Time Scales: Sediment Grain Size as an Example.” Science in China Series D: Earth Sciences 47 (10): 954–60. https://doi.org/10.1360/03yd0160.

Chiu, Tzu-chien, Richard G. Fairbanks, Richard A. Mortlock, and Arthur L. Bloom. 2005. “Extending the Radiocarbon Calibration Beyond 26,000 Years Before Present Using Fossil Corals.” Quaternary Science Reviews 24 (16-17): 1797–1808. https://doi.org/10.1016/j. quascirev.2005.04.002.

Chivas, Allan R, Adriana Garcia, Sander van der Kaars, Martine J. J Couapel, Sabine Holt, Jessica M. Reeves, David J Wheeler, et al. 2001. “Sea-Level and Environmental Changes Since the Last Interglacial in the Gulf of Carpentaria, Australia: An Overview.” Quaternary International 83-85 (September): 19–46. https://doi.org/10.1016/S1040-6182(01)00029-5.

Clark, P. U., J. D. Shakun, P. A. Baker, P. J. Bartlein, S. Brewer, E. Brook, A. E. Carlson, et al. 2012. “Global Climate Evolution During the Last Deglaciation.” Proceedings of the National Academy of Sciences 109 (19): E1134–E1142. https://doi.org/10.1073/pnas.1116619109.

Clarkson, Chris, Zenobia Jacobs, Ben Marwick, Richard Fullagar, Lynley Wallis, Mike Smith, Richard G. Roberts, et al. 2017. “Human Occupation of Northern Australia by

65,000 Years Ago." Nature 547 (7663, 7663): 306–10. https://doi.org/10.1038/nature22968.

Clymo, R. S., and D. Mackay. 1987. "Upwash and Downwash or Pollen and Spores in the Unsaturated Surface Layer of Spahgum-Dominated Peat." New Phytologist 105 (1): 175–83. https://doi.org/10.1111/j.1469-8137.1987.tb00120.x.

Cohen, Andrew S. 2003. Paleolimnology : The History and Evolution of Lake Systems. New York: Oxford University Press. http://proxy-remote.galib.uga.edu/login?url=http://search.ebscohost.com/login.aspx?direct=true&db=cat00002a&AN=gua2927127&site=eds- live.

Commonwealth of Australia, (Geoscience Australia). 2018. "Unfiltered Summary of All Water Observations." 2018. https://maps.dea.ga.gov.au/.

Conedera, Marco, Willy Tinner, Christophe Neff, Manfred Meurer, Angela F. Dickens, and Patrik Krebs. 2009. "Reconstructing Past Fire Regimes: Methods, Applications, and Relevance to Fire Management and Conservation." Quaternary Science Reviews 28 (5-6): 555–76. https://doi.org/10.1016/j.quascirev.2008.11.005.

Conroy, Jessica L., Jonathan T. Overpeck, Julia E. Cole, Timothy M. Shanahan, and Miriam Steinitz-Kannan. 2008. "Holocene Changes in Eastern Tropical Pacific Climate Inferred from a Galápagos Lake Sediment Record." Quaternary Science Reviews 27 (11-12): 1166–80. https://doi.org/10.1016/j.quascirev.2008.02.015.

Cook, Garry D., and Richard G. Heerdegen. 2001. "Spatial Variation in the Duration of the Rainy Season in Monsoonal Australia." International Journal of Climatology 21 (14): 1723–32. https://doi.org/10.1002/joc.704.

Cook, Garry D., Richard J. Williams, Lindsay B. Hutley, Anthony O'Grady P., and Adam C. Liedloff. 2002. "Variation in Vegetative Water Use in the Savannas of the North Australian Tropical Transect." Journal of Vegetation Science 13 (3): 413–18. https://doi.org/10.1111/ j.1654-1103.2002.tb02065.x.

Dam, Herman, Adrienne Mertens, and Jos Sinkeldam. 1994. “A Coded Checklist and Ecological Indicator Values of Freshwater Diatoms from the Netherlands.” Netherlands Journal of Aquatic Ecology 28 (1): 117–33. https://doi.org/10.1007/BF02334251.

Daniau, Anne-Laure, Stéphanie Desprat, Julie C. Aleman, Laurent Bremond, Basil Davis, William Fletcher, Jennifer R. Marlon, et al. 2019. “Terrestrial Plant Microfossils in Palaeoenvironmental Studies, Pollen, Microcharcoal and Phytolith. Towards a Comprehensive Understanding of Vegetation, Fire and Climate Changes over the Past One Million Years.” Revue de Micropaléontologie, March. https://doi.org/10.1016/j.revmic.2019.02.001.

David, Bruno, Jean-Jacques Delannoy, Jerome Mialanes, Christopher Clarkson, Fiona Petchey, Jean-Michel Geneste, Tiina Manne, et al. 2019. “45,610–52,160 Years of Site and Landscape Occupation at Nawarla Gabarnmang, Arnhem Land Plateau (Northern Australia).” Quaternary Science Reviews 215 (July): 64–85. https://doi.org/10.1016/j.quascirev.2019.04.027.

Davies, Sarah J., Henry F. Lamb, and Stephen J. Roberts. 2015. “Micro-XRF Core Scanning in Palaeolimnology: Recent Developments.” In Micro-XRF Studies of Sediment Cores, edited by Ian W. Croudace and R. Guy Rothwell, 17:189–226. Dordrecht: Springer Netherlands. https://doi.org/10.1007/978-94-017-9849-5_7.

De Deckker, Patrick. 2001. “Late Quaternary Cyclic Aridity in Tropical Australia.” Palaeogeography, Palaeoclimatology, Palaeoecology 170 (1-2): 1–9. https://doi.org/10.1016/ S0031-0182(01)00233-4.

De Deckker, Patrick, Timothy T. Barrows, and John Rogers. 2014. “Land–Sea Correlations in the Australian Region: Post-Glacial Onset of the Monsoon in Northwestern Western Australia.” Quaternary Science Reviews 105 (December): 181–94. https://doi.org/10.1016/ j.quascirev.2014.09.030.

De Deckker, Patrick, Allan R. Chivas, J.Michael G. Shelley, and Thomas Torgersen. 1988. “Ostracod Shell Chemistry: A New Palaeoenvironmental Indicator Applied to a Regressive/Transgressive Record from the Gulf of Carpentaria, Australia.” Palaeogeography, Palaeoclimatology, Palaeoecology 66 (3-4): 231–41. https://doi.org/10.1016/0031-0182(88)90201-5.

De Deckker, Patrick, Thierry Corrège, and John Head. 1991. “Late Pleistocene Record of Cyclic Eolian Activity from Tropical Australia Suggesting the Younger Dryas Is Not an Unusual Climatic Event.” Geology 19 (6): 602–5. https://doi.org/10.1130/0091-7613(1991) 019%3C0602:LPROCE%3E2.3.CO;2.

De Deckker, P, N. J Tapper, and S van der Kaars. 2003. “The Status of the Indo-Pacific Warm Pool and Adjacent Land at the Last Glacial Maximum.” Global and Planetary Change 35 (1-2): 25–35. https://doi.org/10.1016/S0921-8181(02)00089-9.

Denniston, R. F., Y. Asmerom, V. J. Polyak, A. D. Wanamaker, C. C. Ummenhofer, W. F. Humphreys, J. Cugley, D. Woods, and S. Lucker. 2017. “Decoupling of Monsoon Activity Across the Northern and Southern Indo-Pacific During the Late Glacial.” Quaternary Science Reviews 176 (November): 101–5. https://doi.org/10.1016/j.quascirev.2017.09.014.

Denniston, R. F., Karl-Heinz Wyrwoll, Y. Asmerom, Victor J. Polyak, William F. Humphreys, John Cugley, David Woods, Zachary LaPointe, Julian Peota, and Elizabeth Greaves. 2013. “North Atlantic Forcing of Millennial-Scale Indo-Australian Monsoon Dynamics During the Last Glacial Period.” Quaternary Science Reviews 72 (July): 159–68. https://doi.org/10. 1016/j.quascirev.2013.04.012.

Denniston, R. F., Karl-Heinz Wyrwoll, V. J. Polyak, Josephine R. Brown, Y. Asmerom, Alan D. Wanamaker, Zachary LaPointe, et al. 2013. “A Stalagmite Record of Holocene Indonesian–Australian Summer Monsoon Variability from the Australian Tropics.” Quaternary Science Reviews 78 (October): 155–68. https://doi.org/10.1016/j.quascirev.2013.08.004.

Devriendt, Laurent. 2011. “Late Quaternary Environment of Palaeolake Carpentaria Inferred from the Chemistry of Ostracod Valves.” Wollongong: University of Wollongong. https://ro.uow.edu.au/theses/3319.

Diefendorf, Aaron F., Kevin E. Mueller, Scott L. Wing, Paul L. Koch, and Katherine H. Freeman. 2010. “Global Patterns in Leaf 13C Discrimination and Implications for Studies of Past and Future Climate.” Proceedings of the National Academy of Sciences 107 (13): 5738–43. https://doi.org/10.1073/pnas.0910513107.

Diffenbaugh, Noah S., Deepti Singh, Justin S. Mankin, Daniel E. Horton, Daniel L. Swain, Danielle Touma, Allison Charland, et al. 2017. “Quantifying the Influence of Global Warming on Unprecedented Extreme Climate Events.” Proceedings of the National Academy of Sciences 114 (19): 4881–6. https://doi.org/10.1073/pnas.1618082114.

Dinerstein, Eric, David Olson, Anup Joshi, Carly Vynne, Neil D. Burgess, Eric Wikramanayake, Nathan Hahn, et al. 2017. “An Ecoregion-Based Approach to Protecting Half the Terrestrial Realm.” BioScience 67 (6): 534–45. https://doi.org/10.1093/biosci/bix014.

DiNezio, Pedro N., and Jessica E. Tierney. 2013. “The Effect of Sea Level on Glacial Indo-Pacific Climate.” Nature Geoscience 6 (6): 485–91. https://doi.org/10.1038/ngeo1823.

Di Nezio, Pedro N., Axel Timmermann, Jessica E. Tierney, Fei-Fei Jin, Bette Otto-Bliesner, Nan Rosenbloom, Brian Mapes, Rich Neale, Ruza F. Ivanovic, and Alvaro Montenegro. 2016. “The Climate Response of the Indo-Pacific Warm Pool to Glacial Sea Level.” Paleoceanography 31 (6): 866–94. https://doi.org/10.1002/2015PA002890.

Douglas, Peter, Mark Brenner, and Jason H. Curtis. 2016. “Methods and Future Directions for Paleoclimatology in the Maya Lowlands.” Global and Planetary Change 138 (March): 3–24. https://doi.org/10.1016/j.gloplacha.2015.07.008.

Douglas, Peter, Mark Pagani, Mark Brenner, David A. Hodell, and Jason H. Curtis. 2012. “Aridity and Vegetation Composition Are Important Determinants of Leaf-Wax Delta D Values in Southeastern Mexico and Central America.” Geochimica et Cosmochimica Acta 97: 24–45. https://doi.org/10.1016/j.gca.2012.09.005.

Eggleton, R. A., G. Taylor, M. Le Gleuher, L. D. Foster, D. B. Tilley, and C. M. Morgan. 2008. “Regolith Profile, Mineralogy and Geochemistry of the Weipa Bauxite, Northern Australia.” Australian Journal of Earth Sciences 55 (sup1): S17–S43. https://doi.org/10.1080/08120090802438233.

Environmental Protection Agency, Brisbane and the Cooperative & Research Centre for Sustainable Development of Tropical Savannas, Darwin.

Environment & Science, Department of. 2018. “WetlandInfo: Wetland Systems.” 2018. https://wetlandinfo.des.qld.gov.au/wetlands.

Environment Science Services, (NQ). 1995. “Stage 1 Overview Reports: Thematic Report 1 of 3 - Natural Resources and Ecology.” Brisbane; Canberra: Cape York Peninsula Land Use Strategy, Department of the Premier, Economic and Trade Development.

Evans, Jay, and Jeremy Russell-Smith. 2020. “Delivering Effective Savanna Fire Management for Defined Biodiversity Conservation Outcomes: An Arnhem Land Case Study.” International Journal of Wildland Fire 29 (5): 386. https://doi.org/10.1071/WF18126.

Farquhar, GD, MH O’Leary, and JA Berry. 1982. “On the Relationship Between Carbon Isotope Discrimination and the Intercellular Carbon Dioxide Concentration in Leaves.” Functional Plant Biology 9 (2): 121–37.

Field, Emily, Sam Marx, Jordahna Haig, Jan-Hendrik May, Geraldine Jacobsen, Atun Zawadzki, David Child, et al. 2018. “Untangling Geochronological Complexity in Organic Spring Deposits Using Multiple Dating Methods.” Quaternary Geochronology 43 (February): 50–71. https://doi.org/10.1016/j.quageo.2017.10.002.

Field, Emily, Hamish A. McGowan, Patrick T. Moss, and Samuel K. Marx. 2017. “A Late Quaternary Record of Monsoon Variability in the Northwest Kimberley, Australia.” Quaternary International 449 (August): 119–35. https://doi.org/10.1016/j.quaint.2017.02.019.

Field, Emily, Jonathan Tyler, Patricia S. Gadd, Patrick Moss, Hamish McGowan, and Sam Marx. 2018. “Coherent Patterns of Environmental Change at Multiple Organic Spring Sites in Northwest Australia: Evidence of Indonesian-Australian Summer Monsoon Variability over the Last 14,500 Years.” Quaternary Science Reviews 196 (September): 193–216. https://doi.org/10.1016/j.quascirev.2018.07.018.

Fink, D., M. Hotchkis, Q. Hua, G. Jacobsen, A. M. Smith, U. Zoppi, D. Child, et al. 2004. “The ANTARES AMS Facility at ANSTO.” Nuclear Instruments and Methods in Physics Research Section B: Beam Interactions with Materials and Atoms 223-224 (August): 109–15. https://doi.org/10.1016/j.nimb.2004.04.025.

Fletcher, William J., Christoph Zielhofer, Steffen Mischke, Charlotte Bryant, Xiaomei Xu, and David Fink. 2017. “AMS Radiocarbon Dating of Pollen Concentrates in a Karstic Lake System.” Quaternary Geochronology 39 (April): 112–23. https://doi.org/10.1016/j.quageo. 2017.02.006.

Fogel, Marilyn L., and Luis A. Cifuentes. 1993. “Isotope Fractionation During Primary Production.” In Organic Geochemistry, edited by Michael H. Engel and Stephen A. Macko, 11:73–98. Topics in Geobiology. Boston, MA: Springer US. https://doi.org/10.1007/978-1- 4615-2890-6_3.

Fox, I. D., V. J Neldner, G. W Wilson, and P. J Bannink. 2001. “The Vegetation of the Australian Tropical Savannas.” Brisbane: Environmental Protection Agency.

Frank, Dorothea, Markus Reichstein, Michael Bahn, Kirsten Thonicke, David Frank, Miguel D. Mahecha, Pete Smith, et al. 2015. “Effects of Climate Extremes on the Terrestrial Carbon Cycle: Concepts, Processes and Potential Future Impacts.” Global Change Biology 21 (8): 2861–80. https://doi.org/10.1111/gcb.12916.

Gagan, Michael K, Erica J Hendy, Simon G Haberle, and Wahyoe S Hantoro. 2004. “Post-Glacial Evolution of the Indo-Pacific Warm Pool and El Niño-Southern Oscillation.” Quaternary International 118-119 (January): 127–43. https://doi.org/10.1016/S1040-6182(03)00134-4.

Gasse, E., and F. A. Street. 1978. “Late Quaternary Lake-Level Fluctuations and Environments of the Northern Rift Valley and Afar Region (Ethiopia and Djibouti).” Palaeogeography, Palaeoclimatology, Palaeoecology 24 (4): 279–”295, 297, 299–325”. https://doi.org/10.1016/0031-0182(78)90011-1.

Gasse, Françoise. 1987. “Diatoms for Reconstructing Palaeoenvironments and Paleohydrology in Tropical Semi-Arid Zones.” Hydrobiologia 154 (1): 127–63. https://doi.org/10.1007/ BF00026837.

Gee, G. W., and J. W. Bauder. 1986. “Particle-Size Analysis.” Edited by A. Klute. Methods of Soil Analysis. Part 1. Physical and Mineralogical Methods. http://proxy-remote.galib.uga.edu/login?url=http://search.ebscohost.com/login.aspx?direct=true&db=lah&AN=19881917517&site=eds-live.

Gell, Peter A., Cooperative Research Centre for Freshwater Ecology, and Australian National Algal Workshop. 1999. An Illustrated Key to Common Diatom Genera from Southern Australia. Thurgoona, NSW: Cooperative Research Centre for Freshwater Ecology.

Gentilli, J., ed. 1971. Climates of Australia and New Zealand. World Survey of Climatology, v.13. Amsterdam, New York: Elsevier Pub. Co.

Geoscience-Australia. 2015. “SRTM 1 Sec DEM Image, Dataset.” Australian Government.

Gill, A. M., P. G. Ryan, P. H. R. Moore, and M. Gibson. 2000. “Fire Regimes of World Heritage Kakadu National Park., Australia.” Austral Ecology 25 (6): 616–25. https://doi.org/10.1111/j.1442-9993.2000.tb00067.x.

Gillespie, Richard. 2019. “A Novel Cellulose-Preparation Method.” Radiocarbon 61 (1): 1–9. https://doi.org/10.1017/RDC.2018.65.

Gillespie, Richard, A P Hammond, K M Goh, P J Tonkin, D C Lowe, R J Sparks, and Gavin Wallace. 1992. “AMS Dating of a Late Quaternary Tephra at Graham’s Terrace, New Zealand.” Radiocarbon; Vol 34, No 1 (1992), January. https://journals.uair.arizona.edu/ index.php/radiocarbon/article/view/1438.

Griffiths, Michael L., Russell N. Drysdale, Michael K. Gagan, Jian-xin Zhao, John C. Hellstrom, Linda K. Ayliffe, and Wahyoe S. Hantoro. 2013. “Abrupt Increase in East Indonesian Rainfall from Flooding of the Sunda Shelf 9500 Years Ago.” Quaternary Science Reviews, Linking Southern Hemisphere records and past circulation patterns:

The AUS-INTIMATE project, 74 (August): 273–79. https://doi.org/10.1016/j.quascirev.2012.07.006.

Griffiths, M. L., R. N. Drysdale, M. K. Gagan, J.-x. Zhao, L. K. Ayliffe, J. C. Hellstrom, W.S. Hantoro, et al. 2009. “Increasing Australian–Indonesian Monsoon Rainfall Linked to Early Holocene Sea-Level Rise.” Nature Geoscience 2 (9): 636–39. https://doi.org/10.1038/ ngeo605.

Grimes, KG, and Andy Spate. 2008. “Laterite Karst.” ACKMA Journal 73: 49–52.

Haberle, Simon G. 2005. “A 23,000-Yr Pollen Record from Lake Euramoo, Wet Tropics of NE Queensland, Australia.” Quaternary Research 64 (03): 343–56. https://doi.org/10.1016/j. yqres.2005.08.013.

Haberle, Simon G, Geoff S Hope, and Sander van der Kaars. 2001. “Biomass Burning in Indonesia and Papua New Guinea: Natural and Human Induced Fire Events in the Fossil Record.” Palaeogeography, Palaeoclimatology, Palaeoecology 171 (3-4): 259–68. https://doi. org/10.1016/S0031-0182(01)00248-6.

Hanebuth, T. 2000. “Rapid Flooding of the Sunda Shelf: A Late-Glacial Sea-Level Record.” Science 288 (5468): 1033–5. https://doi.org/10.1126/science.288.5468.1033.

Harris, Peter T., Andrew D. Heap, John F. Marshall, and Malcolm McCulloch. 2008. “A New Coral Reef Province in the Gulf of Carpentaria, Australia: Colonisation, Growth and Submergence During the Early Holocene.” Marine Geology 251 (1-2): 85–97. https://doi.org/10.1016/j.margeo.2008.02.010.

Hatté, Christine, Jean Morvan, Claude Noury, and Martine Paterne. 2001. “Is Classical Acid-Alkali-Acid Treatment Responsible for Contamination? An Alternative Proposition.” Radiocarbon 43 (2A): 177–82. https://doi.org/10.1017/S003382220003798X.

Haug, Gerald H., Konrad A. Hughen, Daniel M. Sigman, Larry C. Peterson, and Ursula Röhl. 2001. “Southward Migration of the Intertropical Convergence Zone Through the Holocene,” 2001. http://proxy-remote.galib.uga.edu/login?url=http://search.ebscohost.com/login. aspx?direct=true&db=edsjsr&AN=edsjsr.3084483&site=eds-live.

Håkanson, Lars, and M. Jansson. 1983. Principles of Lake Sedimentology. Berlin ; New York: Springer-Verlag.

Head, L., and R. Fullager. 1992. “Palaeoecology and Archaeology in the East Kimberley.”Quaternary Australasia 10 (1): 27–31.

Hembrow, Sarah C., Kathryn H. Taffs, Pia Atahan, Jeff Parr, Atun Zawadzki, and Henk Heijnis. 2014. “Diatom Community Response to Climate Variability over the Past 37,000years in the Sub-Tropics of the Southern Hemisphere.” Science of the Total Environment 468-469 (January): 774–84. https://doi.org/10.1016/j.scitotenv.2013.09.003.

Hesse, Paul P, John W Magee, and Sander van der Kaars. 2004. “Late Quaternary Climates of the Australian Arid Zone: A Review.” Quaternary International 118-119 (January): 87–102. https://doi.org/10.1016/S1040-6182(03)00132-0.

Higham, T. F. G., C. Bronk Ramsey, F. Brock, D. Baker, and P. Ditchfield. 2011. “Radiocarbon Dates from the Oxford AMS System: Datelist 34.” Archaeometry 53 (5): 1067–84. https://doi.org/10.1111/j.1475-4754.2010.00574.x.

Higham, Thomas F. G., Huw Barton, Chris S. M. Turney, Graeme Barker, Christopher Bronk Ramsey, and Fiona Brock. 2009. “Radiocarbon Dating of Charcoal from Tropical Sequences: Results from the Niah Great Cave, Sarawak, and Their Broader Implications.” Journal of Quaternary Science 24 (2): 189–97. https://doi.org/10.1002/jqs.1197.

Higuera, Philip E., Daniel G. Gavin, Patrick J. Bartlein, and Douglas J. Hallett. 2010. “Peak Detection in Sediment - Charcoal Records: Impacts of Alternative Data Analysis Methods on Fire-History Interpretations.” International Journal of Wildland Fire 19 (8): 996. https://doi.org/10.1071/WF09134.

Hitchcock, P., M Kennard, B. Leaver, B. Mackey, P. Stanton, P. Valentine, E. Vanderduys, B. Wannan, W. Willmott, and J. Woinarski. 2013. “The Natural Attributes for World Heritage Nomination of Cape York Peninsula, Australia.” https://www.environment.gov.au/system/ files/resources/5ab50983-6bb4-4d87-8298-f1bcf1ab652a/files/sciencepanelreport.pdf.

Hogg, Alan G, Quan Hua, Paul G Blackwell, Mu Niu, Caitlin E Buck, Thomas P Guilderson, Timothy J Heaton, et al. 2013. “SHCal13 Southern Hemisphere Calibration, 0–50,000 Years Cal BP.” Radiocarbon 55 (4): 1889–1903. https://doi.org/10.2458/azu_js_rc.55.16783.

Hu, Feng Sheng, and Aldo Shemesh. 2003. “A Biogenic-Silica 18O Record of Climatic Change During the Last Glacial–Interglacial Transition in Southwestern Alaska.” Quaternary Research 59 (3): 379–85. https://doi.org/10.1016/S0033-5894(03)00056-5.

Hua, Q., G. E. Jacobsen, U. Zoppi, E. M. Lawson, A. A. Williams, and M. J. McGann. 2001. “Progress in Radiocarbon Target Preparation at the Antares Ams Centre.” Radiocarbon; Vol 43, No 2A (2001), January. https://journals.uair.arizona.edu/index.php/radiocarbon/ article/view/3964.

Ishiwa, Takeshige, Yusuke Yokoyama, Jun’ichi Okuno, Stephen Obrochta, Katsuto Uehara, Minoru Ikehara, and Yosuke Miyairi. 2019. “A Sea-Level Plateau Preceding the Marine Isotope Stage 2 Minima Revealed by Australian Sediments.” Scientific Reports 9 (1): 6449. https://doi.org/10.1038/s41598-019-42573-4.

Jacobel, A. W., J. F. McManus, R. F. Anderson, and G. Winckler. 2016. “Large Deglacial Shifts of the Pacific Intertropical Convergence Zone.” Nature Communications 7 (1): 10449. https://doi.org/10.1038/ncomms10449.

Jiang, Dabang, Zhiping Tian, Xianmei Lang, Masa Kageyama, and Gilles Ramstein. 2015. “The Concept of Global Monsoon Applied to the Last Glacial Maximum: A Multi-Model Analysis.” Quaternary Science Reviews 126 (October): 126–39. https://doi.org/10.1016/j. quascirev.2015.08.033.

Johansen, J. 2010. Diatoms of Aerial Habitats. Edited by Eugene F. Stoermer and John P. Smol. 1. paperback ed. Cambridge: Cambridge University Press.

Johnson, Michelle O., Simon M. Mudd, Brad Pillans, Nigel A. Spooner, L. Keith Fifield, Mike J. Kirkby, and Manuel Gloor. 2014. “Quantifying the Rate and Depth Dependence of Bioturbation Based on Optically-Stimulated Luminescence (OSL) Dates and Meteoric 10 Be.” Earth Surface Processes and Landforms 39 (9): 1188–96. https://doi.org/10.1002/esp.3520.

Jones, M. R., and T. Torgersen. 1988. “Late Quaternary Evolution of Lake Carpentaria on the Australia-New Guinea Continental Shelf.” Australian Journal of Earth Sciences 35 (3): 313–24. https://doi.org/10.1080/08120098808729450.

Juggins, Steve. 2017. Rioja: Analysis of Quaternary Science Data. http://www.staff.ncl.ac. uk/stephen.juggins/.

Kaars, Sander van der, Patrick De Deckker, and Franz X. Gingele. 2006. “A 100 000-Year Record of Annual and Seasonal Rainfall and Temperature for Northwestern Australia Based on a Pollen Record Obtained Offshore.” Journal of Quaternary Science 21 (8): 879–89. https://doi.org/10.1002/jqs.1010.

Kealhofer, Lisa, and Dolores R. Piperno. 1998. “Opal Phytoliths in Southeast Asian Flora.” Smithsonian Contributions to Botany, no. 88: 1–39. https://doi.org/10.5479/si.0081024X. 88.

Kershaw, A. P. 1994. “Pleistocene Vegetation of the Humid Tropics of Northeastern Queensland, Australia.” Palaeogeography, Palaeoclimatology, Palaeoecology 109 (2-4): 399–412. https://doi.org/10.1016/0031-0182(94)90188-0.

Kershaw, A. Peter, Sophie C. Bretherton, and Sander van der Kaars. 2007. “A Complete Pollen Record of the Last 230 Ka from Lynch’s Crater, North-Eastern Australia.” Palaeogeography, Palaeoclimatology, Palaeoecology 251 (1): 23–45. https://doi.org/10.1016/j.palaeo.2007.02.015.

Kershaw, A. P., and H. A. Nix. 1988. “Quantitative Palaeoclimatic Estimates from Pollen Data Using Bioclimatic Profiles of Extant Taxa.” Journal of Biogeography 15 (4): 589. https://doi.org/10.2307/2845438.

Kershaw, Peter, and Sander van der Kaars. 2012. “Australia and the Southwest Pacific.” In Quaternary Environmental Change in the Tropics, edited by Sarah E. Metcalfe and David J. Nash, 236–62. Chichester, UK: John Wiley & Sons, Ltd. https://doi.org/10.1002/9781118336311.ch7.

Kilian, M. R., J. van der Plicht, B. van Geel, and T. Goslar. 2002. “Problematic 14C-AMS Dates of Pollen Concentrates from Lake Gosciaz (Poland).” Quaternary International 88 (1): 21–26. https://doi.org/10.1016/S1040-6182(01)00070-2.

Kitagawa, Hiroyuki, Shafi M. Tareq, Hiroyuki Matsuzaki, Nobuo Inoue, Eiichiro Tanoue, and Yoshinori Yasuda. 2007. “Radiocarbon Concentration of Lake Sediment Cellulose from Lake Erhai in Southwest China.” Nuclear Instruments and Methods in Physics Research Section B: Beam Interactions with Materials and Atoms 259 (1): 526–29. https://doi.org/ 10.1016/j.nimb.2007.01.195.

Kohfeld, K. E., & Harrison, S. P. (2000). How well can we simulate past climates? Evaluating the models using global palaeoenvironmental datasets. Quaternary Science Reviews, 19(1), 321–346. https://doi.org/10.1016/S0277-3791(99)00068-2

Kohn, Matthew J. 2010. “Carbon Isotope Compositions of Terrestrial C3 Plants as Indicators of (Paleo)Ecology and (Paleo)Climate.” Proceedings of the National Academy of Sciences 107 (46): 19691–95. https://doi.org/10.1073/pnas.1004933107.

Krammer, K., Lange-Bertalot, H., 1999. Suesswasserflora von Mitteleuropa, vols. 1e4.Spektrum Akademischer Verlag Heidelberg, Berlin

Krause, Claire E., Michael K. Gagan, Gavin B. Dunbar, Wahyoe S. Hantoro, John C. Hellstrom, Hai Cheng, R. Lawrence Edwards, Bambang W. Suwargadi, Nerilie J. Abram, and Hamdi Rifai. 2019. “Spatio-Temporal Evolution of Australasian Monsoon Hydroclimate over the Last 40,000 Years.” Earth and Planetary Science Letters 513 (May): 103–12. https://doi. org/10.1016/j.epsl.2019.01.045.

Kristensen, Jeppe Aa., Kristina J. Thomsen, Andrew S. Murray, Jan-Pieter Buylaert, Mayank Jain, and Henrik Breuning-Madsen. 2015. “Quantification of Termite Bioturbation in a Savannah Ecosystem: Application of OSL Dating.” Quaternary Geochronology 30 (October): 334–41. https://doi.org/10.1016/j.quageo.2015.02.026.

Kuhnt, Wolfgang, Ann Holbourn, Jian Xu, Bradley Opdyke, Patrick De Deckker, Ursula Röhl, and Manfred Mudelsee. 2015. “Southern Hemisphere Control on Australian Monsoon Variability During the Late Deglaciation and Holocene.” Nature Communications 6 (1, 1): 5916. https://doi.org/10.1038/ncomms6916.

Lamb, Angela L., Melanie J. Leng, Hilary J. Sloane, and Richard J. Telford. 2005. “A Comparison of the Palaeoclimate Signals from Diatom Oxygen Isotope Ratios and Carbonate Oxygen Isotope Ratios from a Low Latitude Crater Lake.” Palaeogeography,

Palaeoclimatology, Palaeoecology 223 (3-4): 290–302. https://doi.org/10.1016/j.palaeo.2005.04.011.

Lambeck, Kurt, Hélène Rouby, Anthony Purcell, Yiying Sun, and Malcolm Sambridge. 2014. “Sea Level and Global Ice Volumes from the Last Glacial Maximum to the Holocene.” Proceedings of the National Academy of Sciences 111 (43): 15296. https://doi.org/10.1073/ pnas.1411762111.

Laws, E. A., Popp, B. N., Bidigare, R. R., Kennicutt, M. C., & Macko, S. A. (1995). Dependence of phytoplankton carbon isotopic composition on growth rate and [CO2)aq: Theoretical considerations and experimental results. Geochimica et Cosmochimica Acta, 59(6), 1131–1138. https://doi.org/10.1016/0016-7037(95)00030-4

Lees, Brian. 2006. “Timing and Formation of Coastal Dunes in Northern and Eastern Australia.” Journal of Coastal Research 221 (January): 78–89. https://doi.org/10.2112/05A-0007.1.

Lees, Brian G. 1992. “Geomorphological Evidence for Late Holocene Climatic Change in Northern Australia.” Australian Geographer 23 (1): 1–10. https://doi.org/10.1080/00049189208703048.

Lees, Brian G., John Stanner, David M. Price, and Lu Yanchou. 1995. “Thermoluminescence Dating of Dune Podzols at Cape Arnhem, Northern Australia.” Marine Geology 129 (1-2): 63–75. https://doi.org/10.1016/0025-3227(95)00112-3.

Lees, Brian G., Lu Yanchou, and John Head. 1990. “Reconnaissance Thermoluminescence Dating of Northern Australian Coastal Dune Systems.” Quaternary Research 34 (2): 169–85. https://doi.org/10.1016/0033-5894(90)90029-K.

Lehmann, Caroline E. R., Sally A. Archibald, William A. Hoffmann, and William J. Bond. 2011. “Deciphering the Distribution of the Savanna Biome.” New Phytologist 191 (1): 197–209. https://doi.org/10.1111/j.1469-8137.2011.03689.x.

Leng, Melanie J., and P. A. Barker. 2006. “A Review of the Oxygen Isotope Composition of Lacustrine Diatom Silica for Palaeoclimate Reconstruction.” Earth-Science Reviews 75 (1-4): 5–27. https://doi.org/10.1016/j.earscirev.2005.10.001.

Leng, Melanie J., and Andrew C. G. Henderson. 2013. “Recent Advances in Isotopes as Palaeolimnological Proxies.” Journal of Paleolimnology 49 (3): 481–96. https://doi.org/10. 1007/s10933-012-9667-5.

Leng, Melanie J, and Jim D Marshall. 2004. “Palaeoclimate Interpretation of Stable Isotope Data from Lake Sediment Archives.” Quaternary Science Reviews 23 (7-8): 811–31. https://doi.org/10.1016/j.quascirev.2003.06.012.

Lewis, Richard J., John Tibby, Lee J. Arnold, Cameron Barr, Jonathan Marshall, Glenn McGregor, Patricia Gadd, and Yusuke Yokoyama. 2020. “Insights into Subtropical Australian Aridity from Welsby Lagoon, North Stradbroke Island, over the Past 80,000 Years.” Quaternary Science Reviews 234 (April): 106262. https://doi.org/10.1016/j.quascirev.2020.106262.

Lewis, Sophie C., Michael K. Gagan, Linda K. Ayliffe, Jian-xin Zhao, Wahyoe S. Hantoro, Pauline C. Treble, John C. Hellstrom, et al. 2011. “High-Resolution Stalagmite Reconstructions of Australian–Indonesian Monsoon Rainfall Variability During Heinrich Stadial 3 and Greenland Interstadial 4.” Earth and Planetary Science Letters 303 (1):133–42. https://doi.org/10.1016/j.epsl.2010.12.048.

Lewis, Stephen E., Craig R. Sloss, Colin V. Murray-Wallace, Colin D. Woodroffe, and Scott G. Smithers. 2013. “Post-Glacial Sea-Level Changes Around the Australian Margin: A. Review.” Quaternary Science Reviews, Linking Southern Hemisphere records and past circulation patterns: The AUS-INTIMATE project, 74 (August): 115–38. https://doi.org/ 10.1016/j.quascirev.2012.09.006.

Liu, Shanshan, Dabang Jiang, and Xianmei Lang. 2018. “A Multi-Model Analysis of Moisture Changes During the Last Glacial Maximum.” Quaternary Science Reviews 191 (July): 363–77. https://doi.org/10.1016/j.quascirev.2018.05.029.

Lough, J. M., L. E. Llewellyn, S. E. Lewis, C. S. M. Turney, J. G. Palmer, C. G. Cook, and A. G. Hogg. 2014. “Evidence for Suppressed Mid-Holocene Northeastern Australian Monsoon Variability from Coral Luminescence.” Paleoceanography 29 (6): 581–94. https://doi.org/10.1002/2014PA002630.

Luly, J. G., J. F. Grindrod, and D. Penny. 2006. “Holocene Palaeoenvironments and Change at Three-Quarter Mile Lake, Silver Plains Station, Cape York Peninsula, Australia.” The Holocene 16 (8): 1085–94. https://doi.org/10.1177/0959683606069398.

Mackenzie, Lydia, Henk Heijnis, Patricia Gadd, Patrick Moss, and J. Shulmeister. 2017. “Geochemical Investigation of the South Wellesley Island Wetlands: Insight into Wetland Development During the Holocene in Tropical Northern Australia.” The Holocene 27 (4): 566–78. https://doi.org/10.1177/0959683616670219.

Mackenzie, Lydia, Patrick Moss, and Sean Ulm. 2020. “A Late-Holocene Record of Coastal Wetland Development and Fire Regimes in Tropical Northern Australia.” The Holocene 30 (10): 1379–90. https://doi.org/10.1177/0959683620932970.

Marchant, Robert, and Henry Hooghiemstra. 2004. “Rapid Environmental Change in African and South American Tropics Around 4000 Years Before Present: A Review.” Earth-Science Reviews 66 (3-4): 217–60. https://doi.org/10.1016/j.earscirev.2004.01.003.

Marlon, Jennifer R., Patrick J. Bartlein, Anne-Laure Daniau, Sandy P. Harrison, Shira Y. Maezumi, Mitchell J. Power, Willy Tinner, and Boris Vanniére. 2013. “Global Biomass Burning: A Synthesis and Review of Holocene Paleofire Records and Their Controls.” Quaternary Science Reviews 65 (April): 5–25. https://doi.org/10.1016/j.quascirev.2012.11.029.

Martin, Len, James Goff, Geraldine Jacobsen, and Scott Mooney. 2019. “The Radiocarbon Ages of Different Organic Components in the Mires of Eastern Australia.” Radiocarbon 61 (1): 173–84. https://doi.org/10.1017/RDC.2018.118.

May, Jan-Hendrik, Frank Preusser, and Luke Andrew Gliganic. 2015. “Refining Late Quaternary Plunge Pool Chronologies in Australia’s Monsoonal ’Top End’.” Quaternary Geochronology 30 (October): 328–33. https://doi.org/10.1016/j.quageo.2015.01.008.

May, J. -H., S. K. Marx, W. Reynolds, L. Clark-Balzan, G. E. Jacobsen, and F. Preusser. 2018. “Establishing a Chronological Framework for a Late Quaternary Seasonal Swamp in the Australian ‘Top End’.” Quaternary Geochronology 47 (August): 81–92. https://doi.org/10. 1016/j.quageo.2018.05.010.

Mays, Jennifer L., Mark Brenner, Jason H. Curtis, Kathryn V. Curtis, David A. Hodell, Alex Correa-Metrio, Jaime Escobar, Andrea L. Dutton, Andrew R. Zimmerman, and Thomas P. Guilderson. 2017. “Stable Carbon Isotopes (13C) of Total Organic Carbon and Long-Chain N-Alkanes as Proxies for Climate and Environmental Change in a Sediment Core from Lake Petén-Itzá, Guatemala.” Journal of Paleolimnology 57 (4): 307–19. https://doi.org/ 10.1007/s10933-017-9949-z.

McCulloch, M. T, P De Deckker, and A. R Chivas. 1989. “Strontium Isotope Variations in Single Ostracod Valves from the Gulf of Carpentaria, Australia: A Palaeoenvironmental Indicator.” Geochimica et Cosmochimica Acta 53 (7): 1703–10. https://doi.org/10.1016/0016-7037(89)90256-1.

McGowan, Hamish A., Lynda M. Petherick, and Balz S. Kamber. 2008. “Aeolian Sedimentation and Climate Variability During the Late Quaternary in Southeast Queensland, Australia.” Palaeogeography, Palaeoclimatology, Palaeoecology 265 (3-4): 171–81. https://doi.org/10. 1016/j.palaeo.2008.05.011.

McGowan, Hamish, Samuel Marx, Patrick T. Moss, and Andrew Hammond. 2012. “Evidence of ENSO Mega-Drought Triggered Collapse of Prehistory Aboriginal Society in Northwest Australia: ENSO MEGA-DROUGHT.” Geophysical Research Letters 39 (22): n/a–n/a. https://doi.org/10.1029/2012GL053916.

McLauchlan, Kendra K., Philip E. Higuera, Jessica Miesel, Brendan M. Rogers, Jennifer Schweitzer, Jacquelyn K. Shuman, Alan J. Tepley, et al. 2020. “Fire as a Fundamental Ecological Process: Research Advances and Frontiers.” Edited by Giselda Durigan. Journal of Ecology 108 (5): 2047–69. https://doi.org/10.1111/1365-2745.13403.

Meredith, W., P. L. Ascough, Michael I. Bird, D. J. Large, C. E. Snape, Y. Sun, and E.L. Tilston. 2012. “Assessment of Hydropyrolysis as a Method for the Quantification of Black Carbon Using Standard Reference Materials.” Geochimica et Cosmochimica Acta 97 (November): 131–47.

Meyers, P. A., and R. Ishiwatari. 1995. “Organic Matter Accumulation Records in Lake Sediments.” In Physics and Chemistry of Lakes, edited by Abraham Lerman, Dieter M. Imboden, and Joel R. Gat, 279–328. Berlin, Heidelberg: Springer Berlin Heidelberg. https://doi.org/10.1007/978-3-642-85132-2_10.

Meyers, P. A., and E. Lallier-Vergès. 1999. “Lacustrine Sedimentary Organic Matter Records of Late Quaternary Paleoclimates.” Journal of Paleolimnology 21 (3): 345–72. https://doi. org/10.1023/A:1008073732192.

Meyers, Philip A. 1997. “Organic Geochemical Proxies of Paleoceanographic, Paleolimnologic, and Paleoclimatic Processes.” Organic Geochemistry 27 (5-6): 213–50. https://doi.org/10. 1016/S0146-6380(97)00049-1.

Meyers, Philip A., and Ryoshi Ishiwatari. 1993. “Lacustrine Organic Geochemistry—an Overview of Indicators of Organic Matter Sources and Diagenesis in Lake Sediments.” Organic Geochemistry 20 (7): 867–900. https://doi.org/10.1016/0146-6380(93)90100-P.

Mooney, S. D., S. P. Harrison, P. J. Bartlein, A.-L. Daniau, J. Stevenson, K. C. Brownlie, S. Buckman, et al. 2011. “Late Quaternary Fire Regimes of Australasia.” Quaternary Science Reviews 30 (1-2): 28–46. https://doi.org/10.1016/j.quascirev.2010.10.010.

Morley, David W., Melanie J. Leng, Anson W. Mackay, Hilary J. Sloane, Patrick Rioual, and Richard W. Battarbee. 2004. “Cleaning of Lake Sediment Samples for Diatom Oxygen Isotope Analysis.” Journal of Paleolimnology 31 (3): 391–401. https://doi.org/10.1023/B: JOPL.0000021854.70714.6b.

Moser, K. A., A. Korhola, J. Wekcström, T. Blom, R. Pienitz, J. P. Smol, M. S. V. Douglas, and M. B. Hay. 2000. “Paleohydrology Inferred from Diatoms in Northern Latitude Regions.” Journal of Paleolimnology 24 (1): 93–107. https://doi.org/10.1023/A:1008173901591.

Moss, Patrick T., Richard Cosgrove, Åsa Ferrier, and Simon G. Haberle. 2012. “Holocene Environments of the Sclerophyll Woodlands of the Wet Tropics of Northeastern Australia.” In Peopled Landscapes, edited by SIMON G. HABERLE and BRUNO DAVID, 34:329–42. Archaeological and Biogeographic Approaches to Landscapes. ANU Press. http://www. jstor.org.elibrary.jcu.edu.au/stable/j.ctt24h85b.17.

Moss, Patrick T., and A. Peter Kershaw. 2007. “A Late Quaternary Marine Palynological Record (Oxygen Isotope Stages 1 to 7) for the Humid Tropics of Northeastern Australia Based on ODP Site 820.” Palaeogeography, Palaeoclimatology, Palaeoecology, Environmental History of the Humid Tropics region of north-east Australia, 251 (1): 4–22. https://doi.org/ 10.1016/j.palaeo.2007.02.014.

Moss, Patrick T., Lydia Mackenzie, Sean Ulm, Craig Sloss, Daniel Rosendahl, Lynda Petherick, Lincoln Steinberger, et al. 2015. “Environmental Context for Late Holocene Human Occupation of the South Wellesley Archipelago, Gulf of Carpentaria, Northern Australia.” Quaternary International 385 (October): 136–44. https://doi.org/10.1016/j.quaint.2015.02.051.

Mueller, N., A. Lewis, D. Roberts, S. Ring, R. Melrose, J. Sixsmith, L. Lymburner, et al. 2016. “Water Observations from Space: Mapping Surface Water from 25 Years of Landsat Imagery Across Australia.” Remote Sensing of Environment 174 (March): 341–52. https://doi.org/10.1016/j.rse.2015.11.003.

Muller, Joanne, Malin Kylander, Raphael A. J. Wüst, Dominik Weiss, Antonio Martinez-Cortizas, Allegra N. LeGrande, Tim Jennerjahn, Herman Behling, William T. Anderson, and Geraldine Jacobson. 2008. “Possible Evidence for Wet Heinrich Phases in Tropical NE Australia: The Lynch’s Crater Deposit.”Quaternary Science Reviews 27 (5): 468–75. https://doi.org/10.1016/j.quascirev.2007.11.006.

Nanson, G. C., T. J. East, and R. G. Roberts. 1993. “Quaternary Stratigraphy, Geochronology and Evolution of the Magela Creek Catchment in the Monsoon Tropics of Northern Australia.” Sedimentary Geology 83 (3-4): 277–302. https://doi.org/10.1016/0037- 0738(93)90017-Y.

Nanson, Gerald C., David M. Price, Stephen A. Short, Robert W. Young, and Brian G. Jones. 1991. “Comparative Uranium-Thorium and Thermoluminescence Dating of Weathered Quaternary Alluvium in the Tropics of Northern Australia.” Quaternary Research 35 (3-Part1): 347–66. https://doi.org/10.1016/0033-5894(91)90050-F.

Negus, Peter M., Cameron Barr, John Tibby, Glenn B. McGregor, Jonathan Marshall, and Jennie Fluin. 2019. “Subtle Variability in Water Quality Structures Tropical Diatom Assemblages in Streams of Cape York Peninsula, Australia.” Marine and Freshwater Research 70 (10): 1358. https://doi.org/10.1071/MF18478.

Neldner, V. J, J. R Clarkson, CYPLUS, and Natural Resources Analysis Program. 1995. Vegetation Survey and Mapping of Cape York Peninsula. Brisbane; Canberra: Office of the Co-ordinator General ; Commonwealth Information Services.

Neulieb, Thomas. 2013. “Potential Pitfalls of Pollen Dating.” Radiocarbon 55 (3–4). https://doi.org/10.2458/azu_js_rc.55.16274.

Neumann, Katharina, Caroline A. E. Strömberg, Terry Ball, Rosa Maria Albert, Luc Vrydaghs, and Linda Scott Cummings. 2019. “International Code for Phytolith Nomenclature (ICPN) 2.0.” Annals of Botany 124 (2): 189–99. https://doi.org/10.1093/aob/mcz064.

Nezio, Pedro N. Di, Axel Timmermann, Jessica E. Tierney, Fei-Fei Jin, Bette Otto-Bliesner, Nan Rosenbloom, Brian Mapes, Rich Neale, Ruza F. Ivanovic, and Alvaro Montenegro. 2016. “The Climate Response of the Indo-Pacific Warm Pool to Glacial Sea Level.” Paleoceanography 31 (6): 866–94. https://doi.org/10.1002/2015PA002890.

Nott, Jonathan F., Edward A. Bryant, and David Price. 1999. “Early-Holocene Aridity in Tropical Northern Australia.” The Holocene 9 (2): 231–36.

Nott, Jonathan F., and David M. Price. 1994. “Plunge Pools and Paleoprecipitation.” Geology, 22 (11): 1047. https://doi.org/10.1130/0091 613(1994)022%3C1047:PPAP%3E2.3.CO;2.

———. 1999. “Waterfalls, Floods and Climate Change: Evidence from Tropical Australia.” Earth and Planetary Science Letters 171 (2): 267–76. https://doi.org/10.1016/S0012- 821X(99)00152-1.

Nott, Jonathan F., David M. Price, and Edward A. Bryant. 1996. “A 30,000 Year Record of Extreme Floods in Tropical Australia from Relict Plunge-Pool Deposits: Implications for Future Climate Change.” Geophysical Research Letters 23 (4): 379–82. https://doi.org/10. 1029/96GL00262.

Oksanen, Jari, F. Guillaume Blanchet, Michael Friendly, Roeland Kindt, Pierre Legendre, Dan McGlinn, Peter R. Minchin, et al. 2019. Vegan: Community Ecology Package. https://CRAN.R-project.org/package=vegan.

Olsson, Ingrid U. 1986. “A Study of Errors in 14C Dates of Peat and Sediment.” Radiocarbon 28 (2A): 429–35. https://doi.org/10.1017/S0033822200007554.

O'Leary, Marion H. 1988. "Carbon Isotopes in Photosynthesis." *Bioscience* 38 (5): 328–36.

Orr, Theresa J., Christopher M. Wurster, Vladimir Levchenko, Philippa L. Ascough, and Michael I. Bird. 2020. "Improved Pretreatment Method for the Isolation and Decontamination of Pyrogenic Carbon for Radiocarbon Dating Using Hydrogen Pyrolysis." *Quaternary Geochronology*, September, 101124. https://doi.org/10.1016/j.quageo.2020. 101124.

Oswald, W. W., P. M. Anderson, T. A. Brown, L. B. Brubaker, S. H. Feng, A. V. Lozhkin,W. Tinner, and P. Kaltenrieder. 2005. "Effects of Sample Mass and Macrofossil Type on Radiocarbon Dating of Arctic and Boreal Lake Sediments." *Holocene* 15 (5): 758–67. https://doi.org/10.1191/0959683605hl849rr.

Pearsall, Deborah M. 2015. *Paleoethnobotany: A Handbook of Procedures*. Third edition. Walnut Creek, California: Left Coast Press Inc.

Peel, M. C., B. L. Finlayson, and T. A. McMahon. 2007. "Updated World Map of the Köppen-Geiger Climate Classification." *Hydrology and Earth System Sciences* 11 (5): 1633–44. https://doi.org/10.5194/hess-11-1633-2007.

Perry, C. A., and K. J. Hsu. 2000. "Geophysical, Archaeological, and Historical Evidence Support a Solar-Output Model for Climate Change." *Proceedings of the National Academy of Sciences* 97 (23): 12433–8. https://doi.org/10.1073/pnas.230423297.

Pessenda, L R, S M Gouveia, and R Aravena. 2001. "Radiocarbon Dating of Total Soil Organic Matter and Humin Fraction and Its Comparison with (Super 14) C Ages of Fossil Charcoal." *Radiocarbon; Vol 43, No 2B (2001)*, January. https://journals.uair.arizona.edu/index.php/ radiocarbon/article/view/3890.

Petherick, L. M., P. T. Moss, and H. A. McGowan. 2011. "Climatic and Environmental Variability During the Termination of the Last Glacial Stage in Coastal Eastern Australia: A Review." *Australian Journal of Earth Sciences* 58 (6): 563–77. https://doi.org/10.1080/ 08120099.2011.566281.

Petherick, Lynda M., Hamish A. McGowan, and Balz S. Kamber. 2009. "Reconstructing Transport Pathways for Late Quaternary Dust from Eastern Australia Using the Composition of Trace Elements of Long Traveled Dusts." *Geomorphology* 105 (1-2): 67–79. https://doi.org/10.1016/j.geomorph.2007.12.015.

Pettitt, P. B, W Davies, C. S Gamble, and M. B Richards. 2003. "Palaeolithic Radiocarbon Chronology: Quantifying Our Confidence Beyond Two Half-Lives." *Journal of Archaeological Science* 30 (12): 1685–93. https://doi.org/10.1016/S0305-4403(03)00070-0.

Piperno, Dolores R. 1995. "Plant Microfossils and Their Application in the New World Tropics." In *Archaeology in the Lowland American Tropics*, edited by Peter W. Stahl, 130–53. Cambridge, UK: Cambridge University Press.

———. 2006. *Phytoliths: A Comprehensive Guide for Archaeologists and Paleoecologists*.Lanham, MD: AltaMira Press.

Piperno, Dolores R., Mark B. Bush, and Paul A. Colinvaux. 1991. “Paleoecological Perspectives on Human Adaptation in Central Panama; II, the Holocene.” *Geoarchaeology* 6 (3): 227–50. http://proxy-remote.galib.uga.edu/login?url=http://search.ebscohost.com/login.aspx?direct=true&db=geh&AN=1992-007471&site=eds-live.

Plicht, J. van der, H. J. Streurman, and J. M. van Mourik. 2019. “Radiocarbon Dating of Soil Archives.” In *Reading the Soil Archives: Unraveling the Geoecological Code of Palaeosols*, edited by J. M. van Mourik and J. van der Meer, 81–114. Developments in Quaternary Science 18. Amsterdam: Elsevier.

Potapova, M. G., A. D. Minerovic, J. Vesela, and C. R. Smith. 2020. “Diatom New Taxon File at the Academy of Natural Sciences (DNTF-ANS).” 2020. http://dh.ansp.org/dntf.

Power, M. J., J. Marlon, N. Ortiz, P. J. Bartlein, S. P. Harrison, F. E. Mayle, A. Ballouche, et al. 2008. “Changes in Fire Regimes Since the Last Glacial Maximum: An Assessment Based on a Global Synthesis and Analysis of Charcoal Data.” *Climate Dynamics* 30 (7-8): 887–907. https://doi.org/10.1007/s00382-007-0334-x.

Prebble, M., R. Sim, J. Finn, and D. Fink. 2005. “A Holocene Pollen and Diatom Record from Vanderlin Island, Gulf of Carpentaria, Lowland Tropical Australia.” *Quaternary Research* 64 (3): 357–71. https://doi.org/10.1016/j.yqres.2005.08.005.

Prentice, I. C., S. F. Cleator, Y. H. Huang, S. P. Harrison, and I. Roulstone. 2017. “Reconstructing Ice-Age Palaeoclimates: Quantifying Low-CO2 Effects on Plants.” *Global and Planetary Change* 149 (February): 166–76. https://doi.org/10.1016/j.gloplacha.2016. 12.012.

Proske, Ulrike, and Simon G Haberle. 2012. “Island Ecosystem and Biodiversity Dynamics in Northeastern Australia During the Holocene: Unravelling Short-Term Impacts and Long-Term Drivers.” *The Holocene* 22 (10): 1097–1111. https://doi.org/10.1177/0959683612441840.

Proske, Ulrike, David Heslop, and Simon Haberle. 2014. “A Holocene Record of Coastal Landscape Dynamics in the Eastern Kimberley Region, Australia.” *Journal of Quaternary Science* 29 (2): 163–74. https://doi.org/10.1002/jqs.2691.

Proske, Ulrike, Janelle Stevenson, Alistair W. R. Seddon, and Kathryn Taffs. 2017. “Holocene Diatom Records of Wetland Development Near Weipa, Cape York, Australia.” *Quaternary International*, Environmental and Climatic Changes Inferred from Sedimentary Records on Asian Shelf Margins: Part I, 440 (June): 42–54. https://doi.org/10.1016/j.quaint.2016.09. 014.

Rangelands Fire Information, North Australia &. 2020. “Data.” 2020. https://www.firenorth. org.au/nafi3/.

Rao, Zhiguo, Wenkang Guo, Jiantao Cao, Fuxi Shi, Hong Jiang, and Chaozhu Li. 2017. “Relationship Between the Stable Carbon Isotopic Composition of Modern Plants and Surface Soils and Climate: A Global Review.” *Earth-Science Reviews* 165 (February): 110–19. https://doi.org/10.1016/j.earscirev.2016.12.007.

Rashid, Irfan, Showkat H. Mir, Débora Zurro, Reyaz A. Dar, and Zafar A. Reshi. 2019. “Phytoliths as Proxies of the Past.” *Earth-Science Reviews* 194 (July): 234–50. https://doi.org/10.1016/j.earscirev.2019.05.005.

Reeves, Jessica M., Helen C. Bostock, Linda K. Ayliffe, Timothy T. Barrows, Patrick De Deckker, Laurent S. Devriendt, Gavin B. Dunbar, et al. 2013. “Palaeoenvironmental Change in Tropical Australasia over the Last 30,000 Years – a Synthesis by the OZ-INTIMATE Group.” *Quaternary Science Reviews* 74 (August): 97–114. https://doi.org/10.1016/j.quascirev.2012.11.027.

Reeves, Jessica M., Allan R. Chivas, Adriana Garcia, and Patrick De Deckker. 2007. “Palaeoenvironmental Change in the Gulf of Carpentaria (Australia) Since the Last Interglacial Based on Ostracoda.” *Palaeogeography, Palaeoclimatology, Palaeoecology* 246 (2-4): 163–87. https://doi.org/10.1016/j.palaeo.2006.09.012.

Reeves, Jessica M., Allan R. Chivas, Adriana Garcia, Sabine Holt, Martine J. J. Couapel, Brian G. Jones, Dioni I. Cendón, and David Fink. 2008. “The Sedimentary Record of Palaeoenvironments and Sea-Level Change in the Gulf of Carpentaria, Australia, Through the Last Glacial Cycle.” *Quaternary International* 183 (1): 3–22. https://doi.org/10.1016/ j.quaint.2007.11.019.

Rehn, Emma. 2020. “Fire and Environmental Change in Northern Australian Savannas During the Holocene.” Cairns: James Cook University.

Rehn, Emma, Cassandra Rowe, Sean Ulm, Craig Woodward, Atun Zawadzki, Geraldine Jacobsen, and M. I. Bird. 2020. “Integrating Charcoal Morphology and Stable Carbon Isotope Analysis to Identify Non-Grass Elongate Charcoal in Tropical Savannas.” *Vegetation History and Archaeobotany* Submitted.

Reimer, Paula J, Edouard Bard, Alex Bayliss, J Warren Beck, Paul G Blackwell, Christopher Bronk Ramsey, Caitlin E Buck, et al. 2013. “IntCal13 and Marine13 Radiocarbon Age Calibration Curves 0–50,000 Years Cal BP.” *Radiocarbon* 55 (4): 1869–87. https://doi.org/ 10.2458/azu_js_rc.55.16947.

Risbey, James S., Michael J. Pook, Peter C. McIntosh, Matthew C. Wheeler, and Harry H. Hendon. 2009. “On the Remote Drivers of Rainfall Variability in Australia.” *Monthly Weather Review* 137 (10): 3233–53. https://doi.org/10.1175/2009MWR2861.1.

Rothwell, R. Guy, and Frank R. Rack. 2006. “New Techniques in Sediment Core Analysis: An Introduction.” *Geological Society, London, Special Publications* 267 (1): 1–29. https://doi.org/10.1144/GSL.SP.2006.267.01.01.

Rowe, Cassandra. 2007. “A Palynological Investigation of Holocene Vegetation Change in Torres Strait, Seasonal Tropics of Northern Australia.” *Palaeogeography, Palaeoclimatology, Palaeoecology* 251 (1): 83–103. https://doi.org/10.1016/j.palaeo.2007.02.019.

———. 2015. “Late Holocene Swamp Transition in the Torres Strait, Northern Tropical Australia.” *Quaternary International* 385 (October): 56–68. https://doi.org/10.1016/j.quaint.2014.07.002.

Rowe, Cassandra, Michael Brand, Lindsay B. Hutley, Christopher Wurster, Costijn Zwart, Vlad Levchenko, and Michael Bird. 2019. “Holocene Savanna Dynamics in the Seasonal Tropics of Northern Australia.” *Review of Palaeobotany and Palynology* 267 (August): 17–31. https://doi.org/10.1016/j.revpalbo.2019.05.004.

Rowe, Cassandra, Christopher M. Wurster, Costijn Zwart, Michael Brand, Lindsay B. Hutley, Vladimir Levchenko, and Michael I. Bird. 2020. “Vegetation over the Last Glacial Maximum at Girraween Lagoon, Monsoonal Northern Australia.”

Russell-Smith, Jeremy. 2016. “Fire Management Business in Australia’s Tropical Savannas: Lighting the Way for a New Ecosystem Services Model for the North?” *Ecological Management & Restoration* 17 (1): 4–7. https://doi.org/10.1111/emr.12201.

Russell-Smith, Jeremy, and Andrew C. Edwards. 2006. “Seasonality and Fire Severity in Savanna Landscapes of Monsoonal Northern Australia.” *International Journal of Wildland Fire* 15 (4): 541. https://doi.org/10.1071/WF05111.

Russell-Smith, Jeremy, Paul G. Ryan, and Richard Durieu. 1997. “A LANDSAT MSS-Derived Fire History of Kakadu National Park, Monsoonal Northern Australial, 1980-94: Seasonal Extent, Frequency and Patchiness.” *The Journal of Applied Ecology* 34 (3): 748. https://doi.org/10.2307/2404920.

Russell-Smith, Jeremy, and Cameron P. Yates. 2007. “Australian Savanna Fire Regimes: Context, Scales, Patchiness.” *Fire Ecology* 3 (1): 48–63. https://doi.org/10.4996/ fireecology.0301048.

Saiz, Gustavo, Iain Goodrick, Christopher Wurster, Paul N. Nelson, Jonathan Wynn, and Michael Bird. 2018. “Preferential Production and Transport of Grass-Derived Pyrogenic Carbon in NE-Australian Savanna Ecosystems.” *Frontiers in Earth Science* 5. https://doi.org/10.3389/feart.2017.00115.

Saiz, G., J. G. Wynn, C. M. Wurster, I. Goodrick, P. N. Nelson, and M. I. Bird. 2015. “Pyrogenic Carbon from Tropical Savanna Burning: Production and Stable Isotope Composition.” *Biogeosciences* 12 (6): 1849–63. https://doi.org/10.5194/bg-12-1849-2015.

Schnurrenberger, Douglas, James Russell, and Kerry Kelts. 2003. “Classification of Lacustrine Sediments Based on Sedimentary Components.” *Journal of Paleolimnology* 29 (2): 141–54. https://doi.org/10.1023/A:1023270324800.

Shi, Li, Paul Gregory, Todd Smith, Prasantha Hapuarachchi, Paul Feikema, Arthur Read, Phillip Reid, et al. 2016. "Climate Data and Their Characterisation for Hydrological and Agricultural Scenario Modelling Across the Fitzroy, Darwin and Mitchell Catchments." https://doi.org/10.25919/5B86ED38D15A6.

Shulmeister, J. 1992. "A Holocene Pollen Record from Lowland Tropical Australia." *The Holocene* 2 (2): 107–16. https://doi.org/10.1177/095968369200200202.

———. 1999. "Australasian Evidence for Mid-Holocene Climate Change Implies Precessional Control of Walker Circulation in the Pacific." *Quaternary International* 57-58 (June): 81–91. https://doi.org/10.1016/S1040-6182(98)00052-4.

Shulmeister, J., and Brian G. Lees. 1992. "Morphology and Chronostratigraphy of a Coastal Dunefield; Groote Eylandt, Northern Australia." *Geomorphology* 5 (6): 521–34. https://doi.org/10.1016/0169-555X(92)90023-H.

———. 1995. "Pollen Evidence from Tropical Australia for the Onset of an ENSO-Dominated Climate at c. 4000 BP." *The Holocene* 5 (1): 10–18. https://doi.org/10.1177/095968369500500102.

Simpson, Gavin L., and H. John B. Birks. 2012. "Statistical Learning in Palaeolimnology." In *Tracking Environmental Change Using Lake Sediments*, edited by H. John B. Birks, André F. Lotter, Steve Juggins, and John P. Smol, 5:249–327. Developments in Paleoenvironmental Research. Dordrecht: Springer Netherlands. https://doi.org/10.1007/978-94-007-2745-8_ 9.

Sloss, Craig R, Luke Nothdurft, Quan Hua, Shoshannah G O'Connor, Patrick T Moss, Daniel Rosendahl, Lynda M Petherick, et al. 2018. "Holocene Sea-Level Change and Coastal Landscape Evolution in the Southern Gulf of Carpentaria, Australia." *The Holocene* 28 (9): 1411–30. https://doi.org/10.1177/0959683618777070.

Sonneman, Jason A, ed. 1999. *An Illustrated Guide to Common Stream Diatom Species from Temperate Australia: Presented at the 2nd Australian Algal Workshop, Adelaide University, 17-19th April, 2000*. Thurgoona, NSW: Cooperative Research Centre for Freshwater Ecology.

Spaulding, S., and M. Edlund. 2010. "Diatoms of North America." 2010. https://diatoms.org/ genera/pinnularia.

Specht, R.L., 1981. Growth indices—Their role in understanding the growth, structure and distribution of Australian vegetation. Oecologia, 50(3), pp.347-356.

Stephens, K., and L. Head. 1995. "Palaeoecology of Archaeological and Swamp Sites in S.E. Cape York Peninsula." *Tempus* 3: 18–32.

Stevens, Nicola, Caroline E. R. Lehmann, Brett P. Murphy, and Giselda Durigan. 2017. “Savanna Woody Encroachment Is Widespread Across Three Continents.” *Global Change Biology* 23 (1): 235–44. https://doi.org/10.1111/gcb.13409.

Stevenson, Janelle, Sally Brockwell, Cassandra Rowe, Ulrike Proske, and Justin Shiner. 2015. “The Palaeo-Environmental History of Big Willum Swamp, Weipa: An Environmental Context for the Archaeological Record.” *Australian Archaeology* 80 (1): 17–31. https://doi.org/10.1080/03122417.2015.11682041.

Stevenson, J, J. R Dodson, and I. P Prosser. 2001. “A Late Quaternary Record of Environmental Change and Human Impact from New Caledonia.” *Palaeogeography, Palaeoclimatology, Palaeoecology* 168 (1-2): 97–123. https://doi.org/10.1016/S0031-0182(00)00251-0.

Stewart, Gr, Mh Turnbull, S Schmidt, and Pd Erskine. 1995. “13C Natural Abundance in Plant Communities Along a Rainfall Gradient: A Biological Integrator of Water Availability.” *Functional Plant Biology* 22 (1): 51. https://doi.org/10.1071/PP9950051.

Stoeckl, Natalie, and Owen Stanley. 2007. “Key Industries in Australia’s Tropical Savannas.” *Australasian Journal of Regional Studies* 13 (3): 255–86.

Stoermer, Eugene F., and John P. Smol, eds. 2001. *The Diatoms: Applications for the Environmental and Earth Sciences*. 1. paperback ed. Cambridge: Cambridge University Press.

Strömberg, Caroline A. E., Regan E. Dunn, Camilla Crifò, and Elisha B. Harris. 2018. “Phytoliths in Paleoecology: Analytical Considerations, Current Use, and Future Directions.” In *Methods in Paleoecology: Reconstructing Cenozoic Terrestrial Environments and Ecological Communities*, edited by Darin A. Croft, Denise F. Su, and Scott W. Simpson, 235–87. Vertebrate Paleobiology and Paleoanthropology. Cham: Springer International Publishing. https://doi.org/10.1007/978-3-319-94265-0_12.

Talbot, Michael R. 2002. “Nitrogen Isotopes in Palaeolimnology.” In *Tracking Environmental Change Using Lake Sediments*, edited by William M. Last and John P. Smol, 2:401–39. Developments in Paleoenvironmental Research. Dordrecht: Kluwer Academic Publishers. https://doi.org/10.1007/0-306-47670-3_15.

Taylor, B., K. Fujioka, and et al., eds. 1992. *Proceedings of the Ocean Drilling Program, 126 Scientific Results*. Vol. 126. Proceedings of the Ocean Drilling Program. Ocean Drilling Program. https://doi.org/10.2973/odp.proc.sr.126.1992.

Testé, Marc, Aline Garnier, Nicole Limondin-Lozouet, Enecon Oxlaj, Cyril Castanet, Louise Purdue, Eva Lemonnier, Lydie Dussol, and Philippe Nondédéo. 2020. “The Phytoliths of Naachtun (Petén, Guatemala): Development of a Modern Reference for the Characterization of Plant Communities in the Maya Tropical Lowlands.” *Review of Palaeobotany and Palynology* 272 (January): 104130. https://doi.org/10.1016/j.revpalbo.2019.104130.

Tibby, J., and S. G. Haberle. 2007. “A Late Glacial to Present Diatom Record from Lake Euramoo, Wet Tropics of Queensland, Australia.” *Palaeogeography, Palaeoclimatology, Palaeoecology* 251 (1): 46–56. https://doi.org/10.1016/j.palaeo.2007.02.017.

Tierney, Jessica E., James M. Russell, and Yongsong Huang. 2010. “A Molecular Perspective on Late Quaternary Climate and Vegetation Change in the Lake Tanganyika Basin, East Africa.” *Quaternary Science Reviews* 29 (5-6): 787–800. https://doi.org/10.1016/j. quascirev.2009.11.030.

Torgersen, T., M. R. Jones, A. W. Stephens, D. E. Searle, and W. J. Ullman. 1985. “Late Quaternary Hydrological Changes in the Gulf of Carpentaria.” *Nature* 313 (6005, 6005): 785–87. https://doi.org/10.1038/313785a0.

Turner, Jonathan N., Anna F. Jones, Paul A. Brewer, Mark G. Macklin, and Sara M. Rassner. 2015. “Micro-XRF Applications in Fluvial Sedimentary Environments of Britain and Ireland: Progress and Prospects.” In *Micro-XRF Studies of Sediment Cores*, edited by Ian W. Croudace and R. Guy Rothwell, 17:227–65. Developments in Paleoenvironmental Research. Dordrecht: Springer Netherlands. https://doi.org/10.1007/978-94-017-9849- 5_8.

Turney, Chris S. M., G. Russell Coope, Doug D. Harkness, J. John Lowe, and Michael J. C. Walker. 2000. “Implications for the Dating of Wisconsinan (Weichselian) Late-Glacial Events of Systematic Radiocarbon Age Differences Between Terrestrial Plant Macrofossils from a Site in SW Ireland.” *Quaternary Research* 53 (01): 114–21. https://doi.org/10.1006/ qres.1999.2087.

Turney, Chris S. M., A. Peter Kershaw, Steven C. Clemens, Nick Branch, Patrick T. Moss, and L. Keith Fifield. 2004. “Millennial and Orbital Variations of El Niño/Southern Oscillation and High-Latitude Climate in the Last Glacial Period.” *Nature* 428 (6980): 306–10. https://doi.org/10.1038/nature02386.

Turney, Chris S. M., A. Peter Kershaw, Sarah James, Nick Branch, Joan Cowley, L. Keith Fifield, Geraldine Jacobsen, and Patrick Moss. 2006. “Geochemical Changes Recorded in Lynch’s Crater, Northeastern Australia, over the Past 50 Ka.” *Palaeogeography, Palaeoclimatology, Palaeoecology* 233 (3): 187–203. https://doi.org/10.1016/j.palaeo.2005.09.009.

Vázquez, Gabriel, Priyadarsi D. Roy, Berenice Solis C., Sean M. Smith M., Ericka Blanco M., and Rufino Lozano-Santacruz. 2017. “Holocene Paleohydrology of the Etzatlán-Magdalena Basin in Western-Central Mexico and Evaluation of Main Atmospheric Forcings.” *Palaeogeography, Palaeoclimatology, Palaeoecology*, September. https://doi.org/10.1016/j.palaeo.2017.08.029.

Veenendaal, Elmar M., Mireia Torello-Raventos, Heloisa S. Miranda, Naomi Margarete Sato, Imma Oliveras, Frank van Langevelde, Gregory P. Asner, and Jon Lloyd. 2018. “On the Relationship Between Fire Regime and Vegetation Structure in the Tropics.” *New Phytologist* 218 (1): 153–66. https://doi.org/10.1111/nph.14940.

Walker, D. 2007. “Holocene Sediments of Lake Barrine, North-East Australia, and Their Implications for the History of Lake and Catchment Environments.” *Palaeogeography, Palaeoclimatology, Palaeoecology* 251 (1): 57–82. https://doi.org/10.1016/j.palaeo.2007.02.025.

Wallis, Lynley. 2003. “An Overview of Leaf Phytolith Production Patterns in Selected Northwest Australian Flora.” *Review of Palaeobotany and Palynology* 125 (3-4): 201–48. https://doi.org/10.1016/S0034-6667(03)00003-4.

Wallis, Lynley A. 2001. “Environmental History of Northwest Australia Based on Phytolith Analysis at Carpenter’s Gap 1.” *Quaternary International* 83-85 (September): 103–17. https://doi.org/10.1016/S1040-6182(01)00033-7.

Wang, Yang, Ronald Amundson, and Susan Trumbore. 1996. “Radiocarbon Dating of Soil Organic Matter.” *Quaternary Research* 45 (3): 282–88. https://doi.org/10.1006/qres.1996.0029.

Weltje, G. J., M. R. Bloemsma, R. Tjallingii, D. Heslop, U. Röhl, and Ian W. Croudace. 2015. “Prediction of Geochemical Composition from XRF Core Scanner Data: A New Multivariate Approach Including Automatic Selection of Calibration Samples and Quantification of Uncertainties.” In *Micro-XRF Studies of Sediment Cores*, edited by Ian W. Croudace and

R. Guy Rothwell, 17:507–34. Developments in Paleoenvironmental Research. Dordrecht: Springer Netherlands. https://doi.org/10.1007/978-94-017-9849-5_21.

Wende, R., G. C. Nanson, and D. M. Price. 1997. “Aeolian and Fluvial Evidence for Late Quaternary Environmental Change in the East Kimberley of Western Australia.” *Australian Journal of Earth Sciences* 44 (4): 519–26. https://doi.org/10.1080/08120099708728331.

Wheeler, Tim, and Joachim von Braun. 2013. “Climate Change Impacts on Global Food Security.” *Science* 341 (6145): 508–13. https://doi.org/10.1126/science.1239402.

Whitmore, Thomas J. 1989. “Florida Diatom Assemblages as Indicators of Trophic State and pH: Florida Diatom Assemblages.” *Limnology and Oceanography* 34 (5): 882–95. https://doi.org/10.4319/lo.1989.34.5.0882.

Williams, Alan N., Sean Ulm, Tom Sapienza, Stephen Lewis, and Chris S. M. Turney. 2018. “Sea-Level Change and Demography During the Last Glacial Termination and Early Holocene Across the Australian Continent.” *Quaternary Science Reviews* 182 (February): 144–54. https://doi.org/10.1016/j.quascirev.2017.11.030.

Wohlfarth, B., G. Skog, G. Possnert, and B. Holmquist. 1998. “Pitfalls in the AMS Radiocarbon-Dating of Terrestrial Macrofossils.” *Journal of Quaternary Science* 13 (2): 137–45. https://doi.org/10.1002/(SICI)1099-1417(199803/04)13:2%3C137::AID-JQS352%3E3.0.CO;2-6.

Wolfe, Brent B., Matthew D. Falcone, Ken P. Clogg-Wright, Cherie L. Mongeon, Yi Yi, Bronwyn E. Brock, Natalie A. St. Amour, William A. Mark, and Thomas W. D. Edwards. 2007. “Progress in Isotope Paleohydrology Using Lake Sediment Cellulose.” *Journal of Paleolimnology* 37 (2): 221–31. https://doi.org/10.1007/s10933-006-9015-8.

Wolin, J. A., and J. R. Stone. 2010. “Diatoms as Indicators of Water-Level Change in Freshwater Lakes.” In *The Diatoms: Applications for the Environmental and Earth Sciences, Second Edition*, 174–85. https://doi.org/10.1017/CBO9780511763175.010.

Wood, Rachel. 2015. “From Revolution to Convention: The Past, Present and Future of Radiocarbon Dating.” *Journal of Archaeological Science*, Scoping the Future of Archaeological Science: Papers in Honour of Richard Klein, 56 (April): 61–72. https://doi.org/10.1016/j.jas.2015.02.019.

Woodroffe, Colin D., B. G. Thom, and John Chappell. 1985. “Development of Widespread Mangrove Swamps in Mid-Holocene Times in Northern Australia.” *Nature* 317 (6039, 6039): 711–13. https://doi.org/10.1038/317711a0.

Wurster, Christopher M., Jon Lloyd, Iain Goodrick, Gustavo Saiz, and Michael I. Bird. 2012. “Quantifying the Abundance and Stable Isotope Composition of Pyrogenic Carbon Using Hydrogen Pyrolysis: Quantifying PC Isotope Composition Using Hypy.” *Rapid Communications in Mass Spectrometry* 26 (23): 2690–6. https://doi.org/10.1002/rcm.6397.

Wurster, Christopher M., Hamdi Rifai, Jordahna Haig, Jupiri Titin, Geraldine Jacobsen, and Michael Bird. 2017. “Stable Isotope Composition of Cave Guano from Eastern Borneo Reveals Tropical Environments over the Past 15,000 Cal Yr BP.” *Palaeogeography, Palaeoclimatology, Palaeoecology* 473 (May): 73–81. https://doi.org/10.1016/j.palaeo.2017.02.029.

Wurster, Christopher M., Hamdi Rifai, Bin Zhou, Jordahna Haig, and Michael I. Bird. 2019. “Savanna in Equatorial Borneo During the Late Pleistocene.” *Scientific Reports* 9 (1, 1): 1–7. https://doi.org/10.1038/s41598-019-42670-4.

Wurster, Christopher M., Gustavo Saiz, Maximilian P. W. Schneider, Michael W. I. Schmidt, and Michael I. Bird. 2013. “Quantifying Pyrogenic Carbon from Thermosequences of Wood and Grass Using Hydrogen Pyrolysis.” *Organic Geochemistry* 62 (September): 28–32. https://doi.org/10.1016/j.orggeochem.2013.06.009.

Wüst, R. A. J., G. E. Jacobsen, H. van der Gaast, and A. M. Smith. 2008. “Comparison of Radiocarbon Ages from Different Organic Fractions in Tropical Peat Cores: Insights from Kalimantan, Indonesia.” *Radiocarbon* 50 (3): 359–72. https://doi.org/10.1017/ S0033822200053492.

Wyrwoll, Karl-Heinz, and Gifford H. Miller. 2001. “Initiation of the Australian Summer Monsoon 14,000 Years Ago.” *Quaternary International* 83-85 (September): 119–28. https://doi.org/10.1016/S1040-6182(01)00034-9.

Xiao, Jule, Zhigang Chang, Ruilin Wen, Dayou Zhai, Shigeru Itoh, and Zaur Lomtatidze. 2009. “Holocene Weak Monsoon Intervals Indicated by Low Lake Levels at Hulun Lake in the Monsoonal Margin Region of Northeastern Inner Mongolia, China.” *The Holocene* 19 (6): 899–908. https://doi.org/10.1177/0959683609336574.

Xu, S., and G. Zheng. 2003. “Variations in Radiocarbon Ages of Various Organic Fractions in Core Sediments from Erhai Lake, SW China.” *Geochemical Journal* 37 (1): 135–44. https://doi.org/10.2343/geochemj.37.135.

Xu, Yantian, Zhongping Lai, and Chang’an Li. 2019. “Sea-Level Change as the Driver for Lake Formation in the Yangtze Plain – A Review.” *Global and Planetary Change* 181 (October): 102980. https://doi.org/10.1016/j.gloplacha.2019.102980.

Yan, Mi, Bin Wang, Jian Liu, Axing Zhu, Liang Ning, and Jian Cao. 2018. “Understanding the Australian Monsoon Change During the Last Glacial Maximum with a Multi-Model Ensemble.” *Climate of the Past* 14 (12): 2037–52. https://doi.org/10.5194/cp-14-2037-2018.

Yokoyama, Yusuke, Anthony Purcell, Kurt Lambeck, and Paul Johnston. 2001. “Shore-Line Reconstruction Around Australia During the Last Glacial Maximum and Late Glacial Stage.” *Quaternary International* 83-85 (September): 9–18. https://doi.org/10.1016/S1040-6182(01)00028-3.

Zech, Michael, Mario Tuthorn, Roland Zech, Frank Schlütz, Wolfgang Zech, and Bruno Glaser. 2014. “A 16-Ka 18O Record of Lacustrine Sugar Biomarkers from the High Himalaya Reflects Indian Summer Monsoon Variability.” *Journal of Paleolimnology* 51 (2): 241–51. https://doi.org/10.1007/s10933-013-9744-4.

Appendix A. Extracted radiocarbon samples with insufficient carbon after combustion

Lab Code	ID	Carbon fraction	Pretreatment	Final weight
Y131U1	32	Charcoal <63 um	ABA	1.65ug
Y133	171	Charcoal >250 um	ABA	3.67ug
Y134	171	Charcoal >63 um	ABA	1.52ug
Y135	171	Charcoal <63 um	ABA	0.46ug
Y136	94	Charcoal >250 um	ABA	3.35ug
Y137	94	Charcoal >63 um	ABA	1.05ug
Y138	94	Charcoal <63 um	ABA	6.03ug
Y139	94	Pollen	ABA	1.71ug
Y331	170	Charcoal <63 um	ABA	NA
Y332	282	Charcoal <63 um	ABA	NA
Y330	71	Charcoal <63 um	ABA	NA
NA	56	PyC	Hypy	NA
NA	56	Charcoal <63 um	ABA	NA
NA	32	Charcoal <63 um	ABA	NA
NA	171	Pollen	ABA	NA
NA	94	Pollen	ABA	NA

Appendix B. Selected photographs of diatoms and phytoliths

Frustulia rhomboides

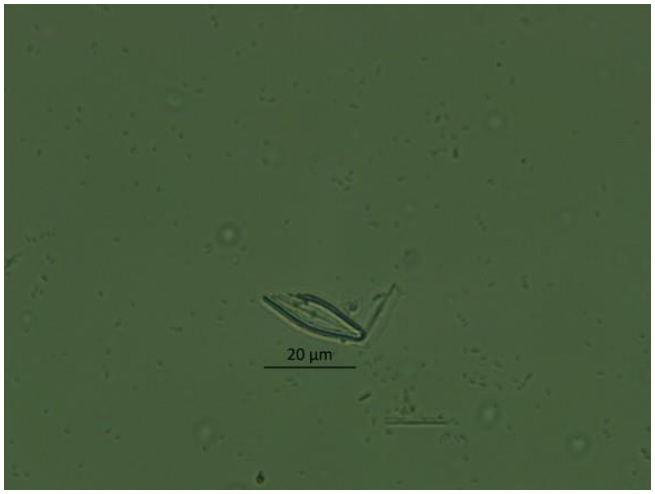

Brachysira brebissoni

Eunotia sp.

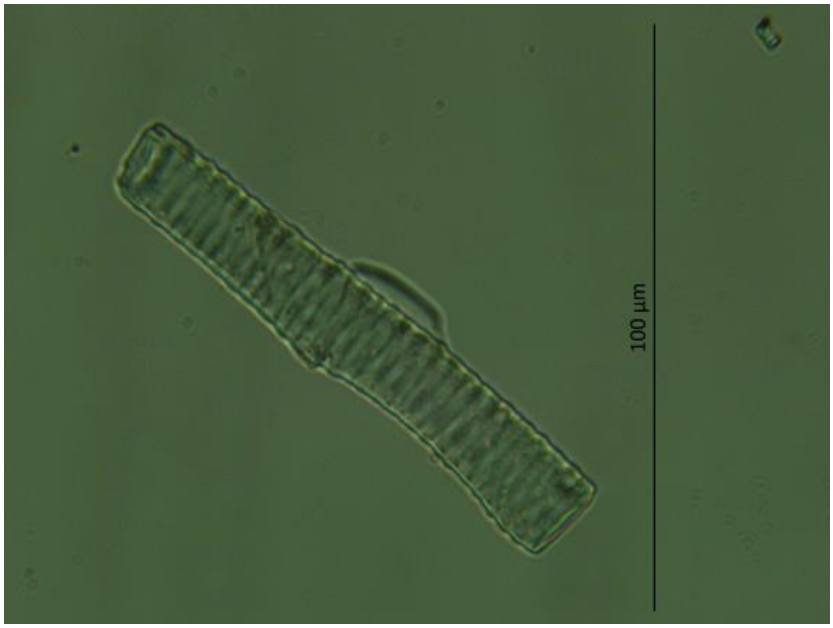

Tracheid phytolith

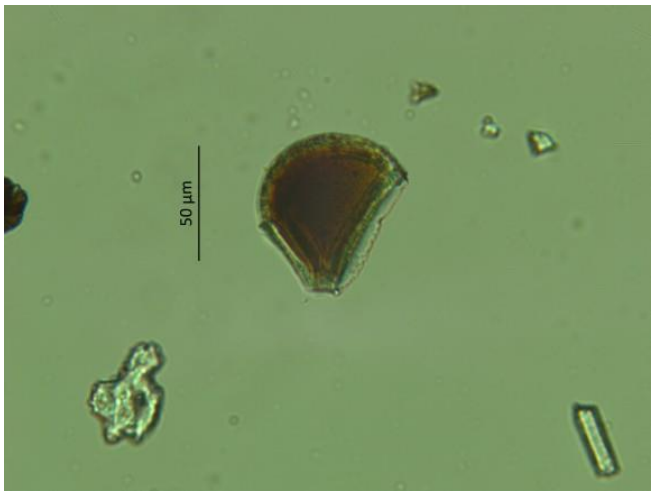

Bulliform phytolith

Acicular phytoliths

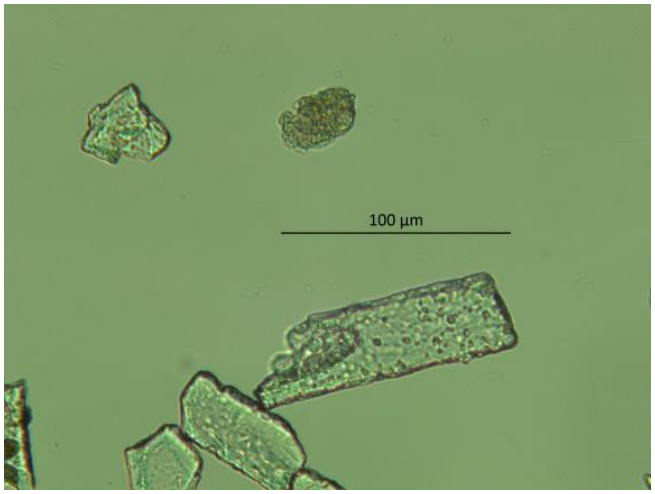

Elongate phytoliths

Appendix C. Data availability

The data collected and analysed in this thesis is available at https://research.jcu.edu.au/data/